G. GIACOMELLI

Magnetic Monopoles.

PROVANDO E RIPROVANDO

LA RIVISTA DEL NUOVO CIMENTO VOL. 7, N. 12 1984

Magnetic Monopoles.

G. GIACOMELLI

Università di Bologna - Bologna, Italia
Istituto Nazionale di Fisica Nucleare - Sezione di Bologna, Italia
CERN - Geneva, Switzerland

(ricevuto il 19 Giugno 1984)

1. – Introduction.

The science of magnetism started with the observation that a number of minerals (like magnetite) attracted pieces of iron. In fact, the word magnetism derives from the Magnesia region in Turkey where some of these minerals were found. The first scientific account of magnetic materials may be traced back to 1269. In a letter written during the siege of the town of Lucera, Italy, the French military engineer Petrus PEREGRINUS DE MARICOURT described the lines of force around a lodestone and noted that they started and terminated at two points, which he called the north and south poles [74P1]. All subsequent observations confirmed that all magnetic objects, that is all the permanent magnets found in Nature and those made by man, are dipoles. But some physicists continued speaking of isolated poles, often for pedagogical reasons. At the beginning of the 19th century there were discussions concerning the magnetic content of matter and some speculations about the possible existence of isolated magnetic charges. In 1904, J. J. THOMSON considered the problem of the motion of an electron in the field of a point magnetic charge. This may be considered a test problem, which was later attacked by many theoreticians.

The modern period started in 1931, when DIRAC introduced the magnetic monopole in order to explain the quantization of the electric charge [31D1]. In his reasoning the quantization of electric charge follows from the existence of at least one free magnetic charge. DIRAC established also the basic relation between the elementary electric charge e and the magnetic charge g

$$g = ng_{\mathrm{D}} = \frac{1}{2}\frac{\hbar c}{e}n \sim \frac{137}{2}en\,, \tag{1.1}$$

where g_{D} is the smallest magnetic charge and n is an integer which in the original proposal could assume the values $n = 1, 2, 3, \ldots$. The existence of magnetic charges and of magnetic currents would symmetrize in form Maxwell's equations, but the symmetry would not be perfect, since the smallest magnetic charge is predicted to be much larger than the smallest electric charge, eq. (1.1). SCHWINGER [68S1] showed that an explanation of the zero mass for the photon may follow from the existence of both electric and magnetic charges. These types of reasoning were the basis for the introduction of what we may now call the «classical magnetic monopole». In this formulation there was no prediction for the monopole mass. A kind of rule of thumb was instead established, assuming that the classical electron radius be equal to the «classical monopole radius» from which one has $m_M \sim g_D^2 m_e/e^2 \sim 4700\, m_e \sim 2.4$ GeV.

A new period started around 1974, when it was realized that the electric charge is naturally quantized in those unified theories of the basic interactions in which electromagnetism is embedded in a spontaneously broken gauge theory and that such unified theories imply the existence of magnetic monopoles, whose properties are calculable [74H1, 74P2]. In a certain sense, the situation was reversed compared to the reasoning of Dirac: the quantization of the electric charge now implied the existence of magnetic monopoles.

In the context of the grand unification of strong, electromagnetic and weak interactions (GUT), the magnetic monopoles appear at the transition corresponding to the spontaneous breaking of the unified group into subgroups, one of which is U_1, which describes electromagnetism. In the language of group theory one has the following transitions, starting, for instance, with the unified group SU_5:

$$(1.2)\qquad \underset{\text{grand unification}}{SU_5} \xrightarrow{10^{15}\,\text{GeV}} \underset{\text{electroweak unification}}{SU_3 \times (SU_2 \times U_1)} \xrightarrow{10^{2}\,\text{GeV}} \underset{\text{separate interactions}}{SU_{3\,\text{colour}} \times U_{1\,\text{e.m.}}}\,.$$

The monopoles are produced at the first transition after which the group U_1 appears for the first time. The lowest monopole mass is related to the mass of the X vector boson, which is the carrier of the unified interaction and defines the unification scale,

$$(1.3)\qquad m_M \geqslant m_X/G\,,$$

where G is the dimensionless unified coupling constant. In GUT one has $m_X \simeq 10^{15}$ GeV and $G = 0.025$; consequently $m_M \geqslant 10^{16}$ GeV $\simeq 0.02$ μg. This is an enormous mass; therefore, magnetic monopoles cannot be produced at any accelerator existing or even conceivable. They could only be primordial.

In the so-called standard model of the big bang, the Universe started in a state of extremely large density and large temperature. As time progressed, the density and temperature decreased, while the particle composition changed. The grand unification of strong and electroweak interactions lasted until when the temperature dropped to $\sim 10^{15}$ GeV. At that moment, $\sim 10^{-35}$ s after the big bang, the phase transition is thought to have occurred during which the GUT monopoles were created as topological defects. The simplest GUT theories yield too many monopoles, while the inflationary scenario leads to a very small number of monopoles.

GUT based on groups larger than SU_5 offers other possibilities for magnetic-monopole charges and masses. In particular, one finds lighter monopoles

($m_M \sim 10^{10}$ GeV) multiply charged. The appearance of intermediate mass scales in these theories provides a mechanism for reducing the number density of monopoles, without invoking the inflationary scenario. If also gravity is brought into the unifying picture, for instance in the form of Kaluza-Klein theories, then monopoles could be much more massive, $m_M \gtrsim 10^{19}$ GeV. Thus the theoretical picture is far from unique: gauge theories of the unified interactions demand the existence of magnetic monopoles, but the prediction of the monopole mass is uncertain by several orders of magnitude, the magnetic charge could be between one and several Dirac units and the expected flux could vary from an extremely small value to a sizable and observable flux.

Magnetic monopoles of lowest mass are expected to be stable, since magnetic charge should be conserved like electric charge. Therefore, the original monopoles produced in the early Universe should still be around as cosmic relics, whose kinetic energy has been strongly affected by their travel history through galactic magnetic fields.

From 1931 many experimenters searched for «classical Dirac monopoles». Searches were made at every new accelerator, which opened up a new energy region. Monopoles were thought to be produced in high-energy reactions of the type

$$(1.4)\qquad e^+ + e^- \rightarrow g + \bar{g}\,, \quad p + p \rightarrow p + p + g + \bar{g}\,, \quad \bar{p} + p \rightarrow g + \bar{g}\,,$$

where g is a monopole and $\bar{g}$ is an antimonopole. These types of searches are still going on at the newest accelerators.

The most direct method of searching for GUT monopoles is to search them as a flux in the cosmic radiation. GUT poles should be characterized by low velocities and relatively large energy losses. After the 1982 excitement, there has been rapid progress in analysing various types of astrophysical and cosmological bounds, in the detailed studies of the energy losses of monopoles in matter and in obtaining new experimental flux upper limits with a large variety of detectors, which quickly increased in size and complexity.

The field of magnetic monopoles has grown considerably in the last few years. It now involves many fields, from particle physics to astrophysics, from the extremely small to cosmology. But, it has to be stressed that most conclusions are highly speculative and give only rough orders of magnitude. Moreover, many calculations do not take into account the developments in related subjects.

This review, though mainly aimed at the experimental aspects of the monopole searches, attempts to be comprehensive and to give a broad overview, sometimes a simple-minded one, of the general field. The Dirac monopole will often be referred to as «classical», in contrast to GUT or cosmic monopoles.

In sect. 2, which deals with theory, the basis of the «classical monopole» and of the «gauge monopole» concepts will be reviewed. The interactions of monopoles with matter and some properties of monopoles most relevant to their detection will be discussed in sect. **3.** Section **4** is devoted to the production and to the history of GUT monopoles from production to our days. In sect. **5** the reader may find a kind of summary of the previous sections. Section **6** reviews the astrophysical limits on cosmic monopole abundance, whilst the searches for classical monopoles will be presented in sect. **7** and those for cosmic monopoles in sect. **8.** The monopole catalysis of proton decay is discussed in sect. **9.** Other types of searches will be briefly mentioned in sect. **10,** while sect. **11** deals with new detectors and sect. **12** with conclusions and future perspectives.

The Gauss CGS symmetric system of units will be used throughout.

2. – Theoretical considerations.

2'1. *The equations of Maxwell.* – With the introductions of magnetic monopoles the equations of Maxwell become symmetrical in form. In the Gauss CGS symmetric system of units one has

$$\operatorname{div}\boldsymbol{E} = 4\pi\varrho_e\,, \tag{2.1}$$

$$\operatorname{div}\boldsymbol{B} = 4\pi\varrho_m\,, \tag{2.2}$$

$$\operatorname{rot}\boldsymbol{E} = \frac{4\pi}{c}\boldsymbol{J}_m - \frac{1}{c}\frac{\partial\boldsymbol{B}}{\partial t}\,, \tag{2.3}$$

$$\operatorname{rot}\boldsymbol{B} = \frac{4\pi}{c}\boldsymbol{J}_e + \frac{1}{c}\frac{\partial\boldsymbol{E}}{\partial t}\,, \tag{2.4}$$

where ϱ_e and ϱ_m are the electric- and magnetic-charge densities, $\boldsymbol{J}_e$ and $\boldsymbol{J}_m$ the electric- and magnetic-current densities. The electric and magnetic charges are integrals of the corresponding charge densities:

$$e = \int_v \varrho_e\,\mathrm{d}v = \frac{1}{4\pi}\oint_S \boldsymbol{E}\cdot\mathrm{d}\boldsymbol{S}\,, \tag{2.5}$$

$$g = \int_v \varrho_m\,\mathrm{d}v = \frac{1}{4\pi}\oint_S \boldsymbol{B}\cdot\mathrm{d}\boldsymbol{S}\,. \tag{2.6}$$

The magnetic charge and the electric charge should be separately conserved. Therefore, one should have a continuity equation for the electric-charge and current densities as well as for the magnetic densities

$$\operatorname{div}\boldsymbol{J}_e + \frac{1}{c}\frac{\partial\varrho_e}{\partial t} = 0\,, \tag{2.7}$$

$$\operatorname{div}\boldsymbol{J}_m + \frac{1}{c}\frac{\partial\varrho_m}{\partial t} = 0\,. \tag{2.8}$$

Electric and magnetic fields applied to an electric or to a magnetic charge give rise to the Lorentz force

$$\boldsymbol{F}_{\mathrm{e}} = e\left(\boldsymbol{E} + \frac{1}{c}\boldsymbol{v}_{\mathrm{e}} \times \boldsymbol{B}\right), \tag{2.9}$$

$$\boldsymbol{F}_{\mathrm{g}} = g\left(\boldsymbol{B} - \frac{1}{c}\boldsymbol{v}_{\mathrm{m}} \times \boldsymbol{E}\right). \tag{2.10}$$

The modified Maxwell's equations (2.1)-(2.4) exhibit a dual symmetry between electricity and magnetism, which is expressed by duality rotations, defined as

$$(\boldsymbol{E}', \varrho_{\mathrm{e}}', \boldsymbol{J}_{\mathrm{e}}') = (\boldsymbol{E}, \varrho_{\mathrm{e}}, \boldsymbol{J}_{\mathrm{e}}) \cos\theta + (\boldsymbol{B}, \varrho_{\mathrm{m}}, \boldsymbol{J}_{\mathrm{m}}) \sin\theta\,, \tag{2.11}$$

$$(\boldsymbol{B}', \varrho_{\mathrm{m}}', \boldsymbol{J}_{\mathrm{m}}') = (\boldsymbol{B}, \varrho_{\mathrm{m}}, \boldsymbol{J}_{\mathrm{m}}) \cos\theta - (\boldsymbol{E}, \varrho_{\mathrm{e}}, \boldsymbol{J}_{\mathrm{e}}) \sin\theta\,, \tag{2.12}$$

where θ is a real number.

The symmetry is even more evident in the relativistic notation. If the electric- and magnetic-current four-vectors are written as

$$J_\mu^{\mathrm{e}} = (\boldsymbol{J}_{\mathrm{e}}, ic\varrho_{\mathrm{e}})\,, \qquad J_\mu^{\mathrm{m}} = (\boldsymbol{J}_{\mathrm{m}}, ic\varrho_{\mathrm{m}})\,, \tag{2.13}$$

the electromagnetic-field strength tensors are

$$F_{ij} = -\varepsilon_{ijk} B_k\,, \qquad F_{i4} = E_4\,, \tag{2.14}$$

$$F^+_{\mu\nu} = \frac{1}{2}\varepsilon_{\mu\nu\alpha\beta}F^{\alpha\beta}\,, \tag{2.15}$$

and Maxwell's equations become

$$\partial^\mu F_{\mu\nu} = \frac{4\pi}{c} J_\nu^{\mathrm{e}}\,, \tag{2.16}$$

$$\partial^\mu F^+_{\mu\nu} = \frac{4\pi}{c} J_\nu^{\mathrm{m}}\,. \tag{2.17}$$

The dual symmetry corresponds now to the relations

$$\begin{pmatrix} F_{\mu\nu} \\ F^+_{\mu\nu} \end{pmatrix} \Rightarrow \begin{pmatrix} \cos\theta & \sin\theta \\ -\sin\theta & \cos\theta \end{pmatrix} \begin{pmatrix} F_{\mu\nu} \\ F^+_{\mu\nu} \end{pmatrix}, \tag{2.18}$$

$$\begin{pmatrix} J_\mu^{\mathrm{e}} \\ J_\mu^{\mathrm{m}} \end{pmatrix} \Rightarrow \begin{pmatrix} \cos\theta & \sin\theta \\ -\sin\theta & \cos\theta \end{pmatrix} \begin{pmatrix} J_\mu^{\mathrm{e}} \\ J_\mu^{\mathrm{m}} \end{pmatrix}. \tag{2.19}$$

2'2. *Point electric charge in the field of a point magnetic charge.* – Let us consider the nonrelativistic motion of an electron (assumed to be a point electric charge without spin) about a fixed (heavy) point magnetic charge (with no spin). If $\boldsymbol{r}_e$ is the position vector of the electric charge with respect to the magnetic charge (fig. 2.1*a*)) the equation of motion is ($\dot{\boldsymbol{r}}_e = \mathrm{d}\boldsymbol{r}_e/\mathrm{d}t$)

$$m_e \ddot{\boldsymbol{r}}_e = \frac{e}{c} \dot{\boldsymbol{r}} \times \boldsymbol{B}, \tag{2.20}$$

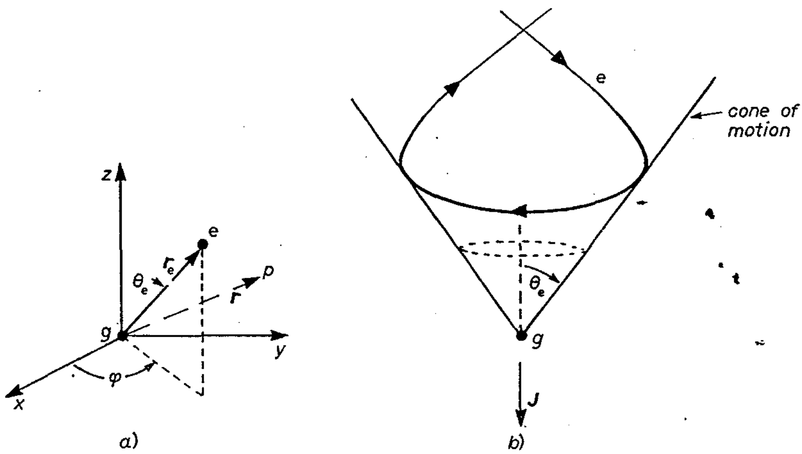

Fig. 2.1. – Motion of an electron e in the field of a point massive magnetic charge g located at the origin 0: *a*) frame of reference and *b*) motion of the electron on a conical surface [82C6].

where the second term represents the Lorentz force. The point monopole generates a magnetic field $\boldsymbol{B} = g\boldsymbol{r}/r^3$. The problem has the following three invariants of motion [82C6].

a) *The kinetic energy*, which is that of the electron

$$T = T_e = \tfrac{1}{2} m_e \dot{r}_e^2 . \tag{2.21}$$

b) *The total angular momentum*, which is the sum of the mechanical and electromagnetic parts

$$\boldsymbol{J} = \boldsymbol{J}_{\text{mech}} + \boldsymbol{J}_{\text{e.m.}} . \tag{2.22}$$

The orbital and the electromagnetic parts of the angular momentum are given by

$$\boldsymbol{J}_{\text{mech}} = \boldsymbol{r}_e \times m_e \dot{\boldsymbol{r}}_e , \tag{2.23}$$

$$\boldsymbol{J}_{\text{e.m.}} = \frac{1}{4\pi c} \int \boldsymbol{r} \times (\boldsymbol{E} \times \boldsymbol{B})\, \mathrm{d}^3 r , \tag{2.24}$$

where $\boldsymbol{E}\times\boldsymbol{B}/4\pi c$ is the electromagnetic momentum density at the point p of position vector $\boldsymbol{r}$, where the fields $\boldsymbol{E}$, $\boldsymbol{B}$ are

$$\boldsymbol{E}=e\,\frac{\boldsymbol{r}-\boldsymbol{r}_e}{|\boldsymbol{r}-\boldsymbol{r}_e|^3}\,,\qquad \boldsymbol{B}=g\,\frac{\boldsymbol{r}}{|\boldsymbol{r}|^3}\,. \tag{2.25}$$

The integration of (2.24) yields ($\hat{r}=\boldsymbol{r}/r$)

$$\boldsymbol{J}_{\text{e.m.}}=\frac{-eg}{c}\,\hat{r}_e\,. \tag{2.26}$$

Therefore,

$$\boldsymbol{J}=\boldsymbol{r}_e\times m_e\dot{\boldsymbol{r}}_e-\frac{eg}{c}\,\hat{r}_e\,. \tag{2.27}$$

c) *Also the radial component of* $\boldsymbol{J}$ *is conserved*

$$J_r=\hat{r}_e\cdot\boldsymbol{J}=-\frac{eg}{c}\,. \tag{2.28}$$

Since both $\boldsymbol{J}$ and J_r are constant in time, also the angle θ_e between $\hat{r}_e$ and $\boldsymbol{J}$ remains constant in time. This means that the electron moves in a conical surface, which has the apex at the monopole position and its axis along the $-\boldsymbol{J}$ direction (fig. 2.1*b*)). The semi-angle θ_e of the cone is

$$\theta_e=\arccos\frac{J_r}{J}=\arccos\frac{eg}{cJ}\,. \tag{2.29}$$

The charges e and g behave as if repelled by one another. Notice the presence of the «field» angular momentum (2.26). If we try to pass an electron through the pole, this field angular momentum suddendly changes sign at the pole position. This problem will be considered again in subsect. **2˙3.6**.

So far our discussion of the electron-monopole system has been done in the context of electromagnetic theory, neglecting spins and radiation effects.

2˙3. *The Dirac quantization condition and the Dirac monopole.*

2˙3.1. The Dirac quantization. In his 1931 paper DIRAC observed that magnetic monopoles can be incorporated into quantum mechanics only if the electric and magnetic charges are quantized. This can be proven in a simple way considering the component of the angular momentum along the $\boldsymbol{r}_e$ direction in the problem of the system made of an electric charge and a magnetic charge analysed classically in the previous subsect. **2˙2**. The quantization condition for the component of the angular momentum (2.28) yields $J_r=\hbar n/2$, that is

$$\frac{eg}{c} = \frac{1}{2}\hbar n, \tag{2.30}$$

where n is an integer. This is the Dirac relation obtained as a consequence of angular-momentum quantization. This is not the original derivation of Dirac. It is also a naive derivation because the quantization condition written is valid only for a Cartesian component and if one neglects spin. Nevertheless, it can be proven that the conclusion is correct and that Dirac's quantization condition is intimately related to the quantization of angular momentum [82C6].

DIRAC emphasized that the mere existence of a single monopole somewhere in the Universe would imply that all electric charges be quantized with the basic electric unit equal to $e = \hbar c/2g$. He proposed that the observed quantization of the electric charge be explained in this way. Conversely, all magnetic charges should be integral multiples of a basic minimal magnetic charge

$$g_D = \frac{\hbar c}{2e} = \frac{e}{2\alpha} = 68.5e, \tag{2.31}$$

where α is the fine-structure constant and e is the basic electric charge, which we assume to be the electron charge. If free quarks with charge $e/3$ exist, then one would expect that the basic magnetic charge be three times larger.

2.3.2. The magnetic-coupling constant. The basic magnetic charge is much larger than the basic electric charge. Thus the introduction of magnetic poles has introduced a formal symmetry in Maxwell's equation, but there is a numerical asymmetry between magnetic and electric effects. The dimensionless magnetic constant (which may be introduced in analogy with the fine-structure constant $\alpha = e^2/\hbar c = 1/137$) is $\alpha_m = g^2/\hbar c = 34.25$. This is a large coupling constant; therefore, the electromagnetic interactions of monopoles are too strong for perturbative theory to be applicable. For example, the elastic scattering of an electron by a magnetic monopole cannot be described by the exchange of a single photon, but one should also consider the exchange of many photons. This is because $\alpha_m\alpha = O(1)$, while in ee scattering one has $\alpha^2 \simeq O(10^{-4})$. In fact, a single Feynman graph for monopole interaction violates some fundamental principles, like unitarity and Lorentz invariance, which can be restored only at a nonperturbative level.

2.3.3. The mass of the Dirac monopole. In the Dirac formulation of the magnetic monopoles there is no prediction for the monopole mass. A kind of rule of thumb was established, assuming that the classical electron radius be equal to the «classical» monopole radius

$$r_e = \frac{e^2}{m_e c^2} = r_M = \frac{g^2}{m_M c^2}, \tag{2.32}$$

from which one has $m_M = m_e g^2/e^2 = 4700 m_e = 2.4$ GeV. The mass of the monopole is expected to be much larger than the mass of the electron because the basic magnetic charge is much larger than the basic electric charge.

2.3.4. The electromagnetic vector potential and the Dirac string. The usual theoretical treatment of the electromagnetic fields is in terms of vector and scalar potentials $(\boldsymbol{A}, i\varphi) = A_\mu$ such that $\boldsymbol{B} = \text{rot}\,\boldsymbol{A}$ and $\boldsymbol{E} = -\text{grad}\,\varphi$. $\boldsymbol{A}$ and φ are determined by $\boldsymbol{B}$ and $\boldsymbol{E}$ up to a group of gauge transformations

$$\boldsymbol{A} \Rightarrow \boldsymbol{A}' = \boldsymbol{A} + \nabla\chi, \qquad \varphi \Rightarrow \varphi' = \varphi - \partial\chi/\partial t, \tag{2.33}$$

where χ is any smooth function of space and time. The field produced by a magnetic pole can be described in this way only if A_μ is allowed to be singular along an arbitrary line (a string) which starts at the pole and goes to infinity (fig. 2.2). This is clearly an unphysical feature, since the singularity in A_μ

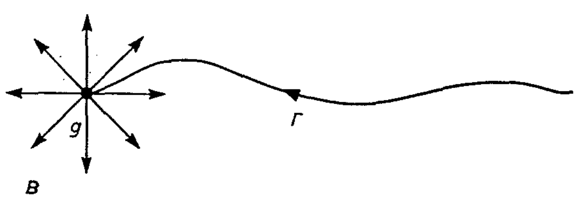

Fig. 2.2. – Illustration of the field produced by a point magnetic pole and of the string which one finds with the use of the vector potential [82C6].

does not correspond to a singularity in the electromagnetic fields. In particular, since the space around a monopole is spherically symmetric and without singularity, the wave function of an electron around the monopole should have no singularity. One can thus require that the string be undetectable by any conceivable method, in particular, by the Aharonov-Bohm effect [59A1].

Let us see how this last requirement leads to the Dirac quantization condition. For this purpose we consider an infinitely long and very thin solenoid. At one end of it there appears to be a magnetic pole with charge g, which produces by Gauss theorem a magnetic flux $\Phi_B = 4\pi g$. Let us now analyse the Aharonov-Bohm effect around the thin solenoid, as illustrated in fig. 2.3. Charged particles emitted by the source A pass through the two slits in the screen B and are detected at C. Without the solenoid S the amplitudes for the passage through the individual slits combine coherently and the probabil density at C is given by $P = |\psi_1 + \psi_2|^2$, where ψ_1 is the probability for pass through the first slit and ψ_2 is that for the passage through the second o

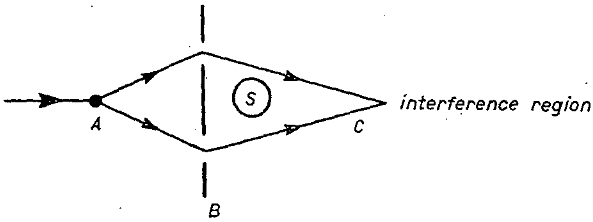

Fig. 2.3. – Illustration of the Aharonov-Bohm experiment.

If the solenoid S is placed between the two slits, the probability density C becomes

$$P' = |\psi_1 + \exp[ie\Phi_B/\hbar c]\psi_2|^2 , \tag{2.34}$$

where e is the charge of the particles emitted in A and Φ_B is the magneti flux through the solenoid. By moving the solenoid and observing the chang in the interference pattern one could detect the presence of the solenoid, unles $\exp[ie\Phi_B/\hbar c] = 1$, which requires $e\Phi_B/\hbar c = 2\pi n$ and thus $eg = \hbar cn/2$, whicl is the Dirac relation.

Many ways of eliminating altogether the string have been discussed b several authors. Wu and Yang [76W1] defined one vector potential A_μ ir one region of space free of monopoles and of strings, and a second vector po- tential A'_μ in a second region, again free of poles and of strings. Thus eithei potential has no singularity in its region of definition. Then, one must make sure that the two vector potentials describe the same physics in the overlap regions, which means that A'_μ should be a gauge transformation of A_μ. Again this condition leads to Dirac's relation.

Cabibbo and Ferrari [62C1] built a quantized theory for the interactions of monopoles and charged particles with the electromagnetic fields, without making use of potentials. Monopoles and charged particles are treated in a symmetrical way and the internal consistency of the theory requires the usual Dirac condition.

2'3.5. Parity conservation and charge conjugation invariance. In the above formulation of the monopole theory the parity P and the conjuga- tion of the electric charge C are not conserved. This is not surprising, since, for instance, a pole is accelerated in the direction of a magnetic field. One may, however, find new symmetries by multiplying P and C by M (M is an operator which changes the magnetic charge) so that $P' = PM$ and $C' = CM$ are conserved. In processes in which monopoles are not present as physical particles, P' and C' are equivalent to the usual operators P and C and no parity or C violation is expected. Thus the existence of monopoles would not contradict the observed P and C conservation in ordinary electromagnetic processes.

2'3.6. Problems with the electron-monopole system. In the semi-classical discussion of subsect. 2'2 it was mentioned that, if an electron passes through a pole, the field angular momentum suddenly changes sign at the pole position. Thus this part of the angular momentum is undefined when the electron and the pole are one on top of the other. In quantum mechanics the difficulty translates into difficulties at the origin of the angular and radial wave functions of the charged particle.

Another peculiar situation arises in a possible bound state of a spinless point magnetic charge with a spinless point electric charge. The total angular momentum for this system may be half-integer because there is an half-integral angular-momentum contribution from the electromagnetic field. Therefore, the composite system has an angular momentum which is not an integral multiple of $\hbar$. Thus, accepting the connection between spin and statistics, the composite system is fermionic and it has been constructed with two bosons. This paradox was given subtle explanations by different authors, who reached the conclusion that the usual connection between spin and statistics remains valid (see, for instance, [76G1]).

2'3.7. Quantum formulation. Quantum electrodynamics for Dirac monopoles was given a complete Hamiltonian formulation by SCHWINGER [66S1-66S3]. He argued that the n-value in the Dirac relation should be restricted to even values. However, most authors do not accept this conclusion since the Aharonov-Bohm effect disappears also for n odd and because there exist 't Hooft-Polyakov monopole solutions with n odd.

It is believed that there is no problem with renormalization and that the same factor renormalizes the electric and the magnetic charge. The Dirac quantization condition should apply to renormalized charges.

A consequence of the quantization of the electric charge is that the group of possible gauge transformations at any given point is a compact group U_1, the group of complex numbers of unit modulus or equivalently of displacements round a circle. The action of a gauge transformation on a wave function is to multiply it by a phase factor $\exp[-iq\chi] = \exp[-iq_0\chi/\hbar]^n$, where $q = nq_0$, n is an integer and q_0 is the basic unit of electric charge. One can think of the factor $\exp[-iq_0\chi/\hbar]$ as the basic gauge transformation. In the Dirac-Yang reasoning the existence of a magnetic monopole brings in charge quantization, from which the compactness of the gauge group follows.

2.4. *Gauge monopoles.*

2.4.1. Monopoles in non-Abelian gauge theories. In 1974 'T HOOFT [74H1] and POLYAKOV [74P2] showed that magnetic monopoles appear as stable solutions of the spontaneously broken Yang-Mills field equations and were required by a large class of theories. Non-Abelian gauge theories have general applications in elementary-particle physics. In particular, the present view on electromagnetism is that it is part of a larger non-Abelian gauge theory characterized by a simple gauge group G, that is a group which has only one coupling constant. G is equipped with a suitable Higgs mechanism, which makes the group to spontaneously break down in subgroups. The assumption that the electromagnetic group U_1 is a subgroup of a larger simple group leads to the conclusion that charge quantization is a consequence of having the group G compact. Since the quantization of the electric charge is already contained in the theory, there is no need to postulate separately the existence of a monopole. Rather one should look if the non-Abelian theory contains magnetic monopoles. As already stated, this was proved by 'T HOOFT and POLYAKOV. The qualitative argument of 't Hooft will be recalled.

Let us consider a sphere with a magnetic flux Φ_B entering at one spot (fig. 2.4). Immediately around the spot, on the circular contour C_0, we must have a magnetic vector potential $\boldsymbol{A}$, with $\oint \boldsymbol{A}\cdot d\boldsymbol{r} = \Phi_B$. The potential may

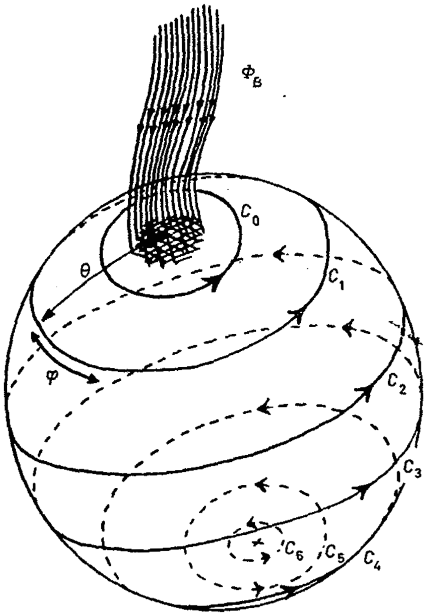

Fig. 2.4. – The circular contours C on a sphere surrounding a magnetic monopole. One deplaces the contour from C_0 to C_1, C_2 etc., until it shrinks at the bottom of the sphere. The requirement is that there be no singularity at that point [74H1].

be obtained from the vacuum by applying a gauge transformation Λ, $\boldsymbol{A} = \nabla\Lambda$, where Λ is multivalued. Now we require that all fields, which transform according to $\psi \to \psi \exp[ni\Lambda]$, remain single valued. This leads to the conclusion that Φ_B must be an integer times 2π and we have a complete gauge rotation along the C_0 contour of fig. 2.4. In an Abelian gauge theory we must necessarily have some other spot on the sphere where the flux lines come out, because the rotation over $2\pi n$ cannot continuously change into a constant value, while we lower the contour C from C_0 to C_1, etc. over the sphere. In a non-Abelian theory with compact covering group, a rotation over 2π may be shifted towards a constant, without any singularity. Thus we may have vacuum all around the sphere with no other lines of force: this leads to the conclusion that a magnetic monopole lies inside the sphere. Notice that there is no singularity anywhere in the sphere, nor is there the need for a Dirac string.

For the explicit proof of the existence of magnetic monopoles in most non-Abelian theories we remind to the original papers [74H1], [74P2] and other specialized papers [82C6].

2.4.2. The «golden triangle». We have discussed some specific connections between charge quantization, spontaneously broken non-Abelian theories and magnetic monopoles. Each of these three concepts suggests the other two. Goldhaber [82G3] pointed out that one is tempted to view the trio as three aspects of a single phenomenon and he called the links between them the «golden triangle» (fig. 2.5). He concluded that it would appear that, unless some additional fundamental effect bars the appearance of isolated monopoles, it becomes a detailed question about the evolution of our Universe whether monopoles are present today. It is very likely that monopoles form part of the fabric of fundamental microphysics, whatever the answer to the observational question.

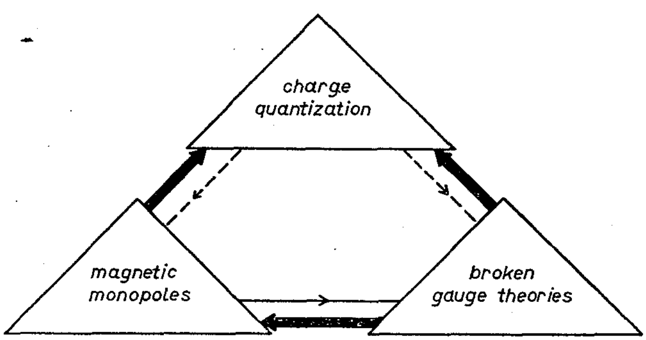

Fig. 2.5. – The «golden triangle». Each directed line indicates the strength of logical connection between two vertices. Charge quantization follows either from monopoles or spontaneously broken non-Abelian gauge theories. The existence of monopoles as stable classical field configurations has been demonstrated for broken gauge theories [82G3].

2.4.3. Size and mass of gauge monopoles. The Dirac and gauge monopoles differ in their internal structure. The Dirac monopole has a point singularity for which a source has to be put in by hand, while the gauge monopole has a smooth internal structure, satisfying the gauge theory equations of the group G without any need of external sources. The size of the gauge monopole is determined by the Compton wave-length of the massive particle associated with the unified field, $r_c \simeq \hbar/m_X$. Inside this radius the massive fields play a role in providing a smooth structure, which rapidly vanishes outside, with an exponential dependence. For $r \gg r_c$ the configuration is indistinguishable from that of the Dirac monopole.

An important feature of a monopole solution with a smooth internal structure is that its mass is calculable, in contrast to the Dirac monopole where it is not. The mass is given by the energy of the minimizing configuration. BOGOMOLNY established a lower bound for the monopole mass, $m_M \geqslant \nu m/\alpha$, where m is the mass of the heavy vector boson, $\alpha = 1/137$ is the fine-structure constant and $\nu = 1$ or $1/4$. In practice we can take the lower bound as a good estimate of the mass.

Specializing to GUT monopoles, we have $m = m_X \simeq 10^{15}$ GeV, $\alpha \to$ unified coupling constant $\simeq 1/40$, $\nu = 1$ (not everybody agrees with this statement, leaving $\alpha \simeq 1/137$) and, therefore, $m_M \geqslant 10^{16}$ GeV. Lower and higher bounds for the mass of the SU_5 monopole have been quoted [83S2, 80S1]: $m = 3m_X/8\alpha = 5 \cdot 10^{16}$ GeV, $m \leqslant m_M < 1.8m$, that is $5 \cdot 10^{16} \leqslant m_M < 9 \cdot 10^{16}$ GeV.

2.4.4. Magnetic charge as a topological number. It can be shown that a small variation in the Higgs field Φ yields no change in the magnetic flux on a closed surface σ, where the flux is produced by one (or more) monopole, and, therefore, no change in the value of the magnetic charge g. This result can be extended to any change in Φ which can be built up by small continous deformations. It means that one can map a closed surface σ in the three-dimensional $\boldsymbol{r}$-space into the sphere $|\Phi| = a$ in Higgs space (fig. 2.6). In topology, such a deformation in Φ is called a homotopy. Mappings which are homotopic (which, therefore, are related to each other by a continuous deformation) have the same value of the topological number N. Monopoles are

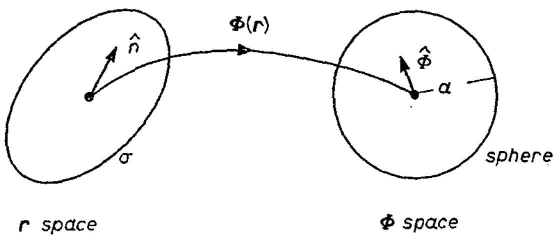

Fig. 2.6. – Mapping from the closed surface σ in three-dimensional $\boldsymbol{r}$-space into the sphere of vacuum solutions for the Higgs field Φ.

classified in the $\pi_2(M_{\mathrm{vac}})$ class, where M_{vac} is the manifold of vacuum solutions for the Higgs field; the subscript 2 in $\pi_2(M_{\mathrm{vac}})$ refers to $N=2$, which corresponds to the number of tangents, which are 2 in a sphere in Φ-space.

In the context of monopoles, examples of homotopies are i) the time development of Φ, ii) the change in Φ under a continuous gauge transformation and iii) the change induced by altering the closed surface σ continuously. As a consequence the magnetic flux (and then the magnetic charge g) is time independent, gauge invariant and unchanged under any continuous deformation of the surface σ containing the monopole or monopoles.

It can be shown that the magnetic charge is an additive quantum number and that it is conserved quantum mechanically as well as classically.

2'4.5. GUT monopoles. The Weinberg-Salam theory of electroweak interactions is described by $SU_{2,\mathrm{L}}\times U_{1,\mathrm{R}}$; this is not a simple group. Therefore, one cannot apply the reasonings of the previous sections and the theory should not contain magnetic monopoles. Thus one should investigate higher unification schemes. The grand unified theories (GUT) of strong, electromagnetic and weak interactions are possibly described by a simple gauge group G_{GUT}. The unification is based on the hypothesis that at sufficiently high energies there is no difference between strong and electroweak forces. This is expected to happen when the energy of each particle is larger than 10^{15} GeV. At lower energies the symmetry should spontaneously break down, the forces are different and the original simple group G_{GUT} breaks down into three subgroups, like those described by (1.2). Examples of G_{GUT} are SU_5, SO_{10}, etc.

At present energies the different coupling constants are vastly different, with $\alpha_{\mathrm{strong}}\gg\alpha_{\mathrm{e.m.}}\neq\alpha_{\mathrm{W}}$. They are expected to vary logarithmically with energy and, if no new physics intervenes in the $(10^2\div10^{15})$ GeV region (the « desert »), they should become comparable at energies of the order of 10^{15} GeV. Figure 2.7 illustrates this situation.

When a large gauge group breaks down, there may be several energy scales corresponding to intermediate stages of breaking. Let us consider, for example, the following chain of breakings:

$$SO_{10}\to SU_5\to SU_{3,\mathrm{colour}}\times SU_{2,\mathrm{L}}\times U_{1,\mathrm{R}}\to SU_{3,\mathrm{colour}}\times U_{1,\mathrm{e.m.}}\,. \tag{2.35}$$

The monopole mass is determined by the mass m acquired by the heavy vector gauge bosons as a result of the first breakdown into subgroups with a U_1 factor, which eventually becomes $U_{1,\mathrm{e.m.}}$. (The precise correspondence with Maxwell's electrodynamic theory should hold only in the Higgs vacuum.) Thus in the chain (2.35) the relevant mass is that acquired by SU_5 bosons as a result of SU_5 breaking down to $SU_{3,\mathrm{colour}}\times SU_{2,\mathrm{L}}\times U_{1,\mathrm{R}}$. If the U_1 factor

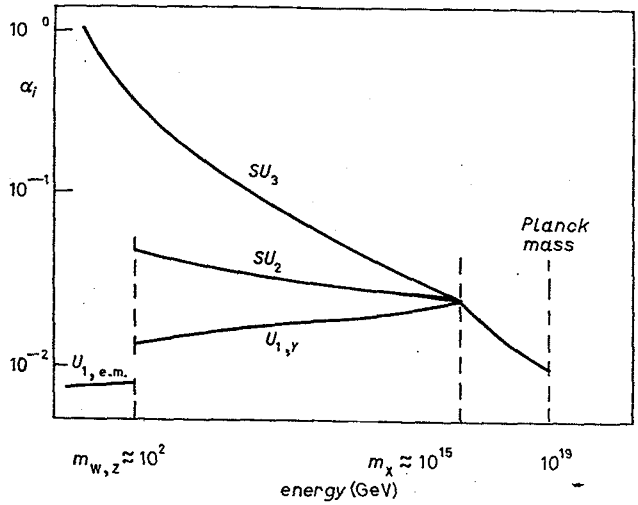

Fig. 2.7. – Qualitative picture of the evolution of the SU_3, SU_2 and U_1 couplings in a grand unified theory such as SU_5: they come together at an energy $m_X \sim 10^{15}$ GeV if the « desert » region between 10^2 and 10^{15} GeV is not populated with particles.

would appear earlier in the chain, the monopole mass would be larger; if it would appear (for the first time) later, the monopole mass would be lighter.

In cosmology, physical GUT monopoles should have appeared at the energy at which the GUT unification stopped, that is at temperatures of $\sim 10^{15}$ GeV. As the temperature became lower than those corresponding to the unified phase, a phase transition should have occurred. The breaking of the symmetry freezed in certain space domains. A GUT monopole can be viewed as the coalescence of these domains to form the magnetic-field distribution of a magnetic monopole, as shown in fig. 2.8.

The sequence of transitions illustrated in (2.35) requires many Higgs fields. Moreover, the final unbroken groups in the sequence are $SU_{3,\text{colour}} U_{1,\text{e.m.}}$: this means that one has to consider the influence of colour. One finds that the Dirac

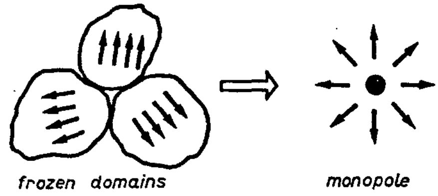

Fig. 2.8. – At $t = 10^{-35}$ s after the « big bang », at the temperature $T \simeq 10^{15}$ GeV, there was the phase transition corresponding to the end of the grand-unification era of strong and electroweak interactions. At that time Higgs fields in causally separated domain directions caused a GUT monopole to be formed where they met.

relation is still valid when monopoles and electric charges of colour singlet particles are involved. For coloured charged particles one would have a modified Dirac relation containing for the electric charge the quantity $q = q_0(K + t_{\text{coul}}/3)$, where K is an integer and $t_{\text{coul}} = 1, 2, 3$ for the three possible cases. This condition could be applied to quarks with charges 1/3 and 2/3, but they would have to be free entities, with only long-range electromagnetic interactions. The connections between magnetic monopoles, fractional charges and confinement have been discussed many times, with various subtle differences [78G2].

It is highly probable that a GUT monopole has a confined colour magnetic charge: for distances smaller than 1 fm we have to consider its effects, which may instead be neglected outside the confinement region.

2·4.6. Quantum formulation. It has to be remarked that the theory of 't Hooft-Polyakov monopoles assumes the validity of semi-classical methods. In particular, it hypothesizes that all quantum fluctuations are small and local. Otherwise, concepts like topological number become irrelevant and the arguments to prove the necessity of monopole existence could not be carried through. As was already stated in the previous section, a complete quantum field theory of Dirac monopoles was discussed several years ago [66S1]. The non-Abelian monopole has an internal structure and a large mass. This requires new analyses of the quantum theory, in particular of the problem of renormalization. Wu and Yang [75W1, 76W1] formulated their approach to the Dirac monopole and then generalized it to the case of a non-Abelian group. In their formulation there is no Higgs field and the monopole is described by a nontrivial fibre bundle with a certain structural group.

2·4.7. Dyons. A dyon is defined as a particle which carries both electric and magnetic charge. Therefore, when at rest, it produces both an electrostatic and a magnetostatic field $\boldsymbol{E} = e\boldsymbol{r}/r^3$, $\boldsymbol{B} = g\boldsymbol{r}/r^3$. For the case of «classical» dyons one may proceed as for «classical» monopoles. We may consider in fig. 2.1 two dyons, one with charges e_1, g_1 and the other with e_2, g_2. The electromagnetic component of the angular momentum is

$$\boldsymbol{J}_{\text{e.m.}} = \int \boldsymbol{r} \times (\boldsymbol{E} \times \boldsymbol{B})\, \mathrm{d}\boldsymbol{r} = -(e_1 g_2 - e_2 g_1)\hat{\boldsymbol{r}} \tag{2.36}$$

and the Dirac quantization condition becomes

$$e_1 g_2 - e_2 g_1 = \frac{\hbar c}{2} n\,. \tag{2.37}$$

If one of the dyons is an ordinary particle with an electric charge e_1, and with $g_1 = 0$, then eq. (2.37) requires that both e_1 and g_2 be quantized as in Dirac's original formulation; but the value of e_2 is not constrained. Semi-classical arguments were used to argue that in a proper quantum-mechanica treatment the dyon charge must be quantized. For instance, if CP is an in variant, then for a dyon (e, g) there must be also a CP conjugate dyon $(-e, g)$ Applying to both dyons relation (2.37) yields the Dirac relation (1.1). Thus if g has the minimal g_D value, then the dyon electric charge is quantized and equal to the minimal electric charge (or twice).

Also 't Hooft-Polyakov dyons satisfy relation (2.37). Quantum fluctuations lead to a quantized electric charge of the dyon, in integral multiples of the minimal electric charge.

Most arguments made for monopoles may be readily extended to dyons. Some gauge models, like SU_5, predict the existence of both monopoles and dyons [80D1]. Dyons should be heavier than electrically neutral monopoles. Consequently, dyons could decay

$$M^{\pm} \to M^0 + e^{\pm} + \text{anything}. \tag{2.38}$$

2'4.8. Monopolonium. An interesting and exotic object is «monopolonium», a pole-antipole system analogous to e^-e^+ positronium. Monopolonium made of GUT poles has some amazing properties, arising from the extremely large pole mass [83H3]. It is a classical system, which decays by classical Larmor radiation for all, but the last fraction of a second of its life.

If the monopole and the antimonopole are in a circular orbit about their c.m., one must have $\overline{m}\omega^2 r = g^2/r^2$, where $\overline{m} = m_M/2$ is the reduced mass of the system. The energy is given by

$$E = \tfrac{1}{2}\overline{m}\omega^2 r^2 - g^2/r = -\tfrac{1}{2}g^2/r. \tag{2.39}$$

The system will lose energy by dipole radiation, with a formula analogous to that for electric charges

$$\frac{dE}{dt} = -2\frac{2}{3}g^2a^2/c^3 = -\frac{64}{3}E^4/g^2m_M^2c^3. \tag{2.40}$$

Integrating (2.40) from the time of formation ($t = t_0$, $r = r_0$) to the final time, one has

$$\tau = t_f - t_0 \simeq m_M^2c^3r_0^3/8g^4. \tag{2.41}$$

Thus the lifetime of the state is determined by the cubic power of the initial radius r_0. The decay of the system may be viewed quantum mechanically as a cascade of jumps through sequentially decreasing principal quantum numbers. The energy of each state is $E = -g^2/2r = -R_m/n^2$, where R_m is the magnetic Rydberg constant $R_m = \overline{m}g^4/2\hbar = 293\,m_M$ (GeV). The instantaneous transition energy is

$$\Delta E = R_m \left[\frac{1}{n^2} - \frac{1}{(n+1)^2}\right]. \tag{2.42}$$

Table I gives the lifetime, the binding and the transition energies, the principal quantum number n and the $\beta = v/c$ of the monopoles in monopolonium. The

TABLE I. – *Monopolonium properties* [83H3].

Classical diameter (cm)	Lifetime (s)	Binding energy (GeV)	Transition energy (eV)	Principal quantum number	$\beta = v/c$
10^{-8}	$3.7 \cdot 10^{22}$	$3.3 \cdot 10^{-5}$	$1.6 \cdot 10^{-7}$	$4.2 \cdot 10^{11}$	$4.1 \cdot 10^{-11}$
10^{-10}	$3.7 \cdot 10^{15}$	$3.3 \cdot 10^{-3}$	$1.6 \cdot 10^{-4}$	$4.2 \cdot 10^{10}$	$4.1 \cdot 10^{-10}$
10^{-13}	$3.7 \cdot 10^{6}$	3.3	5.1	$1.32 \cdot 10^{9}$	$1.3 \cdot 10^{-8}$
10^{-15}	3.7	$3.3 \cdot 10^{2}$	$5.1 \cdot 10^{3}$	$1.32 \cdot 10^{8}$	$1.3 \cdot 10^{-7}$
10^{-18}	$3.7 \cdot 10^{-9}$	$3.3 \cdot 10^{5}$	$1.6 \cdot 10^{8}$	$4.2 \cdot 10^{6}$	$4.1 \cdot 10^{-6}$
10^{-20}	$3.7 \cdot 10^{-15}$	$3.3 \cdot 10^{7}$	$1.6 \cdot 10^{11}$	$4.2 \cdot 10^{5}$	$4.1 \cdot 10^{-5}$
10^{-28}	$3.7 \cdot 10^{-39}$	$3.3 \cdot 10^{15}$	$1.6 \cdot 10^{23}$	$4.2 \cdot 10^{1}$	$4.1 \cdot 10^{-1}$

values were computed by assuming $m_M = 2 \cdot 10^{16}$ GeV and a constant magnetic-coupling constant $\alpha_m = 34.25$ (it should increase to a value of about 40 at the GUT unification energy). The lifetime of monopolonium is 43 d if $r_0 = 10^{-13}$ cm, while $\tau = 10^{11}$ y if $r_0 = 0.1$ Å! This means that monopoloniums formed in the early Universe may have survived until our days.

For transition energies smaller than the pion mass (corresponding to $r > 10^{-18}$ cm) the $M\bar{M}$ system emits photons with an energy spectrum which corresponds first to radiowaves, then in succession to light, X-rays and γ-rays. Radiowaves are emitted for most of the lifetime of monopolonium.

For $r < 10^{-18}$ cm, when the remaining lifetime is only 10^{-9} s, the system radiates photons and gluons. For $r < 10^{-20}$ cm the Z^0 threshold opens up and as many as 10^5 Z^0 may be emitted. Finally, when $r \sim 10^{-28}$ cm $= 1/m_X$, $n = 40$ and $\beta = v/c \to 1$, the two pole cores start to overlap. The system has still $\sim 75\,\%$ of the total energy, which is suddenly released in a very short burst of less than 10^{-38} s, producing ~ 24 heavy particles (12 X, Y bosons, 6 gluons, 2 Z^0, $W^{\pm}$ and 4 Higgs particles), which give rise to roughly 10 leptons, 30 quarks and 6 gluons. The hadron jets, which then follow, should yield approximately 10^7 hadrons. In this last spectacular burst all the particle physics for energies up to the GUT unification energy should be contained!

The binding energy of monopolonia with sizes between 1/10 and 1 Å range from 340 MeV to 3.4 keV. These are the relevant temperatures for $M\bar{M}$ formation and correspond to the Universe age between 10 and 10^4 s, which is the epoch of helium synthesis. The mechanism of monopolonium formation could have been the following: collisions between relatively cool poles and antipoles resulted in loosely bound monopolonia systems by the emission of radiation These states corresponded only to thermal fluctuations, but since the Universe was cooling down, the binding energy exceeded quickly the thermal energy available to dissociate them. The number of monopolonia produced could be $\sim 10^{-18}$ of the number of available monopoles, $n_{M\bar{M}}/n_M \sim 10^{-18}$. Assuming an original monopole density equal to the density required to close the Universe, HILL estimated [83H3] that in a typical cubic light-year one could now have ~ 300 $M\bar{M}$ annihilations per year, leading to radiation at a wave-length of 1 cm with a flux of the order of 10^{-24} eV/cm² s Hz. Current observational limits are at a level of 10^8 times larger (~ 50 microjanski). In general the prospects for monopolonium observation seem to be very small.

The above discussion concerns monopoles without electric charge. The analysis of dyon-dyon states leads to similar results [71B1].

2'5. *Other possibilities.* – From the above discussion we conclude that GUT theories predict the existence of superheavy poles, which carry magnetic charge as well as confined colour magnetic charge. But other possibilities may exist; in particular, one has to investigate more thoroughly the implications of supersymmetric (SUSY) GUT's, of quark and lepton substructures (preons), of unification with gravity as well as the implications of intermediate mass scales. The unification with gravity is often discussed in the context of Kaluza-Klein theories, which define a space-time of dimensions higher than four. In these theories the natural mass scale for magnetic monopoles is the Planck mass, $m_M \sim m_{Pl} \sim 10^{19}$ GeV [83P4].

BARTLETT *et al.* [72B1, 78B1] conjectured that monopoles could be tachyons, that is faster-than-light particles [75M1, 77P1]. LONDON introduced Z_n poles (a Z_2 monopole is its own antimonopole). Such monopoles could arise in successive steps of SO_{10} breakings [83W2]. Models of hadrons in which quarks possess both electric and magnetic charges (dyons) have been discussed. Some authors identified colour with the magnetic charge [79S1].

3. – Interactions of magnetic monopoles with matter.

3'1. *Introduction.* – The study of the interactions of magnetic monopoles in matter is important in order to understand i) the formation of bound systems of monopoles and atomic nuclei and ii) the energy loss of monopoles in matter in general and in particle detectors in particular.

The relatively long-range interaction of the monopole magnetic charge with the nuclear magnetic dipole leads to the formation of bound systems, with binding energies in the range $(1 \div 100)$ keV and with typical linear sizes of the order of 10 fm. Since the scales of these systems are approximately the same as those of mesic atoms, the name «monopolic atoms» has been used in the literature [83B1]. Furthermore, monopoles and atomic nuclei may be bound together by electrons, in a way similar to the chemical binding of molecules. For these systems the typical linear size is of the order of 1 Å and the binding energy is of the order of 1 eV. These systems may be referred to as « monopolic molecules ». The formation of monopolic atoms and molecules may affect the energy loss in matter and the cross-section for the monopole catalysis of proton decay [83B5].

There is considerable interest in determing the rate at which monopoles lose energy in various astrophysical objects, such as the Earth and the stars, in order to establish the likelihood of primordial monopoles being trapped in these objects. There is an even greater interest in the question of whether the quantity and quality of energy lost by magnetic monopoles in particle detectors is adequate for monopole detection. For classical monopoles their mass should be sufficiently small so that acceleration of the monopoles by magnetic fields to relativistic velocities is practically inevitable. For such velocities the monopole energy loss is $(g/e)^2 \simeq 4700$ times the energy loss of a minimum ionizing electric charge. Thus the energy loss of a classical monopole would be enormous, more than enough to enable them to be easily detected with almost any kind of particle detectors. Furthermore, the energy loss would be large enough to stop a considerable fraction of monopoles in the Earth, so that searches for monopoles trapped in Earth matter would be particularly meaningful. Instead GUT monopoles have such large masses that it is difficult to accelerate them to large velocities. The study of the energy loss of slow moving monopoles becomes thus of great practical interest.

3'2. *The magnetic-monopole–magnetic-dipole interaction.* – The long-range interaction of a magnetic monopole with a fermion is due to the « magnetostatic » interaction between the pole magnetic charge and the magnetic-dipole moment of the fermion, including its anomalous part [77K1, 83B1].

Let us consider again the problem of the interaction of a point magnetic charge with a point electron, as in fig. 2.1*a*). But, now, the electron has spin $s_e = 1/2$ and magnetic moment $\mu_e = -e\hbar/2m_e c$. At the point r_e, where one has a magnetic field $B = g/r^2 = \hbar c/2er^2$, the electron feels the Lorentz force $|\boldsymbol{F}_L| = v\hbar/2r_e^2$ and the additional force

$$|\boldsymbol{F}_D| = |-\nabla(\boldsymbol{\mu}_e \cdot \boldsymbol{B})| = \frac{\hbar^2}{2m_e r_e^3}. \tag{3.1}$$

The ratio of the two forces is

$$\frac{F_L}{F_D} = \frac{v m_e r_e}{\hbar} = \frac{v}{\alpha c}\frac{r_e}{a_0}, \tag{3.2}$$

where $a_0 = 0.53$ Å is the first Bohr radius. For small velocities ($v < \alpha c$) and/or small distances ($r_e < a_0$) the force F_D arising from the coupling between the monopole magnetic charge and the electron dipole magnetic moment is domir over the Lorentz force. The situation is opposite to that encountered in dinary atomic physics, where spin coupling provides fine and hyperfine stı tures, negligible in first approximation.

The interaction energy arising from the magnetic-charge–magnetic-dir interaction is given by

$$W_{\mathrm{D}} = -\boldsymbol{\mu}_{\mathrm{e}}\cdot\boldsymbol{B} = \hbar^2/4m_{\mathrm{e}}r_{\mathrm{e}}^2 . \tag{3.3}$$

The dipole energy (3.3) for an electron at $r_{\mathrm{e}} = a_0$ is $W_{\mathrm{D}} \simeq 7$ eV, which comparable to the binding energy of an atom; thus one expects a sizat deformation of an atomic system when a monopole passes inside or close an atom.

For a proton ($\mu_{\mathrm{p}} \simeq 2.8\, e\hbar/2m_{\mathrm{p}}c$) at a distance $r = 1$ fm from the mon pole one has $W_{\mathrm{D}} \simeq 2.8\hbar^2/2m_{\mathrm{p}}r^2 \simeq 29$ MeV, a value larger than the bindin energy of nucleons in nuclei; thus one expects deformations of the nucleu when a monopole passes close to it.

3'3. *Monopolic atoms.* – For a nucleus with spin $\boldsymbol{s}_{\mathrm{A}}$ and magnetic momen $\boldsymbol{\mu}_{\mathrm{A}} = (e\hbar/2m_{\mathrm{A}}c)K\boldsymbol{s}_{\mathrm{A}}$, where $K \simeq A$ is the gyromagnetic factor, the dipole Hamiltonian $W_{\mathrm{D}} = -\boldsymbol{\mu}_{\mathrm{A}}\cdot\boldsymbol{B}$ is attractive for a suitable spin orientation. One can have monopole-nucleus bound states if the total Hamiltonian, inclusive of the centrifugal barrier part (W_{C}),

$$W_{\mathrm{tot}} = W_{\mathrm{D}} + W_{\mathrm{C}} = -(\hat{s}\cdot\hat{r})\frac{k\hbar^2}{4m_{\mathrm{A}}r^2} + \left(J+\frac{1}{2}\right)^2\frac{\hbar^2}{2m_{\mathrm{A}}r^2} \tag{3.4}$$

is attractive. This is the case for nuclei with large and positive anomalous magnetic moments, like proton, aluminium, etc. The dipole approximation is not adequate for distances smaller than the nuclear radius.

The bound-state spectrum for the monopole-proton system has some unfamiliar features compared to ordinary atomic spectra (table II) [8401]. The state with binding energy E_{B} equal to the proton mass is controversial. Notice that one has a sequence of bound states with zero total angular momentum.

TABLE II. – *The lowest monopole-proton $\boldsymbol{J} = 0$ bound states, characterized by the N-value, the binding energy (E_{B}), the size (r) and the wave-length (λ) of the photon emitted in radiative capture from an initial state of zero kinetic energy* [8401]. *The $N = 0$ state is not found by all authors.*

N	E_{B}	r	λ (Å)
3	0.04 eV	0.23 Å	$3\cdot 10^5$
2	105 eV	460 fm	120
1	263 keV	9 fm	0.048
0	938 MeV?		

Since the monopole-proton bound states all have $J = 0$, there will not be any cascade decay, contrary to what happens in the case of μ-mesic atoms. Following the capture to an excited state, the system can only relax via collisional de-excitation or two-photon emission.

The bound states may be produced via radiative capture

$$M+p \to (M+p)_{\text{bound}} + \gamma \tag{3.5}$$

with cross-sections of the order of $(1 \div 10)$ mb for a monopole with $\beta = 10^{-3} \div 10^{-4}$ (fig. 3.1). The capture will predominantly take place from an initial $J=1$ state. A $\beta = 10^{-4}$ monopole would have a mean free path of ~ 200 m in water for being captured in a Mp bound state with $E_B = 263$ keV, with the emission

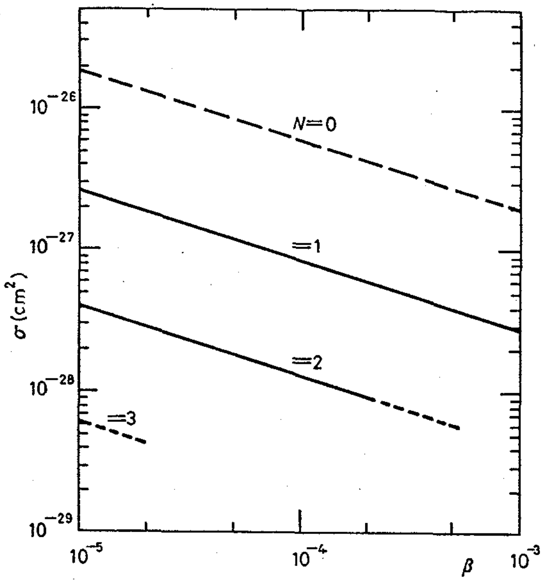

Fig. 3.1. – Cross-sections for radiative capture of protons by magnetic monopoles *vs.* their β. The labels N refer to the various bound states of table II. The result for $N = 0$ and for $N = 3$ are rough estimates [84O1].

of a 263 keV photon. If the lowest-energy state exists, the emission of 938 MeV photons would lead to even more spectacular events.

Monopole-nucleus bound states should exist for many nuclei which have a relatively large gyromagnetic factor K. The binding energies of the ground states should be larger than few tens of keV, while typical sizes should be of the order of 10 fm [83B1]. Goebel [83G5] estimated a radiative-capture cross-section $\sigma_c \simeq 0.3$ mb for monopoles with $\beta = 10^{-3}$ in ^{27}Al nuclei. The ground state of the M ^{27}Al system should have a binding energy of 0.56 MeV.

3˙4. *Monopolic molecules.* – In addition to the two-body bound states has been shown that there exist three-body bound states consisting of a mo pole, a proton and an electron with binding energies of ~ 1 eV. These sta have atomic dimensions, $\sim 10^{-8}$ cm; the radiative-capture cross-sections also atomic for sufficiently low-velocity monopoles. It would seem that mo poles of very low velocities would find their best state as a $(\mathrm{Mpe})^-$ molecu

3˙5. *Nuclear reactions induced by magnetic monopoles.* – The magnetic i teraction between a monopole and a nucleon is so strong that a monopo passing close to a nucleus could induce some nuclear reactions, like the fissio of ^{235}U. As illustrated in fig. 3.2, the magnetic moments of the close-by nucleor

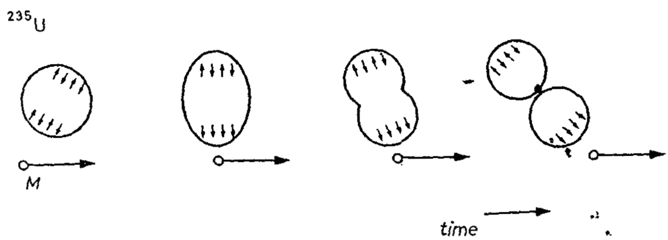

Fig. 3.2. – Illustration of a monopole-nucleus interaction that can result in nuclear fission. The shape of the heavy nucleus and the distributions of the nucleon magnetic moments are shown before, during and after the passage ot the monopole [83B2].

of the nucleus become oriented in the direction of the monopole, while the nucleons on the opposite side are almost unperturbed, since they lie in a weaker magnetic field. Thus the nucleus becomes locally polarized and the close-by nucleons are attracted by the monopole: the nucleus becomes elongated by a sort of a tidal effect, and the deformation could result in nuclear fission [83B2, 83L2]. Presumably only exothermic reactions can be induced, since the c.m. collision energy $E \simeq m_N v^2/2$ is very small for slow monopoles. If it really occurs, monopole-induced fission could lead to another method of monopole detection and could be another energy source.

The magnetic interaction between a monopole and a nucleon could also produce a sort of nuclear Drell effect, whose result could be an excited nucleus, which could subsequently de-excite by β-decay [83L2].

3˙6. *Energy losses of fast monopoles.* – A monopole moving with velocity v produces an electric field whose lines of force lie in a plane perpendicular to the monopole trajectory. At a distance r from the monopole the field is (neglecting the $\partial B/\partial t$ term of eq. (2.3))

$$E = \frac{\beta\gamma g r}{(r^2 + \gamma^2 v^2 t^2)^{3/2}}. \tag{3.6}$$

In matter this field may ionize or excite the nearby atoms or molecules.

The interaction with matter of poles having velocities $v > 10^{-2}\,c$ is well understood: a monopole with magnetic charge g behaves as an equivalent electric charge $(Ze)^2_{\text{eq}} = g^2\beta^2$. The ionization energy losses may be described by the Bohr Bethe-Bloch formula as corrected by AHLEN [80A1, 83A7]. For an incoming particle with electric charge Ze one has

$$(3.7)\qquad \left(\frac{\mathrm{d}E}{\mathrm{d}x}\right)_{\mathrm{e}} = \frac{4\pi N_{\mathrm{e}} Z^2 e^4}{m_{\mathrm{e}} c^2 \beta^2}\left[\ln\frac{2m_{\mathrm{e}}c^2\beta^2\gamma^2}{I_{\mathrm{e}}} - \beta^2 - \delta_{\mathrm{e}}/2 - B_{\mathrm{e}}\right]$$

and for a magnetic monopole in a nonconducting material

$$(3.8)\qquad \left(\frac{\mathrm{d}E}{\mathrm{d}x}\right)_{\mathrm{m}} = \frac{4\pi N_{\mathrm{e}} g^2 e^2}{m_{\mathrm{e}} c^2}\left[\ln\frac{2m_{\mathrm{e}}c^2\beta^2\gamma^2}{I_{\mathrm{m}}} - \frac{1}{2} + \frac{K_{\mathrm{m}}}{2} - \frac{\delta_{\mathrm{m}}}{2} - B_{\mathrm{m}}\right],$$

where $K_{\mathrm{m}} = 0.406$ for poles with $g = g_{\mathrm{D}}$ (0.346 for $g = 2g_{\mathrm{D}}$), $\beta = v/c$, $\gamma^2 = 1/(1-\beta^2)$, N_{e} is the number density of electrons, m_{e} is the electron mass, $I_{\mathrm{e,m}}$ and $\delta_{\mathrm{e,m}}$ are the mean ionization potential and density effect corrections for the electric and magnetic projectiles. In eqs. (3.7) and (3.8) one has assumed that the atoms of the medium are light enough and β to be large enough so that shell effect corrections can be neglected. Although I_{m} and δ_{m} should be fundamentally different from I_{e} and δ_{e}, the differences vanish in the limit of small densities. Thus one can practically set $I_{\mathrm{m}} = I_{\mathrm{e}}$ and $\delta_{\mathrm{m}} = \delta_{\mathrm{e}}$. For $\beta\gamma < 2$ one has $\delta_{\mathrm{e}} = 0$, while, for $\beta\gamma > 100$, $\delta_{\mathrm{e}} \simeq 3.7 + 4.6 \log \beta\gamma$. In eq. (3.9) the extra Bohr correction term B_{m} may probably be neglected; its value is quite dependent on higher-order QED effects (for $g = g_{\mathrm{D}}$, $B_{\mathrm{m}} \simeq 0.248$).

Formulae (3.7) and (3.8) are valid under the assumption that all collisions of the projectile with the electrons of the medium are either close or distant. In the close collisions the energy transfers are so large that the electrons can be regarded as free. The energy lost in each distant collision is very small, so that the electrons cannot be considered free. But it is legitimate to consider the excitation of an atom as a perturbation; for most distant collisions the impact parameter is large enough that one can assume the dipole approximation. According to AHLEN the hypothesis that there exists a small fraction of collisions that do not satisfy either the close or distant collision approximations is adequate for $\beta \geqslant 0.04$.

In table III are given the values of the mean ionization potential I_{e} in various materials. In fig. 3.3 and 3.4 are shown the energy losses of monopoles in silicon and in hydrogen, respectively. A numerical formula is given in subsect. 5.1.

TABLE III. – *Mean ionization potentials in various materials* [80A1].

Z	Material	I_e (eV)
1	H_2 gas	18.5
1	H liquid	20.7
2	He gas	42.3
6	C saturated condensed compound	77.3
10	Ne gas	133.0
14	Si solid	169.0
26	Fe solid	275.0
50	Sn solid	498.0
82	Pb solid	793.0
92	U solid	884.0

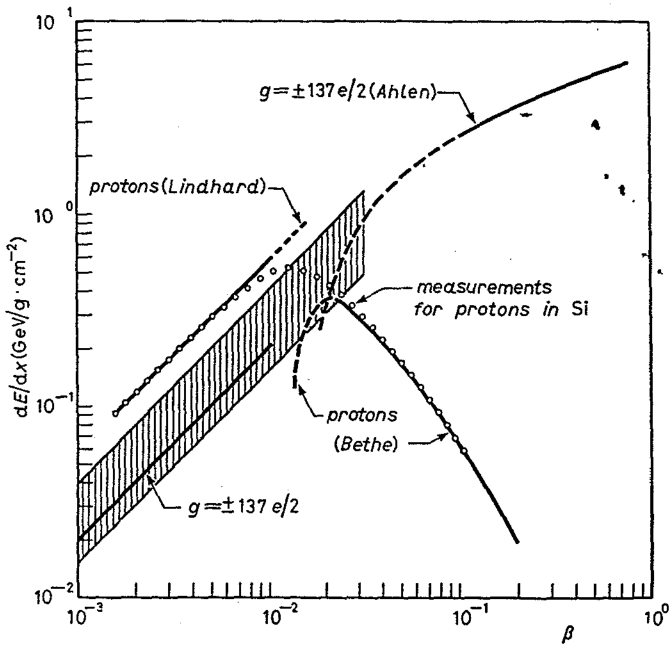

Fig. 3.3. – Stopping powers in silicon for protons and for monopoles with $g = g_D$. Solid lines are calculations using low- and high-velocity approximations as explained in the text. Dashed lines are extrapolations of the various theories into regions of questionable validity. The Bethe calculation does not include shell corrections. The shaded region indicates the estimated range of errors for the slow monopole stopping power. The open circles are the averaged values of measurements of proton stopping power in silicon [80A1].

3'7. *Energy losses of slow monopoles—The Fermi-gas approximation.* – A considerable amount of work has been done on the evaluation of energy losses of slow electrically charged particles and, more recently, on slow magnetically charged particles [82R3, 83A1, 83A7]. One of the most successful models has

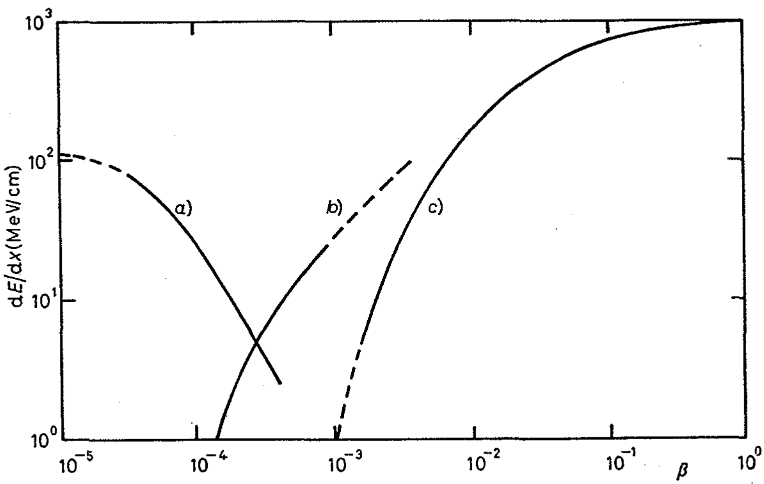

Fig. 3.4. – The energy loss, in MeV/cm, of magnetic monopoles in liquid hydrogen as a function of β [83B7]. Curve *a*) corresponds to elastic monopole-hydrogen atom scattering; curve *b*) corresponds to interactions with level crossings [83D1]; curve *c*) describes the ionization energy loss. The dashed parts of the curves correspond to velocity ranges where the approximations used in the calculations may break down.

been that in which the properties of the stopping material have been approximated by those of a free (degenerate) gas of electrons. This is clearly appropriate for interactions with the conduction electrons of metallic absorbers. For nonmetallic absorbers it represents a reasonable approximation for heavy atoms ($Z \geqslant 10$) for which the Thomas-Fermi description is valid. The first calculation of Fermi and Teller was refined by LINDHARD, who obtained for electrically charged particles in heavy materials

$$-\left(\frac{\mathrm{d}E}{\mathrm{d}x}\right)_e = \frac{4}{3\pi}\,\frac{m_e^2 Z^2 e^4 v}{\hbar^3}\left[\ln \pi\left(\frac{v_F}{\alpha c}\right)^{1/2} + \frac{\alpha c}{\pi v_F} + (\ln \pi - 1)/2\right], \tag{3.9}$$

valid for projectile velocities $v < v_F$, where the Fermi velocity $v_F \simeq \hbar(3\pi^2 N_e)^{\frac{1}{3}}/m_e \simeq \simeq \alpha \simeq 1/137 \simeq 10^{-2}$. The projectile velocity is also limited at low values, since the energy transfer ΔW from the monopole to a bound electron with a characteristic atomic velocity v_F should be larger than the energy level spacing of the atom. The kinematic limit of the energy transfer is $\Delta W = 2m_e v(v + v_F) \simeq \simeq 2m_e v v_F$, from which $\beta > I/2m_e\beta_F$.

(3.7) describes well the experimental data for protons with $\beta > 3\cdot 10^{-2}$, while (3.9) describes the proton data for $10^{-3} < \beta < 10^{-2}$ (see fig. 3.3).

AHLEN and KINOSHITA have extended the technique of Lindhard to compute the energy loss of monopoles in Fermi gases. They used the relation $\mathrm{d}E/\mathrm{d}x = gH$, where H is the magnetic field induced at the pole position by eddy currents. Their result is

$$\left(\frac{\mathrm{d}E}{\mathrm{d}x}\right)_{\mathrm{m}} = \frac{2\pi N_{\mathrm{e}} g^2 e^2 v}{m_{\mathrm{e}} c^2 v_{\mathrm{F}}}\left[\ln\frac{1}{Z_{\min}} - \frac{1}{2}\right]. \tag{3.10}$$

For *nonconductors* eq. (3.10) is expected to be valid for $10^{-4} \leqslant \beta \leqslant 10^{-2}$, with the parameter $Z_{\min} = \hbar/2m_{\mathrm{e}} v_{\mathrm{F}} a_0$. $a_0 = 0.5 \cdot 10^{-8}$ cm is roughly the « mean free path » of an electron bound in an atom. N_{e} is the density of nonconducting electrons in the material. For nonconductors this is the only term, while in *conductors* one should add a second term, which depends on the conduction electrons. In fact, eq. (3.10) describes more properly the conduction case and is valid for all $\beta \leqslant 10^{-2}$, with the parameters $Z_{\min} = \hbar/2mv_{\mathrm{F}}\Lambda$, $\Lambda \simeq 50aT_{\mathrm{m}}/T$, a = lattice parameter; T_{m} is the melting temperature of the metal and T the actual temperature; N_{e} is the density of conduction electrons.

3'8. *The response of scintillators.* – The response of a detector does not depend only on the energy losses, but also on the specific features of the detector. The response of plastic scintillators to the passage of low-velocity magnetic monopoles has been estimated by considering the valence electrons of the material as a Fermi gas with an energy gap $E_{\mathrm{G}} \sim 5$ eV, which corresponds to the first excited electronic energy level of a benzene ring [83A1].

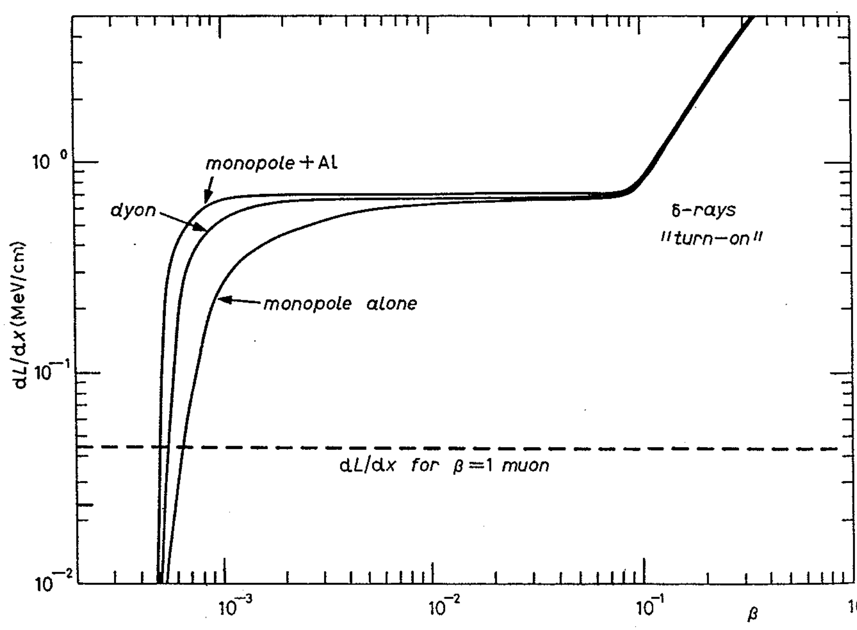

Fig. 3.5. – Estimates of the scintillation light yield in Ne 110 scintillator as a function of the magnetic-monopole velocity $\beta = v/c$ [83A1]. The plateau yield around $\beta \simeq 10^{-2}$ is probably 30% higher.

Ahlen and Tarlé [83A1] have used the above results to calculate the scintillation yield of a magnetic monopole in Ne 110, fig. 3.5. Curves for a bare monopole with $g = g_D$ and for a monopole bound with a proton are given. Note the presence of a threshold at $\beta \simeq 6\cdot10^{-4}$, above which the light signal is quite large compared to that of a relativistic muon. The threshold is due to the two-body kinematic constraint for $E_G = 5$ eV. The threshold could be reduced by reducing the energy gap, for instance with acrylic-based naphtalene scintillators or with scintillators containing pentacene fluormolecules. The light yield in fig. 3.5 shows the characteristic saturation effect present in solid materials at high β. For $\beta > 0.1$ the light yield should increase because of the production of δ-rays. The light yields of fig. 3.5 are lower limits, because any other effect should effectively lower the threshold and increase the light.

3'9. *The Drell effect.* – The energy losses of monopoles with $10^{-4} < \beta < 10^{-3}$ are mainly due to excitations of the atoms. Atoms of size a will see the field of the moving pole as a pulse with frequencies $\omega_m \simeq \beta/a$. Thus excitations of frequencies $\omega_X \leqslant \omega_m$ will be induced in the atom (*). The characteristic energy shift due to a monopole at a distance $a = 0.5$ Å from an atomic electron is $eg/2m_e a^2 \simeq 7$ eV. Hence a monopole passing within the atom produces substantial level mixings and crossings.

Let us follow qualitatively what happens in the case of a monopole passing through a hydrogen atom. As the monopole approaches the atom from a large distance, the energy levels of the atom split in the characteristic Zeeman pattern due to a uniform magnetic field. In particular, the excited $n = 2$ levels start to move down in energy, while the $n = 1$ level with $m_j = +1/2$ starts to move up (fig. 3.6). For zero impact parameter along the z-axis the z-component of the total angular momentum

$$J_z = \boldsymbol{r}_e \times (\boldsymbol{p} - e\boldsymbol{A}) + \boldsymbol{\sigma}_e/2 - \hat{n}/2 \tag{3.11}$$

is conserved. $\boldsymbol{r}_e$ is the electron co-ordinate relative to the proton (located at the origin) and $\hat{n}$ is the unit vector from the pole to the electron. Since $\hat{n}$ changes sign as the monopole moves from the far left to the far right, the z-component of the electron's angular momentum must change. Thus the ground-state electron with $m_j = -1/2$ will spin flip to $m_j = +1/2$ as the monopole traverses left to right; instead the one with $m_j = +1/2$ will be raised to an excited state with $n > 1$ and $m_j = +3/2$. On the way up this level will cross the one moving down from $m_j = -3/2$ to the ground state with $m_j = -1/2$.

For a monopole along a path of nonzero impact parameter b, one has two

(*) The radiative lifetime of an excited atom $((10^{-8} \div 10^{-9})$ s) is much longer than the transit time of a monopole ($a/\beta c \sim 10^{-15}$ s if $\beta \sim 10^{-4}$).

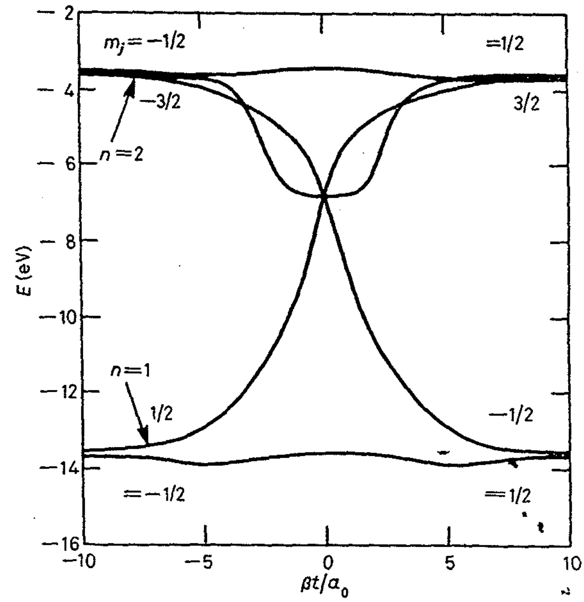

Fig. 3.6. – The energy levels for atomic hydrogen before (left), during (centre) and after (right) the passage of a magnetic monopole [83D1].

possibilities: For $b < b_{min}$ such as $\beta/b > \omega_{min}$ there will be level mixing. For $b > b_{min}$ the adiabatic approximation is applicable and the electron would follow the level pattern, with mixing but not crossing. Thus an electron in either of the two degenerate ground states would remain in the ground state.

The energy loss in hydrogen due to this mechanism (Drell effect) is given by [83D1]

$$\left(\frac{dE}{dx}\right)_m \simeq 370\beta(1-\beta_c^2/\beta^2)^{3/2}\,(\text{GeV cm}^2\,\text{g}^{-1})\,, \tag{3.12}$$

where $\beta_c = (2m_H \Delta E)^{1/2} \simeq 1.2 \cdot 10^{-4}$ is a threshold velocity. The losses in hydrogen are shown in fig. 3.4, curve b). In the $10^{-4} < \beta < 10^{-3}$ range this effect yields losses about an order of magnitude larger than ionization losses.

The Drell mechanism is effective as long as the monopole-atom collision energy exceeds the spacing of atomic levels. The effect may be used for practical detection either by observing the photon emitted in the de-excitation of the excited atom or by observing the ionization caused by the energy transfer from the excited atoms to complex molecules with a small ionization potential (Penning effect). Helium plus CH_4 seem to be good working gases (see subsect. 8'3). Calculations of the Drell effect in complex molecules are presently not available.

3'10. *Energy losses at very low velocities* ($\beta < 10^{-4}$). – Magnetic monopoles with velocities smaller than $10^{-4}\,c$ cannot excite atoms; they can only lose energy in elastic collisions with atoms or with nuclei.

3'10.1. Monopole-atom elastic scattering. At very low velocities the dynamics of the process is still dominated by the coupling of the electron magnetic moments with the monopole magnetic field. A rough estimate of the energy loss may be obtained considering the elastic interaction of a structureless atom, characterized only by its magnetic moment, with the monopole. In the limit of very low velocities one has [83B7]

$$\frac{\mathrm{d}E}{\mathrm{d}x} \simeq N_{\mathrm{a}} E_{\mathrm{c.m.}} \sigma \simeq N_{\mathrm{a}} \hbar^2 / m_{\mathrm{e}}\,, \tag{3.13}$$

where N_{a} is the number of atoms/cm^3. If $N_{\mathrm{a}} \simeq 4\cdot 10^{22}$ atoms/cm^3, one has $\mathrm{d}E/\mathrm{d}x \sim 32$ MeV/cm (liquid hydrogen). The results of a more precise calculation [84B1] are shown in fig. 3.4. The energy is released to the medium in the form of elastic vibrations and/or infra-red radiation (thermal and acoustic energy).

Ahlen *et al.* [82A2] give the following formula for the energy loss from elastic collisions of monopoles with atoms of Si:

$$\frac{\mathrm{d}E}{\mathrm{d}x} \simeq \frac{0.79}{4}\left[1.31 + \ln\beta - \ln\frac{\beta}{137e}\right]. \tag{3.14}$$

For $\beta = 10^{-3}$ eq. (3.14) gives an energy loss which is $\sim 7\,\%$ of the stopping power due to ionization. The relative contribution of (3.14) to the total energy loss increases as β decreases.

3'10.2. Monopole-nucleus elastic scattering. For monopole-nucleus elastic collisions two effects have to be considered. The first is due to the interaction of the monopole magnetic charge with the magnetic moment of the nucleus. It leads to a formula like (3.13):

$$\frac{\mathrm{d}E}{\mathrm{d}x} \simeq \frac{N_{\mathrm{a}} \hbar^2 \mu_{\mathrm{p}}}{m_{\mathrm{p}} \mu_{\mathrm{e}}} (\simeq 0.1\ \mathrm{MeV/cm\ in\ liquid\ H_2}). \tag{3.15}$$

The second effect is due to the interaction of the confined chromomagnetic charge of the monopole with the confined colour charge of the nucleus. It leads to S-wave scattering, like between two nuclei; very roughly one has

$$\frac{\mathrm{d}E}{\mathrm{d}x} \simeq \frac{\pi r^2 m_{\mathrm{p}} c^2 N_{\mathrm{a}}}{4} \beta^2 (\simeq 0.3\beta^2\ \mathrm{MeV/cm\ in\ liquid\ H_2}). \tag{3.16}$$

3.11. *Energy losses in superconductors.* – The linear velocity dependence of the energy losses of slow monopoles in conductors seems to be well established and there is no reason to suspect the existence of a velocity threshold. Extrapolating formula (3.10) to superconductors, letting $\Lambda \to \infty$, one would at first sight expect an enormous energy loss. However, in the region close to the monopole trajectory the magnetic field would be larger than the critical field of the superconductor. If the critical field is 1 kG, then in a cylinder of radius $r \simeq 600$ Å the material stops being superconductor. This corresponds to a large impact parameter. Thus the functional dependence of the energy losses in a superconductor should not be different than that in a normal conductor. $\mathrm{d}E/\mathrm{d}x$ will depend linearly on β and on the conductivity σ, and be of order 100 MeV/g cm^{-2} at $\beta \sim 10^{-3}$.

In superconductors there is an additional component of stopping power. If a pole passes through a superconductor of thickness x, there will be a magnetic flux $\Phi_B = 2\pi\hbar c/e$ (equal to two flux quanta of superconductivity) which threads the quenched cylinder after the monopole is gone. The magnetic field in the cylinder is given by $\Phi_B/\pi r^2$ and the energy by $x\Phi_B^2/8\pi^2 r^2 = x\hbar^2 c^2/2e^2 r^2$. This yields $\mathrm{d}E/\mathrm{d}x \sim 42$ MeV/cm. It is a small fraction of the stopping power at $\beta \simeq 10^{-3}$, but, since it is β-independent, it dominates for $\beta < 10^{-4}$.

De Rujula *et al.* [84B5] and Allega *et al.* [83A6] analysed in detail the energy losses in superconductors and also the signal and the noise in a « sonic antenna » detector. They follow the notations used in gravitational-wave research and express the signal energy E_s in units of temperature $T_s = E_s/K_B$, where K_B is the bulk modulus of the antenna. For a 10 cm long antenna they obtain for aluminium

$$T_s(\mathrm{Al}) = 1700\ \mathrm{K}\ (\beta - \beta_0)^2, \tag{3.17}$$

with $\beta_0 = 10^{-4}$. The signals from different materials and the noise temperatures, present and future, are shown in fig. 3.7.

3.12. *Track-etch detectors.* – The passage of heavily ionizing particles may be permanently recorded in some insulating materials, which range from plastic sheets like CR39, lexan (makrofol E), kapton and nitrocellulose to glasses and to minerals like mica and obsidian. These materials may be considered as threshold devices, with no time resolution and with thresholds which depend on the material and on the type of chemical etching.

The latent track may be made visible by proper chemical etching. The etching velocity along the latent track (v_T) is faster than the general etch rate (v_G). Therefore, with strong etching one may obtain a hole in a sheet of the sensitive material. The hole is located where the ionizing particle passed and may be detected by observation with normal optical microscopes or by

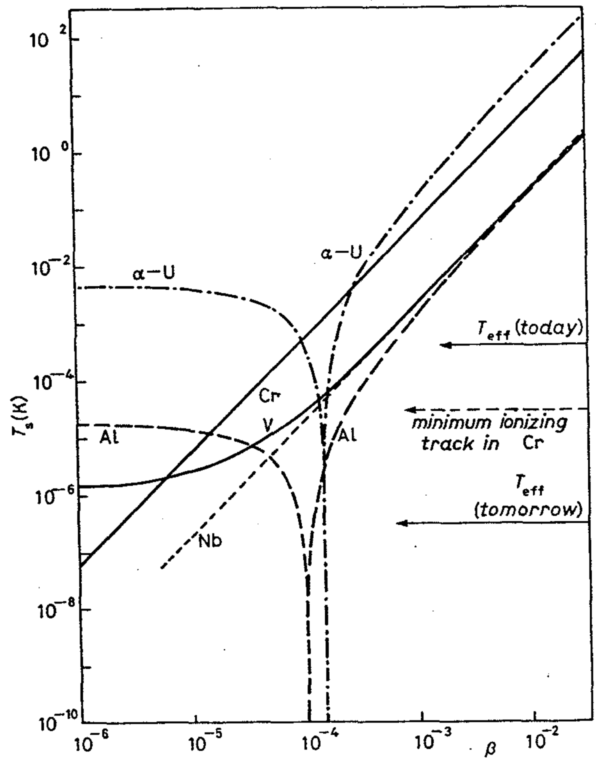

Fig. 3.7. – Signal temperature per eigenmode for a variety of materials at very low temperatures, as a function of monopole velocity. T_{eff} (today) and T_{eff} (tomorrow) indicate effective total noise temperatures that have been, or soon will be, achieved in practice. Also shown in the figure is the signal temperature for a minimum ionizing track in Cr [84B5]. $l = 10$ cm.

other means. For instance, one may measure the electrical resistance of a portion of a plastic sheet positioned between two electrodes, one of which is wet [83A4]; or one can use ammonia vapour on one side of the plate: when there is a hole, the ammonia vapour passes to the other side developing a blueprint sheet [82K2].

Etching a layer for a short time yields two etched cones on each side of the sheet (fig. 3.8) [82B2]. The primary ionization rate may be determined from the geometry of the etched cones. For CR39 this technique is particularly successful, yielding measurements of the electric charge of heavy nuclei to a precision of $0.1e$ if one uses several layers of plastic sheets, placed perpendicular to the incoming ions.

Figure 3.9 shows the response of several track-recording solids as a function of Z/β, the ratio of charge to velocity of the incident particle. The response may be given as the ratio v_T/v_G, or diameter of hole$/2v_G t$.

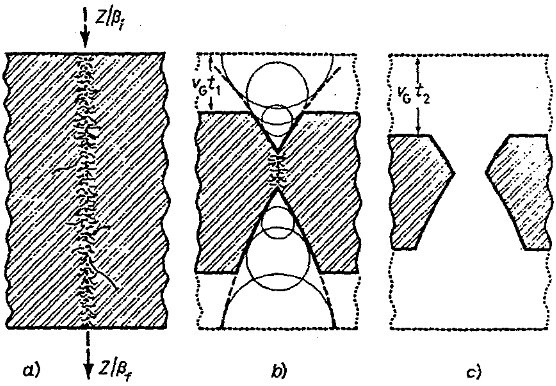

Fig. 3.8. – Track-etching technique for particle identification: *a*) sketch showing dense core of radiation-damaged material and delta-rays; *b*) development of conical etch pits at the intersection of the trajectory with the surface; *c*) development of a hole after prolonged etching [82B2].

Track-etch detectors are sensitive to the restricted energy loss, that is to the fraction of the energy loss rate which is concentrated in a diameter smaller than 1 μm along the direction of the primary particle. The restricted energy loss is mainly due to short delta-rays. Scintillators are instead sensitive mainly to high-energy delta-rays, because of radiation quenching in the dense core region near the particle trajectory. In a certain sense a track-etch detector is complementary to a scintillator, because it is insensitive to the energy deposited in the halo and sensitive only to the energy deposited in the core. The reason is that chemical etching takes place preferentially where the density of energy deposited is large.

From the above considerations and from direct measurements with heavy

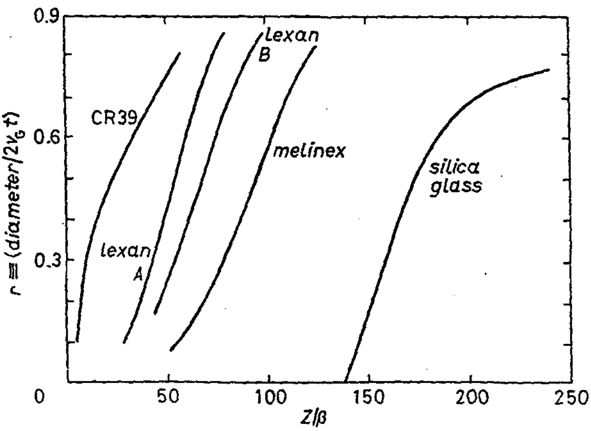

Fig. 3.9. – Response of several track-etch detectors as a function of Z/β. Lexan *A* and lexan *B* refer to the responses of lexan etched in two different reagents [82B2].

ions one may conclude that CR39 has a practical threshold at $Z/\beta \simeq 5$, which corresponds to a restricted energy loss of $\simeq 25$ MeV cm^2 g^{-1} (with delta-rays having energies lower than 200 eV). In order to compute the velocity threshold of monopoles, one has to assume a formula for their energy loss and establish the etching procedure. The formula of Ritson, taking 3 eV for the effective energy gap in CR39, and considering an etching from 1.7 mm to 0.2 mm thickness, predicts an effective threshold around $\beta_M \simeq 2\cdot 10^{-3}$. It is not clear how reliable this number is. One may assume that the conservative threshold values are the following (in parenthesis are indicated the optimistic values):

$$\begin{array}{llll} \text{CR39} \ \beta > 0.02 & (\beta \geqslant 0.003), & \text{nitrocellulose} \ \beta > 0.04 & (\beta \geqslant 0.01), \\ \text{lexan} \ \beta > 0.3 & (\beta \geqslant 0.03), & \text{kapton} \quad \beta \geqslant 0.8 & (\beta \geqslant 0.4), \\ \text{mica} \ \beta n \geqslant 2 & (\beta n \geqslant 1.0). & & \end{array}$$

3'13. *Energy losses of monopoles in celestial bodies.* – In order to asses the likelihood of monopoles being stopped in a celestial body, if they strike it, one needs to know the stopping power of monopoles in that body. For very low β ($< 10^{-4}$) the main energy losses in the Earth are due to i) monopole-atom elastic scattering (probably velocity independent and of the order of 20 MeV g^{-1} cm^2), ii) eddy current losses $\mathrm{d}E/\mathrm{d}x \sim (10 \div 30)\beta$ GeV g^{-1} cm^2 (here the uncertainty arises from the uncertainty in the validity at low β of the formula for nonconducting electrons), iii) nuclear stopping power $(\mathrm{d}E/\mathrm{d}c)_n \simeq$ $\simeq 0.1$ MeV g^{-1} cm^{-2}. One may conclude that the Earth should stop all monopoles with $\beta \leqslant 10^{-4}$. Similar estimates for other celestial bodies lead to the conclusion that monopoles may be stopped if they have

$$\text{Moon} \quad \beta < 5\cdot 10^{-5}, \qquad \text{Earth} < 10^{-4}, \qquad \text{Jupiter} < 3\cdot 10^{-4}, \qquad \text{Sun} < 10^{-3}.$$

4. – GUT monopoles. Production and history.

4'1. *Introduction.* – GUT monopoles should have been produced at the phase transition, which occurred at $t \sim 10^{-35}$ s after the big bang (fig. 4.1), when the unifying gauge symmetry group broke down into smaller subgroups, one of which was U_1. The estimates of monopole production rates in the simplest GUT models yield very large numbers. At least one monopole was produced per event horizon. If the expansion of the Universe proceeded in an orderly way between 10^{-35} s and 10^{-6} s, when the quarks formed the nucleons, one should have expected a production of about one monopole per 10^5 nucleons, which is clearly too much by many orders of magnitude.

One way out of this and of other dilemmas is based on the hypothesis of inflation [81G4]. At the end of the GUT era the radius of the Universe in-

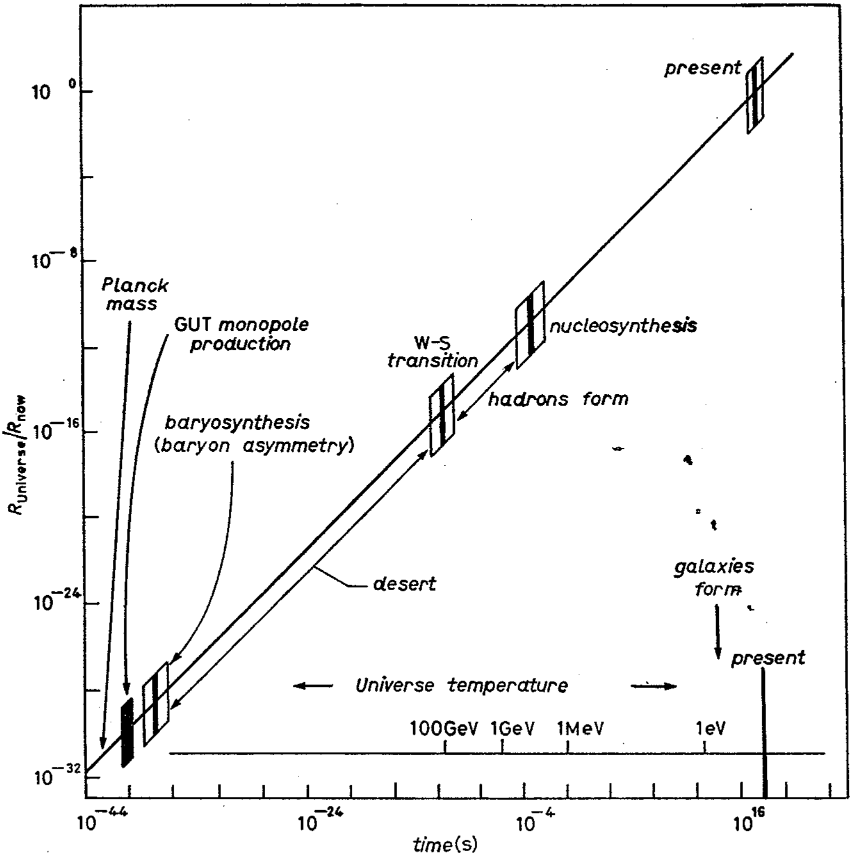

Fig. 4.1. – Illustration of the phase transitions in the early Universe.

creased exponentially before resuming normal expansion. This may lead to one or few horizons in the early Universe and thus to a very small number of monopoles, even one in the whole Universe. Another possible way out is based on GUTs with intermediate mass scales. These theories offer novel possibilities for monopole charges and masses and they also provide a mechanism for suppressing their number density to cosmologically acceptable levels and which may still be detectable.

A second mechanism of monopole production, via very-high-energy reactions of the type $\bar{q}q \to \overline{M}M$, could have occurred immediately after the GUT phase transition. This mechanism is of great interest if the number of monopoles produced at the phase transition was very low.

4.2. *The early Universe.* – In the standard scenario, the early Universe was homogeneous, isotropic and radiation dominated (that is $KT \gg mc^2$ for any of the particles present). For that period ($t < 10^{10}$ s, $kT > 10$ eV) a few simple formulae connect the time t, the temperature T, the mass density ϱ, the entropy density $s = S/v$ and the radius R (CGS system of units):

$$t \simeq \frac{3.3\cdot 10^{20}}{\sqrt{N^*}T^2} \simeq \frac{2.4}{\sqrt{N^*}[KT(\mathrm{MeV})]^2}, \tag{4.1}$$

$$\varrho \simeq \frac{3}{32\pi G t^2} \simeq \frac{4.5\cdot 10^5}{t^2} \simeq 4.2\cdot 10^{-36} N^* T^4, \tag{4.2}$$

$$s \simeq \frac{S}{v} = \frac{2\pi^2}{45} N^* \frac{K(KT)^3}{(\hbar c)^3} \simeq 5.0\cdot 10^{-15} N^* T^3, \tag{4.3}$$

where K is Boltzmann's constant and N^* is the total effective number of helicity states of different particle species. N^* is equal to the number of boson states plus 7/8 of the number of fermion states, $N^* = N_B + (7/8)N_F$. In a typical GUT model $N^* \simeq 160$ for $t < 10^{-35}$ s; it decreased to ~ 100 after the end of the grand-unification era and is now 4-5 [80K1]. In each phase of the Universe, during which N^* remained constant, there was a state of thermal equilibrium. As the Universe expanded and cooled, several phase transitions happened and the number of particle species effectively present decreased. If the Universe expanded adiabatically, one had $SR^3 \simeq$ const and $TR \simeq$ const. R is the scaling function in the Robertson-Walker metric $\mathrm{d}s^2 = c^2\mathrm{d}t^2 - R^2\,\mathrm{d}\sigma^2$. As long as N^* is constant, $T \sim 1/R$. Over long periods the $T \sim 1/R$ relation is only approximate because as T decreased also N^* decreased.

During the radiation era the Einstein equation, which describes the time development of the scaling function R, was

$$\left(\frac{\dot R}{R}\right)^2 \simeq \frac{8\pi\hbar c}{3m_{\mathrm{Pl}}^2}\varrho \simeq 5.4\cdot 10^{-7}\varrho, \tag{4.4}$$

CGS units. The Planck mass and time are

$$m_{\mathrm{Pl}} = \sqrt{\hbar c/G} \simeq 2.2\cdot 10^{-5}\ \mathrm{g} \simeq 1.2\cdot 10^{19}\ \mathrm{GeV}, \qquad t_{\mathrm{Pl}} = \hbar/m_{\mathrm{Pl}}c^2 \simeq 5.4\cdot 10^{-44}\ \mathrm{s}.$$

4'3. *Simple models of monopole production—monopoles are too many.* – The GUT phase transition involved a change from a symmetric state to some nonsymmetric state. The order parameter for the transition is φ, where $\varphi = 0$ in the symmetric state and is different from zero in the nonsymmetric state. φ represents the expectation value of some field responsible for the symmetry breaking, *e.g.* a Higgs field.

Figure 4.2 illustrates the behaviour of the Higgs potential at different temperatures in the early Universe. At temperatures larger than the critical temperature T_c, corresponding to the GUT phase transition, the effective potential $V(\Phi)$ of the Higgs fields Φ had an absolute minimum at $\Phi = 0$ (for any $T > T_c$).

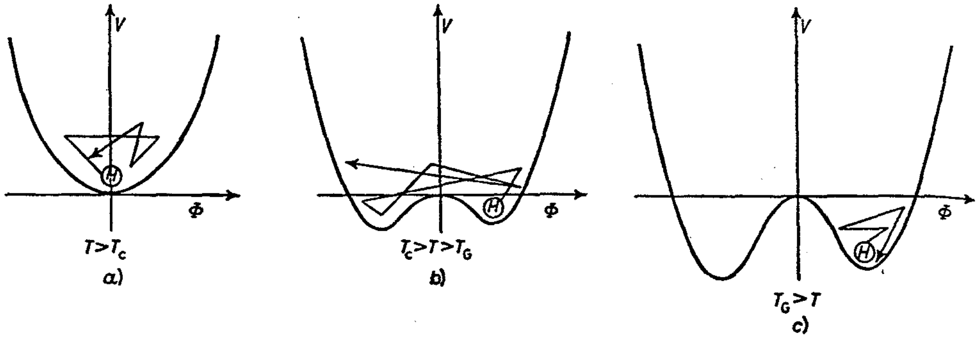

Fig. 4.2. – Illustration of the Higgs potential at different temperatures: *a*) at high temperatures, $T > T_c \simeq 10^{15}$ GeV, the potential has a minimum at $\Phi = 0$; *b*) for intermediate temperatures, $T_c > T > T_G$, the minimum of the potential is at $\langle\Phi\rangle \neq 0$, but the thermal fluctuations of $\langle\Phi\rangle$ are large so that it can go over the central hump; *c*) at lower temperatures, $T < T_G$ (T_G = Ginzburg temperature), one has $\langle\Phi\rangle \neq 0$, the Higgs field no longer fluctuates over the hump [82N1].

For $T < T_c$ the value $\Phi = 0$ became a local maximum (fig. 4.2*b*)). The absolute minimum of $V(\Phi)$ was at $|\langle\Phi\rangle| \neq 0$ and the compact GUT group, for instance SU_5, broke down into smaller subgroups. The magnitude of $\langle\Phi\rangle$ grew as T decreased. For temperatures T just below T_c the difference $\Delta V = V(\langle\Phi\rangle = 0) - V(\Phi_{min})$ was small and random thermal fluctuations of the Higgs field back and forth across the local maximum at $\Phi = 0$ were common. As the Universe cooled, a temperature T_G was reached such as, for $T < T_G$, the fields Φ only fluctuated in the local minimum, without the possibility of crossing the maximum at $\Phi = 0$. At $T = T_G$ (T_G = Ginzburg temperature) the Higgs fields tend to freeze-in with fixed nonzero vacuum expectation values pointing in different internal group directions in different domains of space (fig. 2.8), something as a ferromagnet, when it is cooled before the Curie point. At T_G we may imagine the space split into regions of linear dimensions equal to the Higgs correlation length

$$\xi_G \simeq \frac{1}{h^2 T_G}\frac{\hbar c}{K} \simeq \frac{1}{4.4 h^2 T_G}, \tag{4.5}$$

where h^2 is the Higgs coupling. Within each region the Higgs field is aligned, but its directions in different regions are uncorrelated. Occasionally, at the corners where the domains met, one had monopoles. If the probability of this happening is p, then the number density of monopoles produced at T_G was

$$n_{M,in} \simeq p\xi_G^{-3} \simeq p h^6 T_G^3 (K/\hbar c)^3 \simeq 10\, h^6 T_G^3 . \tag{4.6}$$

p is related to the geometry of the gauge group and is typically of the order of $p \sim 1/10$. If $ph^6 \sim 10^{-6}$ and $T_G \sim 10^{14}$ GeV, then $n_{M,in} \sim 10^{77}$ poles/cm^3.

The relative monopole densities may be defined as

$$r = n_M/T^3\,, \qquad \hat{r} = n_M/\hat{s} \simeq 45ph^6/2\pi^2N^*\,, \tag{4.7}$$

where $\hat{s} = S/vK$ is the entropy density per unit K. $\hat{r}$ is roughly constant during an adiabatic expansion (except for the effect of $M\overline{M}$ annihilation). KIBBLE [80K1, 81K1] estimated the initial relative monopole densities (at $T = T_G$) to be ($K = \hbar = c = 1$ and $N^* \sim 160$)

$$r_{in} \simeq ph^6 \sim 10^{-6}\,, \qquad \hat{r}_{in} \sim 10^{-8}\ \text{poles/particle}\,. \tag{4.8}$$

The above estimate depends on various assumptions about the monopole production mechanism. It is, therefore, of interest to find a limit independent of these details. EINHORN *et al.* [80E1] pointed out that within the context of classical relativity and standard cosmology one could obtain an upper bound on ξ (and thus a lower bound on $\hat{r}_{in}$) by considering particle horizons at $T = T_G$. A photon moving along a geodesic, beginning at $t = 0$, travels a proper distance $2ct$; so one may assume that the Higgs fields at two points separated by more than $2ct$ are uncorrelated. Choosing $\xi = 2ct$, with t given by (4.1), yields

$$r_{in} = \frac{p}{\xi^3 T_G^3} > \frac{pT_G^3 N^{*3/2}}{(2\times 3.3\cdot 10^{20} c)^3}\,, \tag{4.9}$$

which at $T_G = 3\cdot 10^{14}$ GeV and $N^* \sim 100$ gives

$$r_{in} > 10^{-10}\,, \qquad \hat{r} > 10^{-13}\ \text{poles/particle}\,. \tag{4.10}$$

After production the monopole density n_M is expected to follow the equation

$$\frac{dn_M}{dt} = -Dn_M^2 - 3\frac{\dot{R}}{R}n_M\,, \tag{4.11}$$

where the first term on the right-hand side describes monopole-antimonopole annihilation, while the second term describes the dilution of monopoles due to the cosmological expansion. The annihilation process should have been effective only in the early Universe for $T \geqslant 10^{12}$ GeV, when the monopole density in the Universe was large [79P1]. The final result of the calculations is that $\hat{r}_{fin} \simeq 10^{-10}$ if $\hat{r}_{in} \geqslant 10^{-10}$, while $\hat{r}_{fin} \simeq r_{in}$ if $\hat{r}_{in} < 10^{-10}$. These numbers are many orders of magnitude larger than present cosmological bounds (see sect. 6). The monopole «problem» may be summarized recalling the following numbers:

$$\hat{r}_{in} > 10^{-13}\,, \qquad \hat{r}(T = 1\ \text{MeV}) < 10^{-19}\,, \qquad \hat{r}_{now} < 10^{-24}\,.$$

Many theoreticians tried to find mechanisms to suppress the production of monopoles, or ways to annihilate them. For instance, at the phase transition at the end of the electroweak unification ($t \sim 10^{-10}$ s) the mean pole-antipole distance could have been $\sim 10^{-13}$ cm. The poles could have been connected with the antipoles by flux strings, with string tensions, which could give rise to longitudinal vibrations leading to large energy losses and then to pole-antipole annihilations [80L1].

4.4. *The inflationary scenario—monopoles are too few.* – The prediction of large monopole production was based on the smallness of the casual length at $T = T_G$. The number of monopoles can be reduced if the phase transition occurs much later, at a smaller temperature (probably $T \sim 10^9$ GeV), after extreme supercooling. Under these circumstances the Universe expands exponentially, $R(t) \approx \exp[\chi t]$, with $\chi = (8\pi/3)G\varrho_0 \simeq 10^{10}$ GeV. This is the «inflationary» scenario. In this case the Higgs field Φ «rolls» down the potential of fig. 4.3. The initial roll-over is slow and during this time the original

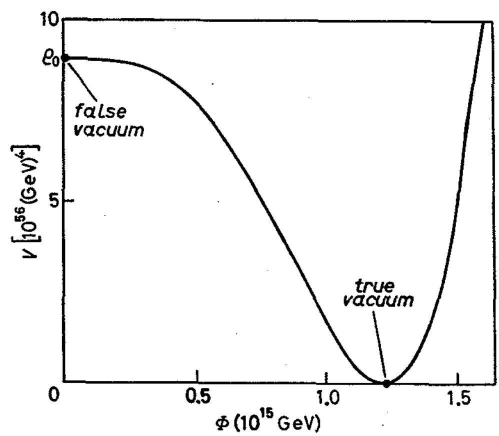

Fig. 4.3. – Details of the Higgs potential in SU_5 [82G3].

bubbles which are supercooling grow in size by a huge factor. When the Φ field reaches the steep part of the potential, it falls quickly to the bottom and oscillates about the minimum, with a time scale which is fast compared to the expansion rate. The oscillation dumping corresponds to particle decays into other species. This releases energy (which is the latent heat of the phase transition): the temperature rises considerably, may be to one-sixth of T_c.

This «inflationary» scenario leads to a drastic reduction of the number of produced monopoles. In fact, the entire Universe may evolve from a single fluctuation, thus leading to 1 or zero monopoles. But in recently proposed two-component inflation, the monopole fluxes could be detectable [84E4].

4.5. *Thermal production of monopoles.* – When the temperature of the Universe was still close to the critical temperature, high-energy collisions between two particles could have produced a monopole-antimonopole pair (for instance, $X+\bar{X} \to M+\bar{M}$). In the original scenario, where the number of monopoles is large, this process is negligible. In the inflationary scenario, where the number of monopoles may be very small, the production by a thermal mechanism acquires more importance.

Let us consider thermal production of monopoles immediately after the GUT phase transition, at the temperature $T_r \simeq T_c/6 \simeq m_X/6$ to which the Universe had reheated immediately after the supercooling phase. Thermal production will be suppressed by a Boltzmann factor [82L2]

$$f^2 \simeq \exp[-2m_M/T_r] \tag{4.12}$$

assuming that $M\bar{M}$ pairs were produced by other particles in thermal equilibrium. For $m_M \geqslant m_X/\alpha_{GUT}$, with $\alpha_{GUT} \simeq 1/40$, the suppression factor becomes

$$f^2 \simeq \exp[-2m_M/T_r] \simeq \exp[-12/\alpha_{GUT}] \simeq \exp[-480] \simeq 10^{-208}, \tag{4.13}$$

which leads to no observable monopole production. COLLINS *et al.* [84C1] state that during the reheating process the effective monopole mass may have oscillated about m_M, as the vacuum expectation value of the scalar field oscillated about the minimum of the scalar potential. Because of this effect, thermal monopole production is greatly increased, with the exponent (4.13) being multiplied by a factor much smaller than one, depending on the form of the scalar potential and on the details of reheating.

4.6. *The history of* GUT *magnetic monopoles after production.* – As the Universe expanded and cooled down, the monopoles should have lost energy, like any other particle. The poles were in thermal equilibrium with other particles via reactions of the type $M+e^- \rightleftarrows M+e^-$. The thermal equilibrium should have lasted until the time of positron-electron annihilation ($t \sim 10$ s, $T \sim 0.5$ MeV). At this time the monopoles would have had kinetic energies of the order of 1 MeV and velocities $\beta \sim 10^{-8}$. After this time the monopoles were effectively decoupled from the other particles present in the Universe.

They would still participate in the general cooling of the Universe, reaching $\beta \sim 10^{-10}$ during the epoch of galaxy formation. As matter (including poles) started to condense (gravitationally) into galaxies, galactic magnetic fields developed through the dynamo mechanism. These fields started to act as monopole accelerators.

Magnetic poles inside the galaxies should have been accelerated, preferentially in the plane of the galaxy (fig. 4.4), by magnetic fields of the order of $B = (2 \div 5) \cdot 10^{-6}$ G acting over distances comparable to the radii of the galaxies

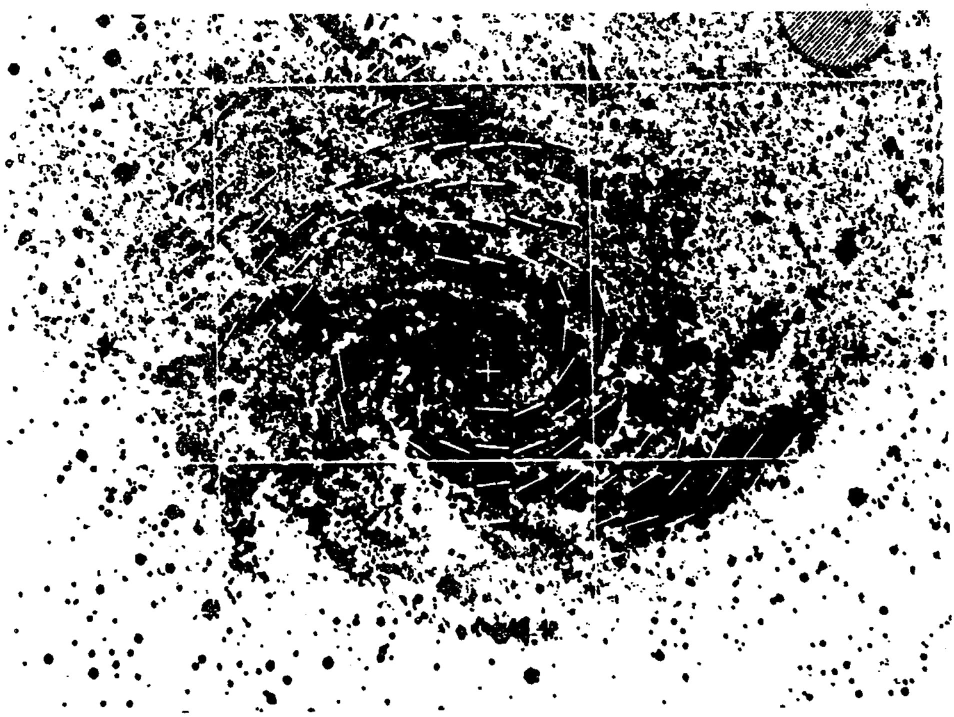

Fig. 4.4. – Directions of the magnetic fields in a typical galaxy.

($r \sim 5 \cdot 10^{22}$ cm). Monopoles would thus start to spiral outward in the galaxies and after times of the order of 10^7 y could be ejected with velocities $v \sim (1 \div 3) \cdot 10^{-2}\, c$. These relatively fast poles would have had the time to encounter several galaxies, where they could be accelerated or deaccelerated. On the average this would cause no net change of energy in the monopole, nor in the field of the galaxies. The poles ejected from galaxies would give rise to an isotropic intergalactic flux of relatively high-energy monopoles.

Like ordinary matter, which prefers being concentrated in galaxies, stars and planets, monopoles also should probably cluster. We may expect to have a sizable fraction of them, with velocities of the order of $10^{-3}\, c$, bound to the Galaxy. Similarly, monopoles with $\beta \sim 10^{-4}$ may be bound to the solar system and could be travelling like little asteroids; some monopoles could also orbit around the Earth.

4.7. *Flux of* GUT *poles arriving on Earth.* – On the basis of what has been said, we could anticipate that on Earth should arrive a flux of cosmic poles having a velocity spectrum whose flux decreases with increasing velocity (fig. 4.5). The minimum pole velocity is equal to the escape velocity (table IV).

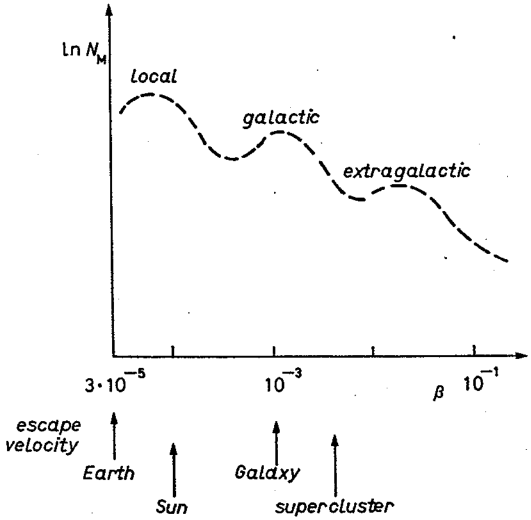

Fig. 4.5. – Sketch of the possibly expected flux of cosmic monopoles arriving on Earth plotted *vs.* the β of the monopoles. The various peaks correspond to poles bound locally, bound to the Galaxy and to the extragalactic flux. Notice that the vertical scale is arbitrary. In the horizontal scale the escape velocities from various astrophysical systems are indicated.

TABLE IV. – *Escape velocities from typical astrophysical systems. The table gives also the values of the monopole kinetic energies for* $m_M = 10^{16}$ GeV. *Note that poles with* $\beta = 10^{-4}$ *may be stopped by the Earth; poles with* $\beta = 10^{-3}$ *may be stopped by a star.*

System	Escape velocity β	Kinetic energy (GeV)
cluster of galaxies	$3\cdot10^{-3}$	$5.0\cdot10^{10}$
Galaxy	10^{-3}	$5.0\cdot10^{19}$
solar system	10^{-4}	$5.0\cdot10^{7}$
Earth	$3.77\cdot10^{-5}$	$6.8\cdot10^{6}$

There may be peaks in the spectrum corresponding to poles trapped locally ($\beta \simeq 10^{-4}$), to poles bound in the Galaxy ($\beta \simeq 10^{-3}$) and to extragalactic poles ($\beta > 10^{-2}$). The extragalactic flux of monopoles should be isotropic, while the lower β fluxes are probably concentrated in the planes of the orbits.

5. – Summary of the properties of magnetic monopoles.

5·1. *Properties based on the Dirac relation.* – In this section we will summarize the main features of magnetic monopoles, which can be obtained from eq. (1.1), assuming $n = 1$ and that the elementary electric charge is that of the electron.

5'1.1. Magnetic charge.

$$g_D = \frac{\hbar c}{2e} = \frac{137}{2} e = 3.29 \cdot 10^{-8} \text{ CGS units}. \tag{5.1}$$

If the elementary electric charge would be that of quarks, with charge 1/3, one would have an elementary magnetic charge three times larger. A similar situation arises if $|n| > 1$. The magnetostatic field near a monopole is shown in fig. 5.1.

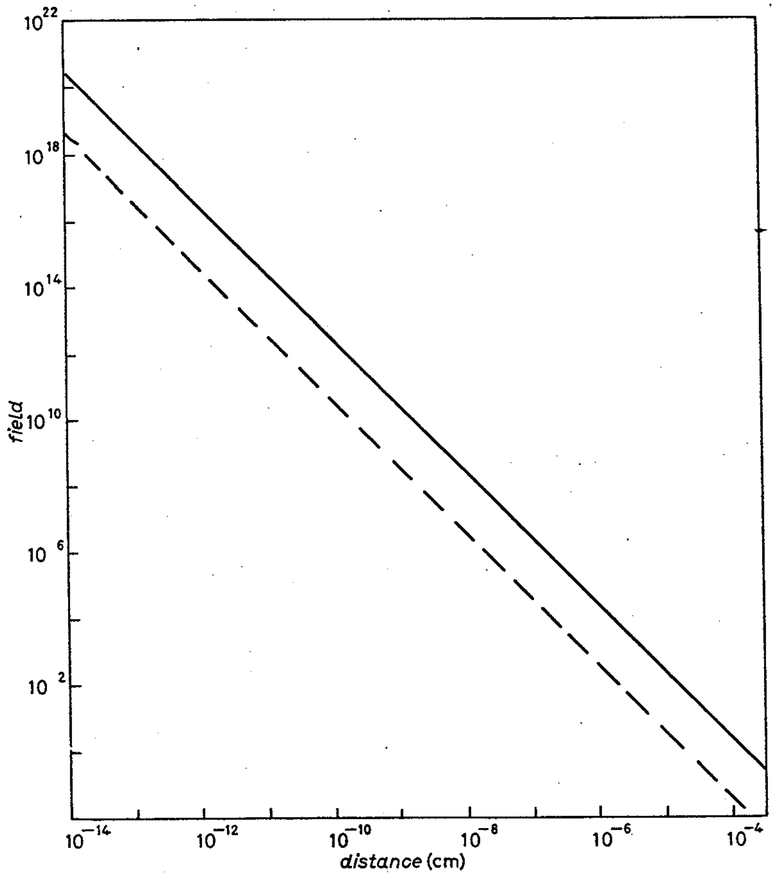

Fig. 5.1. – Magnetostatic field near a magnetic monopole with one unit of Dirac charge (———). For comparison it is also shown the electrostatic field near a unit electric charge (— — —) (both in the Gauss CGS system of units).

5'1.2. Coupling constant. In analogy with the fine-structure constant $\alpha = e^2/\hbar c = 1/137$ one defines a dimensionless magnetic-coupling constant

$$\frac{g_D^2}{\hbar c} = \frac{e^2}{\hbar c}\left(\frac{g_D}{e}\right)^2 = \frac{1}{137}\left(\frac{137}{2}\right)^2 = 34.25\,. \tag{5.2}$$

5·1.3. Energy W acquired in a magnetic field B:

$$W = g_D Bl = 20.5\,\text{keV/G cm}\,. \tag{5.3}$$

Because of the large g-value, monopoles acquire large energies even in modest magnetic fields acting over short distances.

5·1.4. Ionization energy losses for $\beta > 0.04$. The moving monopole creates an electric field which ionizes the medium. The pole behaves as if it has an equivalent electric charge $e_{eq} = g_D \beta n$:

$$\left(\frac{dE}{dx}\right)_m = \left(\frac{dE}{dx}\right)_e \left(\frac{g_D}{e}\right)^2 (n\beta)^2\,, \tag{5.4}$$

where $(g_D/e)^2 = (137/2)^2 = 4700$. For $\beta \geqslant 0.04$ the energy loss is described by eq. (3.8), which may be approximated as follows (in carbon):

$$\left(\frac{dE}{dx}\right)_{m,\,\text{ioniz}} \simeq 0.72(9.0 + \ln \beta^2)\,(\text{GeV g}^{-1}\,\text{cm}^2)\,. \tag{5.5}$$

5·1.5. Energy losses in a nonconductor for $10^{-4} < \beta < 10^{-2}$. In this velocity range the energy loss computed with the Fermi model of the atom is given by (3.10). For carbon

$$\left(\frac{dE}{dx}\right)_{m,C} \simeq 18\beta\,(\text{GeV g}^{-1}\,\text{cm}^2)\,. \tag{5.6}$$

5·1.6. Energy losses in a conductor. For $\beta < 10^{-4}$ only the term due to the conduction electron should be considered (eq. (3.1)). Specializing to aluminium ($v_F = 6.8 \cdot 10^{-3}\,c$, $a = 4 \cdot 10^{-8}$ cm, $T_m = 660\,°\text{C} = 933$ K, $n_c \simeq 3$, $N_{ec} \simeq 1.8 \cdot 10^{23}$ conduction electrons/cm³), one has

$$\left(\frac{dE}{dx}\right)_{m,\,Al} \simeq 130\beta\,(\text{GeV g}^{-1}\,\text{cm}^2)\,. \tag{5.7}$$

Other authors [72M1, 82F1] predict a similar β-dependence, with numerical coefficients which differ by $\sim 30\,\%$: (5.7) saturates for $\beta > 5 \cdot 10^{-3}$ to ~ 1 GeV g^{-1} cm^2.

In the $10^{-4} < \beta < 10^{-2}$ region one should add to (5.7) the contribution of eq. (3.11) with nonconducting electrons:

$$\left(\frac{dE}{dx}\right)_{m,\,Al} \simeq (20 + 130)\beta\,(\text{GeV g}^{-1}\,\text{cm}^{-2})\,. \tag{5.7a}$$

Furthermore, one should add a contribution from the Drell effect.

5.1.7. Drell effect. The energy losses due to the Drell effect for $10^{-4}<\beta<10^{-3}$ are (eq. (3.12) for H)

$$\text{(5.8a)} \qquad \text{in H} \qquad \frac{\mathrm{d}E}{\mathrm{d}x}=370\beta\left(1-\frac{1.4\cdot10^{-8}}{\beta^2}\right)^{3/2}(\mathrm{GeV\,cm^2\,g^{-1}}),$$

$$\text{(5.8b)} \qquad \text{in He} \qquad \frac{\mathrm{d}E}{\mathrm{d}x}=150\beta\left(1-\frac{8.6\cdot10^{-9}}{\beta^2}\right)^{3/2}(\mathrm{GeV\,cm^2\,g^{-1}}).$$

This energy loss is the dominant one in the $10^{-4}<\beta<10^{-3}$ range. The Drell effect has an effective threshold at $\beta_{\mathrm{H}}\sim1.2\cdot10^{-4}$ and $\beta_{\mathrm{He}}\sim9.3\cdot10^{-5}$.

5.1.8. Elastic collisions with atoms and nuclei. For $\beta<10^{-4}$ monopoles can only lose energy in elastic collisions with atoms or nuclei. In the limit of very low velocities the nuclear energy losses in liquid hydrogen are

$$\text{(5.9)} \qquad \left(\frac{\mathrm{d}E}{\mathrm{d}x}\right)_{\text{m-atom}}\simeq 100\ \mathrm{MeV/cm},$$

$$\text{(5.10)} \qquad \left(\frac{\mathrm{d}E}{\mathrm{d}x}\right)_{\text{m-nucleus}}\simeq (0.1+0.3\beta^2)\ \mathrm{MeV/cm}.$$

5.1.9. Energy losses in ferromagnetic materials. A slowly moving monopole may align the magnetic domains of ferromagnetic materials. The energy loss connected with this mechanism becomes relatively large at very low monopole velocities, when monopoles can efficiently align magnetic domains. MARTEMYANOV *et al.* [72M1] found for iron

$$\text{(5.11)} \qquad \frac{\mathrm{d}E}{\mathrm{d}x}=\frac{1.3\cdot10^{-3}}{\beta^2}\ (\mathrm{eV/cm}).$$

Energy losses by hysteresis in ferromagnetic materials should be small ($\leqslant 0.1$ MeV/cm) [82L1].

5.1.10. Nuclear capture. The mean free path for the capture of a nucleus by a moving monopole with $\beta\sim10^{-3}$ is of the order of 200 m of water to capture a proton or of 1 km of earth to capture an aluminium nucleus. It is probable that all cosmic poles arriving on Earth have captured a proton.

5.1.11. Trapping of monopoles in ferromagnetic materials. Magnetic monopoles may be trapped in bulk paramagnetic and ferromagnetic materials by an image force, which, in ferromagnetic materials, may reach the value of $\sim$10 eV/Å (11 eV/Å in iron, 3.5 in magnetite). The binding energy in paramagnetic materials is $\sim$200 eV.

5.1.12. Induced electromotive force. A moving monopole produces an electric field (eq. (3.6)). Thus an electromotive force (eq. (11.1)) and a current (Δi) is induced when a monopole passes through a coil. The case of a normal coil is analysed in subsect. **11.1.3**; for a superconducting coil with N turns and inductance L, one has

$$\Delta i = 4\pi N ng/L = 2\,\Delta i_0\,, \tag{5.12}$$

where Δi_0 is the current change corresponding to a change of one unit of the

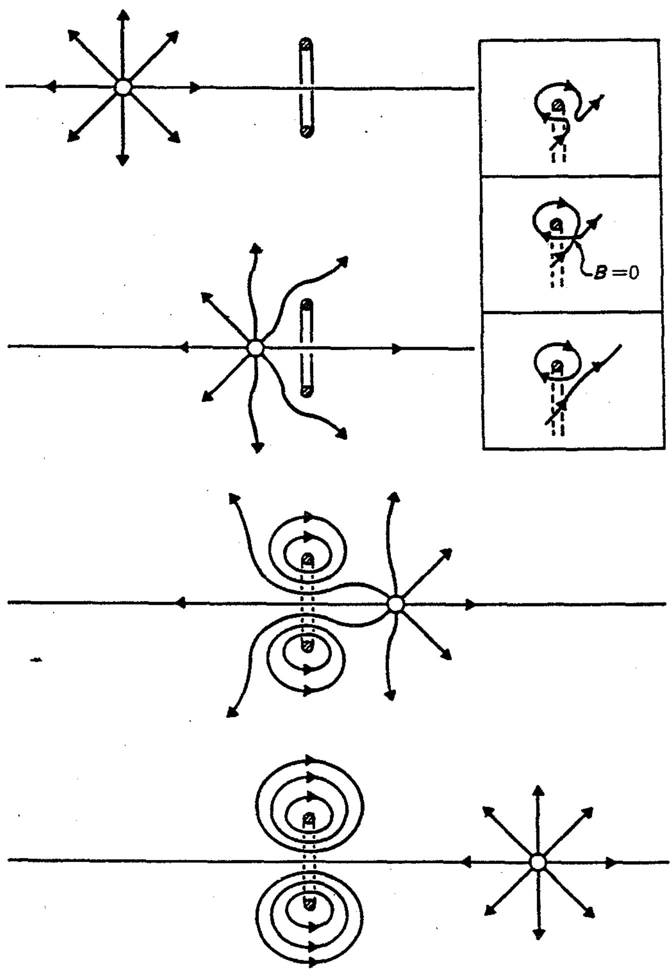

Fig. 5.2. – Illustration of the magnetic-field lines as a monopole passes through a superconducting ring [83C3]. When the pole is still far away from the ring (top view), its magnetic field is the symmetric field of a point magnetic charge. As the pole approaches the superconducting ring, the field is distorted. The distortion continues when the pole passes through the ring, where it leaves some lines of force. After the passage one has the lines of force of a point magnetic charge plus the trapped lines around the coil.

flux quantum of superconductivity, $\Phi_0 = \hbar c/2e$. (In practice $\Delta i \sim 10^{-9}$ A, $L \sim$ few μH, energy $\sim 4 \cdot 10^{-17}$ erg.) Figure 5.3 illustrates the magnetic-field lines as a monopole passes through a superconducting ring [83C3]. The change

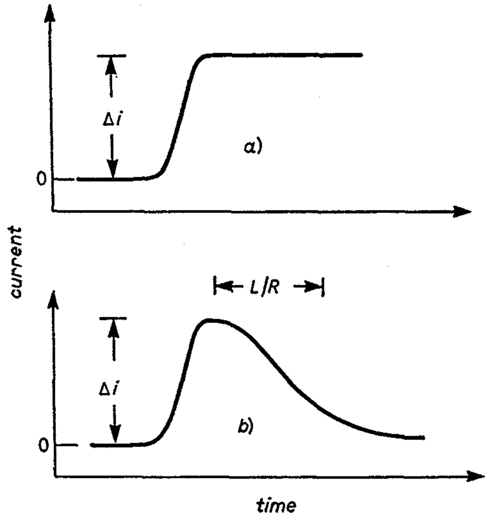

Fig. 5.3. – Illustration of the time variation of the current induced in a coil with self-induction L and resistance R. The rise time of the current is connected to the radius of the coil and to the velocity of the pole, $\Delta t \sim r/\gamma v$. The induced current Δi is persistent in a superconducting coil (a)) and is transient with a characteristic time L/R for a normal coil (b)) [83T2].

in current will occur with a characteristic time given by $b/\gamma v$, where b = radius of coil, v = velocity of monopole. Figure 5.4 illustrates the time variation of the induced current. The change in the current and thus in the field may be observed with a SQUID magnetometer (subsect. **8**'2).

5'2. *Properties of* GUT *monopoles.*

5'2.1. Mass. Grand unified theories of strong and electroweak interactions predict the existence of magnetic monopoles with large masses. Among their most remarkable properties one may recall that GUT poles may carry a screened non-Abelian colour magnetic field and fractional fermion number. Electrically charged dyons may arise as quantum-mechanical excitations of GUT poles and may carry an anomalous electric charge. Though in the following we shall mostly assume a mass $m_M \sim 10^{16}$ GeV for the stable monopole, the situation is theoretically more complex. At the 1983 Monopole Workshop,

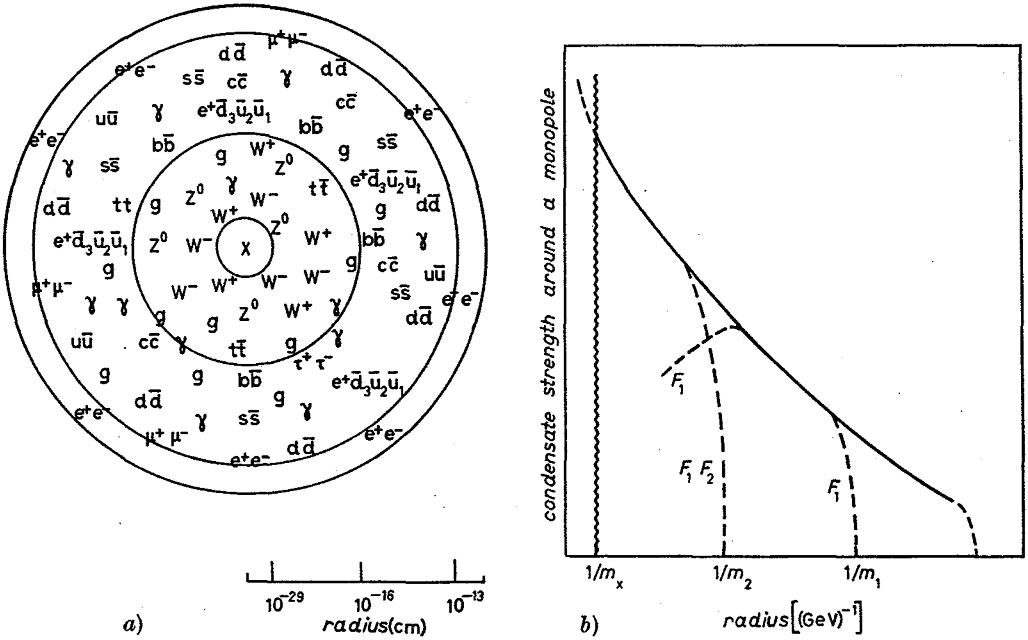

Fig. 5.4. – *a*) Illustration of the GUT monopole structure. The sketch illustrates various regions corresponding to i) grand unification ($r\sim 10^{-29}$ cm; inside this core one may find virtual X-mesons); ii) electroweak unification ($r\sim 10^{-16}$ cm; inside one may find virtual $W^{\pm}$, Z); iii) the confinement region ($r\sim 10^{-13}$ cm; inside one may find virtual γ, gluons and a condensate of fermion-antifermion, 4 and 6 fermion virtual pairs). *b*) Sketch of the $f\bar{f}$ condensate strengths around a monopole. Condensates involving fermions of mass m_f are exponentially damped at radii larger than $1/m_f$. For radii larger than few fm one has the field of a point magnetic charge $B = g/r^2$.

there were discussions about monopoles with

$$(5.13)\qquad \begin{cases} g = g_D\,, & 10^{16} < m_M < 10^{19}\,\text{GeV}\,,\\ g = g_D\,, & m_M \sim 10^4\,\text{GeV}\,,\\ g = 2g_D\,, & 10^{10} < m_M < 10^{16}\,\text{GeV}\,. \end{cases}$$

Moreover, Kaluza-Klein theories may predict $m_M \geqslant 10^{19}$ GeV and very small radii, so that one could ask if the monopole could be a black hole.

5.2.2. Size and structure. The GUT magnetic pole is pictured as having (see fig. 5.4)

a core with a radius $r_c \simeq 1/m_X \simeq 10^{-29}$ cm (the core would be larger for lower-mass monopoles, smaller for higher masses (10^{-32} cm for $m_M \simeq 10^{19}$ GeV));

a region up to $r\sim 10^{-16}$ cm, where virtual W^+, W^- and Z^0 may be present;

a confinement region with $r_{\rm conf} \sim 1$ fm; the monopole may have a chromomagnetic charge confined in the same region as for the colour charges;

a fermion-antifermion condensate region up to $r_f \sim 1/m_f$; the condensate may contain 4 fermion baryon-number-violating terms up to confinement;

for r larger than ~ 3 fm the GUT monopole should behave as a point Dirac monopole, which generates a magnetic field $B = g/r^2$ (fig. 5.1).

One may think that going through the monopole one sees a «small universe», with different regions full of different virtual particles (from the outside: fermion-antifermion, quanta of nonunified forces, particles typical of the unified electroweak interactions and finally the core with X-bosons).

6. – Cosmological and astrophysical bounds on GUT poles.

Several upper limits for the monopole flux were obtained on the basis of cosmological and astrophysical considerations. Most of the bounds have to be considered as rough orders of magnitude only.

6'1. *Limit from the mass density of the Universe.* – The cosmological bound may be obtained requiring that the present monopole mass density be smaller than the critical density ϱ_c of the Universe, that is the minimum density which would close the Universe. The actual matter density of the Universe including the dark matter seems to be somewhat smaller. It is probably a theoretical prejudice to consider that $\varrho_{\rm true} \simeq \varrho_c$. This implies that the observed Hubble expansion of the Universe should not be distorted strongly. In terms of the Hubble constant H_0 and of the gravitational constant G the critical mass density is given by

$$\varrho_c = \frac{3H_0^2}{8\pi G} \simeq 1.9 \cdot 10^{-29} h_0^2 \simeq 1.1 \cdot 10^{-29}\,({\rm g\,cm^{-3}})\,, \tag{6.1}$$

where h_0, with $0.5 < h_0 < 1$, expresses our ignorance on H_0; for numerical estimates the value $h_0 = 0.75$ will be used. If the monopole mass density $\varrho_{\rm M}$ should be smaller than the critical mass density ($\varrho_{\rm M} = n_{\rm M} m_{\rm M} < \varrho_c$) one should have for the monopole number density, $n_{\rm M}$,

$$n_{\rm M} < \frac{\varrho_c}{m_{\rm M}} \simeq 1.2 \cdot 10^{-21}\, h_0^2\,({\rm poles/cm^3})\,. \tag{6.2}$$

The relation between monopole number density and monopole flux F per unit solid angle yields

$$F = \frac{n_{\rm M} v_{\rm M}}{4\pi} = \frac{n_{\rm M} c}{4\pi}\beta < 3 \cdot 10^{-12}\, h_0^2 \beta\,({\rm cm^{-2}\,s^{-1}\,sr^{-1}})\,. \tag{6.3}$$

Figure 6.1 shows the flux upper limit for cosmic poles as a function of the pole mass for $\beta = 10^{-3}$. If the poles are clustered in galaxies like ordinary matter, the limits should be $\sim 10^5$ times less stringent. Figure 6.2 shows the cosmological bound plotted *vs.* pole velocity for several pole masses.

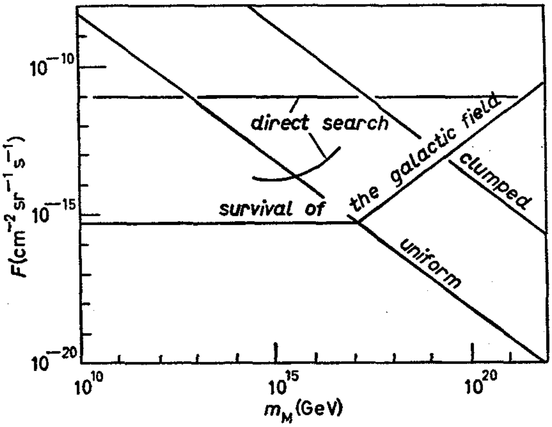

Fig. 6.1. – Cosmological and astrophysical bounds *vs.* the monopole mass for poles with velocity $10^{-3}\,c$. The cosmological bound is given for a uniform density of poles (curve labelled uniform) and for monopoles clustered like ordinary matter (curve labelled clumped). The astrophysical bound was obtained from the survival of the galactic magnetic field. Also indicated are limits from direct searches with induction devices and electronic experiments.

The monopole number density (6.2) may be rewritten in terms of the entropy density $\hat{r} = n_M/\hat{s}$, where $\hat{s} = S/vK$ (see subsect. 4'3). In the matter era one has $\hat{s} \simeq 270\,T^3 \simeq 2s_\gamma \simeq 7n_\gamma$, where s_γ and n_γ are the entropy and number densities of the cosmic electromagnetic radiation. At present $T \simeq 2.7$ K, $n_\gamma \simeq 400$ photons/cm³, $\hat{s} \simeq 2500$ cm^{-3} and

$$\hat{r}_{\text{now}} = \frac{n_M}{\hat{s}} \leqslant 5\cdot 10^{-25}\,h_0^2\,. \tag{6.4}$$

6'2. *Limit from the primordial helium abundance.* – It is possible to derive a bound on the monopole density at the time of the nucleosynthesis (at a temperature $T \simeq 1$ MeV and a cosmic time $t \simeq 220$ s) by requiring that the successful calculation of the primordial helium abundance be preserved until present observations. This implies that the energy density in monopoles $(= n_M m_M c^2)$ be smaller than the energy density in known forms. One has

$$\hat{r}\,(1\,\text{MeV}) = \frac{n_M}{\hat{s}} \leqslant \frac{3}{4}\,\frac{T}{m_M} \simeq 8\cdot 10^{-20}\,. \tag{6.5}$$

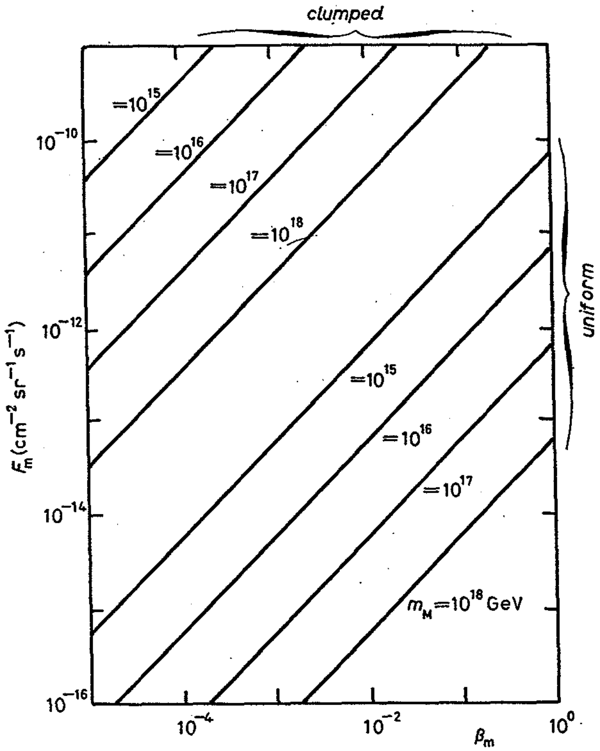

Fig. 6.2. – Cosmological bound plotted *vs.* monopole velocity for several monopole masses ($10^{15} \div 10^{18}$) GeV. The bounds are given for a uniform and for a clumped distribution of monopoles.

6'3. *Limits from galactic, intergalactic and stellar magnetic fields.*

6'3.1. Galactic fields. The Parker limit. Most celestial bodies possess large-scale magnetic fields (fig. 4.4). The magnetic field in our Galaxy is stretched in the azimuthal direction along the spiral arms, and is very probably due to the nonuniform rotation of the Galaxy. This mechanism should generate a magnetic field with a time scale approximately equal to the rotation period of the Galaxy ($\tau \sim 10^8$ y). Since magnetic poles are accelerated in magnetic fields, they would gain energy, which is taken from the stored magnetic energy. An upper bound for the monopole flux may be obtained by requiring that the kinetic energy gained per unit time by the magnetic poles be equal to or smaller than the magnetic energy generated by the dynamo effect. The rate of energy acquired per unit volume by poles in a field B is

$$\frac{\mathrm{d}W_\mathrm{m}}{\mathrm{d}t\,\mathrm{d}v} = \boldsymbol{J}_\mathrm{m} \cdot \boldsymbol{B}\,, \tag{6.6}$$

where the magnetic-current density is $\boldsymbol{J}_m = g n_M \boldsymbol{v}_M$ and $\boldsymbol{v}_M$ is the average pole velocity. The magnetic energy density generated per unit time is

$$\frac{dW_D}{dt\,dv} = \frac{\varrho_B}{\tau_B} = \frac{B^2}{8\pi\tau_B}, \tag{6.7}$$

where $\varrho_B = B^2/8\pi$ is the energy density in a magnetic field $\boldsymbol{B}$ and τ_B is the typical time to regenerate the magnetic field. The condition $\boldsymbol{J}_m \cdot \boldsymbol{B} < B^2(8\pi\tau_B)^{-1}$ leads, assuming that v_M is parallel to B over large distances, to

$$n_M < \frac{B}{8\pi\tau_B g v_M}, \tag{6.8}$$

$$F = \frac{n_M v_M}{4\pi} \leqslant \frac{B_{gal}}{32\pi^2\tau_B g} = \simeq 10^{-16} \text{ poles cm}^{-2}\,\text{s}^{-1}\,\text{sr}^{-1}, \tag{6.9}$$

where $B_{gal} \simeq 3\cdot10^{-6}$ G. This is the well-known Parker bound obtained assuming that v_M is parallel to B over large distances. This cannot be exactly correct. Thus monopoles should acquire smaller energies and so the corresponding energy is removed from the galactic field. TURNER, PARKER and BOGDAN [82T1] examined this problem in more detail and found that, as long as monopole velocities are below a certain critical value β_c, the approximation of neglecting the directionality of the magnetic field is reasonable, while for $\beta > \beta_c$ one has to consider the angle between $\boldsymbol{\beta}$ and $\boldsymbol{B}$. The critical velocity may be estimated as the velocity that a monopole acquires in a typical galactic coherent length $l_c \sim 10^{21}$ cm, $\beta_c = (2gBl_c/m_M c^2)^{1/2} \simeq 3.5\cdot10^{-3}$. The result is

$$\begin{cases} \text{for } \beta \leqslant 3\cdot10^{-3}: & F_G \leqslant 10^{-15}\,\text{cm}^{-2}\,\text{s}^{-1}\,\text{sr}^{-1}; \\ \text{for } \beta > 3\cdot10^{-3}: & F_G \leqslant 10^{-15}\,(\beta/\beta_c)^2\,\text{cm}^{-2}\,\text{s}^{-1}\,\text{sr}^{-1}. \end{cases} \tag{6.10}$$

The one-order-of-magnitude change between (6.9) and (6.10) should not be worried about, since most astrophysical limits represent order of magnitude only.

6.3.2. Limit from the intergalactic field. Stronger limits may be obtained applying the Parker argument to the intergalactic magnetic field and to the magnetic field of some particular stars. RAPHAELI and TURNER [83R1] assumed the existence in the local group of galaxies of an intercluster field $B_{IC} \sim 3\cdot10^{-8}$ G with a regeneration time $\tau_{IC} \sim 10^9$ y. Applying the same reasoning discussed in the previous section, they obtained

$$\begin{cases} \text{for } \beta < 10^{-3}: & F_{IC} < 2\cdot10^{-19}\,\text{cm}^{-2}\,\text{s}^{-1}\,\text{sr}^{-1}, \\ \text{for } \beta > 10^{-3}: & F_{IC} < 2\cdot10^{-19}\dfrac{\beta}{10^{-3}}\,\text{cm}^{-2}\,\text{s}^{-1}\,\text{sr}^{-1}. \end{cases} \tag{6.11}$$

The above hypotheses for B_{IG}, for τ_{IG} and for the whole mechanism are clearly more questionable than those used for our Galaxy.

6'3.3. Limit from peculiar $A4$ stars. Peculiar $A4$ stars have their magnetic fields in the direction opposite to that expected from their rotation. This may be explained assuming that the fields have been «frozen in» at the formation time of the stars, estimated to be $t_s \sim 5\cdot 10^8$ y ago.

A typical galactic monopole with $\beta \sim 10^{-3}$ should lose enough energy when traversing an $A4$ star to be stopped; thus the number of monopoles in the star will increase with time (neglecting $M\bar{M}$ annihilations inside the star). The poles would be accelerated in the magnetic field, which should, therefore, decrease with increasing time. Repeating the Parker argument [83R2] one has for the number density of monopoles in the star an equation similar to (6.8) with $B \simeq 10^3$ G and $\tau_B \simeq 5\cdot 10^8$ y. The monopole velocity is now a drift velocity, which may be estimated equating the rate of energy loss of the monopole in the star to the rate of energy gained in the magnetic field ($w = gB$). The energy lost in the star medium may be obtained treating the star as an electron gas: $\mathrm{d}E/\mathrm{d}x \simeq 0.48\beta_d$ erg/cm. This leads to a drift velocity $\beta_d = gB/0.48$. The total number of poles in the star (given approximately by the pole number density times the volume of the star) should be equal to that determined by integrating the arriving flux on the surface of the star over its lifetime

$$N_t = \frac{4}{3}\pi R_s^3 n_{Ms} = F 4\pi t_s\; R_s^2\,,$$

which leads to

$$F = \frac{n_{Ms} R_s}{3\pi t_s} < 3\cdot 10^{-20}\,\mathrm{cm}^{-2}\,\mathrm{s}^{-1}\,\mathrm{sr}^{-1}\,, \tag{6.12}$$

using $R_s = 10^{11}$ cm. This limit should apply to the flux of poles with $\beta < 3\cdot 10^{-3}$, since faster poles would pass through the star without stopping. It is a strong limit, but it is not clear how good are all the assumptions.

6'3.4. Limitations of the previous analyses. WASSERMAN *al.* [84W1] reported recently the results of numerical simulations designed to evaluate the possibility that magnetic poles are a prominent constituent of the Galaxy. They assumed that the Galaxy consists of a stellar disk made of ordinary matter, surrounded by a spherical halo containing equal numbers of poles and antipoles. They further assumed that in the plane of the Galaxy there is a smooth magnetic field, generated by the dynamo effect, not by magnetic charges. In practice they modelled the galactic field as if it were made by a toroidal solenoid of height $h \simeq R_{\mathrm{Galaxy}}$, as sketched in fig. 6.3. The total mass of the pole-antipole halo was assumed to be twice that of the stellar disk.

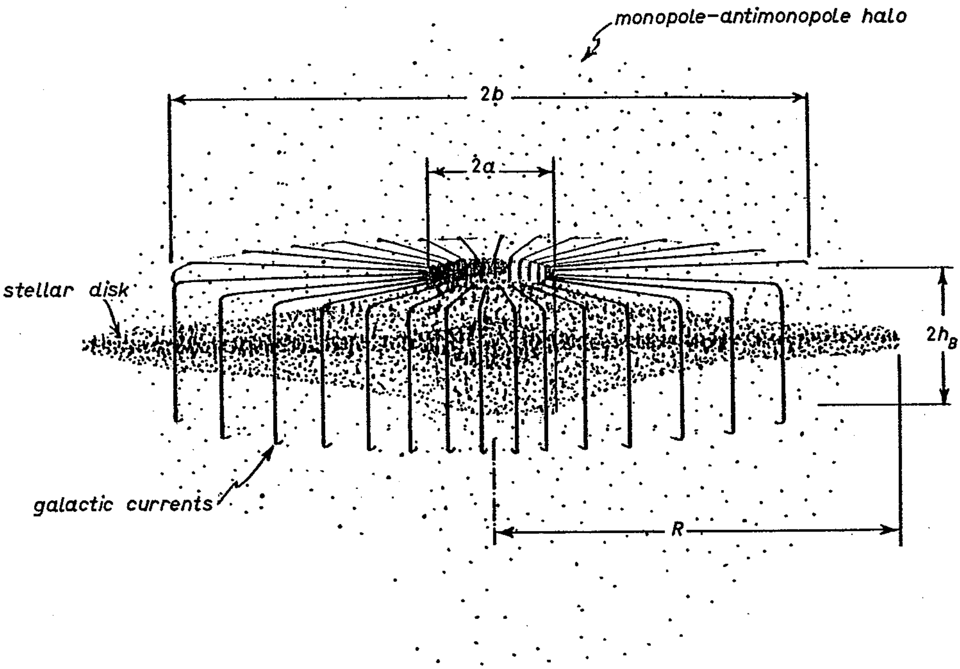

Fig. 6.3. – Model of the Galaxy, made of a stellar luminous disc and of a monopole-antimonopole halo. The galactic magnetic field is assumed to be a toroidal field arising from galactic currents in the coil [84W1].

Nevertheless, many of their conclusions can be applied to the general case in which only a fraction of the total halo mass is in magnetic monopoles. (They further used $m_{\mathrm{M}} = 7 \cdot 10^{19}$ GeV, but what is important is the total mass density of poles.)

The time evolution of the magnetic field was computed using the complete Faraday law, that is

$$\text{(6.13)} \qquad \operatorname{rot} \boldsymbol{E} = -\frac{1}{c}\frac{\partial \boldsymbol{B}}{\partial t} + \frac{4\pi}{c}\boldsymbol{J}_{\mathrm{m}},$$

where $\boldsymbol{J}_{\mathrm{m}}$ is the magnetic-current density. In the simulation the galactic electric currents were assumed to be driven by a battery of constant strength and subject to resistive decay with a characteristic time scale t_B. The magnetic current $I_{\mathrm{m}}(t)$ through any single loop in the solenoid was computed from the orbits of individual magnetic charges.

Figure 6.4 shows the numerical results for the time dependence of $B(t)$, the magnetic field at a radius $r = 0.5\,R_{\text{Galaxy}}$ (inside the solenoid), and for the magnetic current $I_{\mathrm{m}}(t)$. The results of the simulation indicate that both $B(t)$ and $I_{\mathrm{m}}(t)$ oscillate with a period approximately equal to the rotation period of the Galaxy. This oscillatory behaviour contradicts the basic hypothesis under-

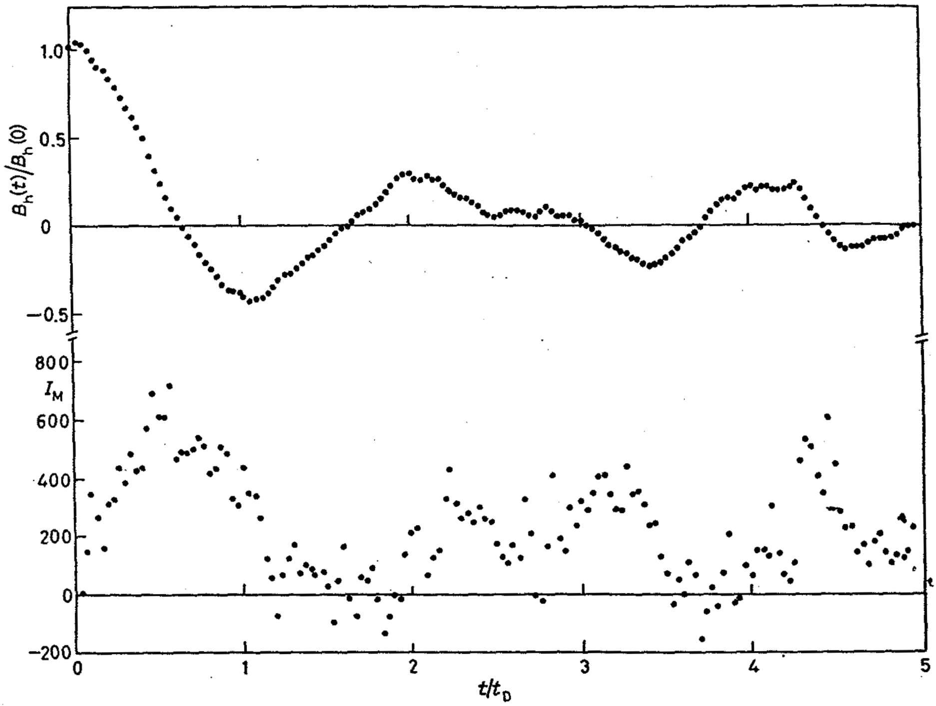

Fig. 6.4. – Galactic magnetic field and magnetic current plotted *vs.* time (t_D is the revolution time of the galaxy) [84W1].

lying the Parker bound, that monopoles accelerated by the galactic field drain energy permanently from it. In practice one has a back-action of the pole-antipole plasma on the magnetic field; this back-action is ignored in the derivation of the Parker bound and other similar bounds, where the time dependence of $\boldsymbol{B}$ is not taken into account in a self-consistent way. WASSERMAN *et al.* conclude that the Parker bound is not valid in general (*) and that the effective time decay of the magnetic field is longer, thus relaxing the bound (probably by an order of magnitude).

6'4. *Limits from terrestrial properties.*

6'4.1. Monopoles trapped in the Earth. Cosmic magnetic monopoles may be stopped by the Earth if they have $\beta < 10^{-4}$. The number of poles

(*) According to WASSERMAN *et al.* the magnetic-field decay is due to higher-order effects, like Landau damping, magnetic charges leaving the finite volume in which $\boldsymbol{B}$ is confined and radial drift of the magnetic plasma due to the centrifugal acceleration of individual charges.

stopped by the Earth over the entire Earth history should be

$$N_M = FS\Omega t = F4\pi^2 R_E^2 t_E \,, \tag{6.14}$$

where $R_E = 6.5\cdot 10^8$ cm is the Earth radius and $t_E \simeq 5\cdot 10^9$ y is the Earth lifetime.

Massive monopoles are affected by both gravity and magnetism. The magnetic and gravitational forces on a GUT pole are about equal at a radius $R = 0.18 R_E$, that is well inside the Earth core [80C1]. The poles stopped by the Earth will reach thermal velocities and will fall to the Earth core, unless they get bound in a ferromagnetic material. The fate of poles in the Earth core depends primarily on the features of the magnetic field in the core.

6.4.2. Magnetic energy dissipated by poles trapped in the Earth. The monopoles trapped in the Earth core should have velocities v_c determined by the balance between their kinetic energy and the potential energy in the Earth magnetic field: $\beta_c \simeq 1.2\cdot 10^{-5}$.

An upper limit on the number density of poles in the core (n_{Mc}) is obtained requesting that the magnetic energy dissipated by the monopoles trapped in the core by their doing work against the Earth's magnetic field be less than the total available magnetic energy stored during the characteristic growth time τ_{BE} of the geomagnetic field. We obtain again eq. (6.8), which in the present case yields $n_{Mc} < B_c/8\pi\tau_{BE} g v_c \simeq 1.1\cdot 10^{-9}$ poles/cm³. The total number of poles present in the Earth core ($r_c \simeq r_E/2$),

$$M_{M\,tot} < n_{Mc} v_c = n_{Mc} \frac{4}{3}\pi R_c^3 \simeq 1.5\cdot 10^{17} \,, \tag{6.15}$$

should approximately equal the total number of poles in the whole Earth. The ratio of the total number of monopoles to the total number of nucleons in the Earth ($N_{N\,tot} \simeq 3.7\cdot 10^{51}$) should be $(N_M/N_N)_{tot} < 4\cdot 10^{-35}$, from which

$$F < \frac{N_{M\,tot}}{4\pi^2 R_E^3 t_E} \simeq 3\cdot 10^{-19}\ \text{cm}^{-2}\,\text{s}^{-1}\,\text{sr}^{-1} \,. \tag{6.16}$$

6.4.3. Pole-antipole annihilation in the Earth core. As an example of other limits we shall recall that obtained by CARRIGAN [80C1, 80C2] on the number of poles trapped in the Earth from an estimate of the heat flow out of the Earth's core due to pole-antipole annihilations during periods of magnetic-field reversals. Assuming that $\sim 25\,\%$ of the observed heat flow come from pole-antipole annihilation, that the surface heat flow is $3\cdot 10^{20}$ erg s^{-1} and that only a fraction of poles could annihilate (say 10^{-2}), he obtained an upper limit for the monopole to baryon ratio at $\sim 2\cdot 10^{-28}$, corresponding to a flux of poles with $\beta < 10^{-4}$ of $F < 3\cdot 10^{-13}\,\text{cm}^{-2}\,\text{s}^{-1}\,\text{sr}^{-1}$. It is difficult to ascribe a precision to these numbers based on such speculative mechanisms.

6'5. *Monopole term in the magnetic fields of celestial bodies.* – For the Sun, the Earth, the Moon and other bodies of the solar system exist now detailed measurements of the radial component of the magnetic field and thus of the net magnetic flux Φ_B from that body. One can, therefore, check and measure a possible monopole term in the magnetic field. Such a monopole term could, for instance, arise from the presence in that body of an excess ΔN_{M} of magnetic monopoles of one sign, or from a possible magnetic structure of the proton or neutron. In formulae

$$\Phi_B = 4\pi R^2 B_{\text{R}} = 4\pi(g\,\Delta N_{\text{M}} + g_{\text{p}} N_{\text{p}} + g_{\text{n}} N_{\text{n}})\,, \tag{6.17}$$

from which

$$g\,\Delta N_{\text{M}} + g_{\text{p}} N_{\text{p}} + g_{\text{n}} N_{\text{n}} = B_{\text{R}} R_{\text{R}}^3\,, \tag{6.18}$$

where R is the radius of the celestial body, B_{R} is its surface radial magnetic field, g_{p} and g_{n} the possible magnetic charges of the proton and of the neutron. In practice formula (6.18) will yield an upper limit either for ΔN_{M} (that is the excess monopoles of one charge) or for the magnetic charge of the proton (g_{p}) or neutron (g_{n}).

6'5.1. The magnetic-monopole term in the Sun. In 1972 WILCOX noted that solar data indicated a net outward magnetic flux from the Sun [72W2, 74S1]. The observations concerned the quiet periods of the Sun (with a minimum of sunspots). The net outward magnetic flux corresponds to a radial field of ~ 1 G at the surface of the Sun. From (6.18) assuming $g_{\text{p}} = g_{\text{n}} = 0$, we have a limit on an excess of north poles

$$\Delta N_{\text{M}} \leqslant \frac{(B_{\text{R}} R^2)_{\text{Sun}}}{g} \simeq 1.5\cdot 10^{29}\ \text{poles} \tag{6.19}$$

or to a ratio ($N_{\text{N Sun}} = 1.2\cdot 10^{57}$ nucleons) $\Delta N_{\text{M}}/N_{\text{N}} \leqslant 1.2\cdot 10^{-28}$ poles/nucleon.

ALVAREZ [82A5] speculated that, if an excess of north poles existed in the Sun, they had to have masses of the order of 10^{12} GeV in order to balance their gravitational attraction to the Sun with their mutual magnetic repulsion. An alternative possibility could be that $g_{\text{p}} \neq 0$ (the Sun contains 73 % free protons and 25 % helium; one can assume that it is made only of protons). In this case

$$g_{\text{p}} \leqslant \frac{(B_{\text{R}} R^2)_{\text{Sun}}}{N_{\text{p}}} \simeq 4\cdot 10^{-36}\ \text{CGS units}\,. \tag{6.20}$$

6·5.2. The Moon. Using magnetometer observations aboard the satellite Explorer 35 orbiting the Moon, SHATTEN [83S1] made measurements of the surface magnetic fields and thus of the net magnetic flux from the Moon. He found $B \leqslant 10^{-6}$ G and $\Phi_B \simeq B\pi R^2_{\text{Moon}} \leqslant 1.1 \cdot 10^{11}$ G cm². Thus one has

$$\Delta N_{\text{M}} < 9 \cdot 10^{17} \text{ poles}, \qquad N_{\text{M}}/N_{\text{N}} < 2 \cdot 10^{-32} \text{ poles/nucleon} \tag{6.21}$$

or $(g_{\text{p}} + g_{\text{n}})/2 < 7 \cdot 10^{-4}$ CGS units.

Notice that these good limits are obtained because the Moon has no detectable magnetic-dipole field and because $g_{\text{p}} \sim B_{\text{R}} \times R^2/m$ with R^2/m differing at most by two orders of magnitude for the different bodies of the solar system.

6·5.3. The Earth. The above arguments may be repeated for the Earth $(B_{\text{r}} < 0.1\,\text{G})$. One obtains

$$\Delta N_{\text{M}} < 1.3 \cdot 10^{24} \text{ poles}, \qquad \Delta N_{\text{M}}/N_{\text{N}} < 3 \cdot 10^{-28} \text{ poles/nucleon} \tag{6.22}$$

or

$$\frac{g_{\text{p}} + g_{\text{n}}}{2} < 1.2 \cdot 10^{-35} \text{ CGS units}. \tag{6.23}$$

7. – Experimental searches for classical monopoles.

In the early 1970's, the « classical » monopole was considered to be a member of the family of « well-known undiscovered objects ». Searches were made at every new higher-energy accelerator, in cosmic rays and in bulk matter [70G1].

7·1. *Accelerator searches.* – If monopoles could be produced at high-energy accelerators, they would be highly relativistic; therefore, they would ionize heavily. Broadly speaking, the searches for free magnetic poles produced at accelerators may be classified into two groups: i) *direct detection* of monopoles, immediately after their production in high-energy collisions; ii) *indirect searches*, where monopoles are searched for a long time after their production. A broad class of experiments could be classified as indirect.

7·1.1. Direct searches. Examples of direct searches are the recent experiments performed with track-etch detectors at SLAC [82K2], at PETRA [83M2], at the CERN ISR [75G1, 78H1] and at the CERN $\text{p}\bar{\text{p}}$ collider [83A4]. A set of thin plastic sheets of CR39 or of kapton or of nitrocellulose and/or of makrofol E (lexan) surrounded an intersection region. Kapton was placed inside the vacuum chamber, the other plastics outside. Heavily ionizing magnetic poles produced in e^+e^-, pp or $\bar{p}p$ collisions should have crossed some of the plastic sheets. One of the sheets was developed « strongly » and scanned quickly with one of the methods described in subsect. 3.12; if a signal was found, a second sheet was developed « lightly » and was scanned with optical microscopes.

The experiments at the e^+e^- storage rings placed an upper-limit cross-section of $\sim 10^{-37}$ cm^2, which is about three orders of magnitude smaller than the QED cross-section for point particles. These experiments would exclude poles with masses up to 16 GeV. The new experiment at the CERN $p\bar{p}$ collider, using kapton foils inside the vacuum chambers and CR39 outside, established an upper limit of $\sigma \leqslant 3 \cdot 10^{-32}$ cm^2 for monopoles with masses up to 150 GeV.

7'1.2. Indirect searches. Examples of indirect searches at high-energy accelerators are those which have been performed at the CERN ISR [78C1], IHEP [72G1], Fermilab [73C1, 74C1, 75E1], CERN SPS [83B9] and at other lower-energy accelerators [61F1, 63A1, 66A1, 81G1] using ferromagnetic materials. For instance, in the experiment at the CERN SPS, the 400 GeV protons interacted (before reaching a beam dump) in a series of targets made of compacted ferromagnetic tungsten powder. The poles produced in high-energy pp, pn and also $\pi\mathcal{N}$ collisions should have lost quickly their energy and be brought to rest inside the target, where they are assumed to be bound. More specifically, in this experiment the monopoles should be trapped in one of the small powder pieces of ferromagnetic tungsten. This should avoid the possibility of monopole-antimonopole annihilations. Later on the targets were placed in front of a pulsed solenoid, capable of giving a magnetic field of more than 200 kG. This should have been large enough to extract (at $\sim$ 50 kG) and accelerate the monopoles, which should have been detected in nuclear emulsions and in plastic sheets.

In this sort of experiments one can in principle obtain very good cross-section upper limits, since one can integrate the production over long time intervals. But one has to guess the behaviour of monopoles in matter. In fact, each experimental group took special precautions to avoid possible pitfalls; examples of these precautions are the above-mentioned segmentation of the targets, the use of stripper foils before acceleration, in order to dislodge the paramagnetic molecules which may attached to a monopole, etc.

Figure 7.1 summarizes schematically, as a function of the monopole mass, the production cross-section upper limits (at the 95 % c.l.) in $p\mathcal{N}$ and e^+e^- collisions. Figure 7.2 summarizes the same limits as a function of the monopole magnetic charge. Solid lines refer to « direct » measurements, dashed lines to « indirect » measurements at high-energy accelerators. In fig. 7.3 are also shown dotted lines which refer to cross-sections obtained from cosmic-ray experiments. Table V gives a summary of the recent searches at the highest-energy accelerators.

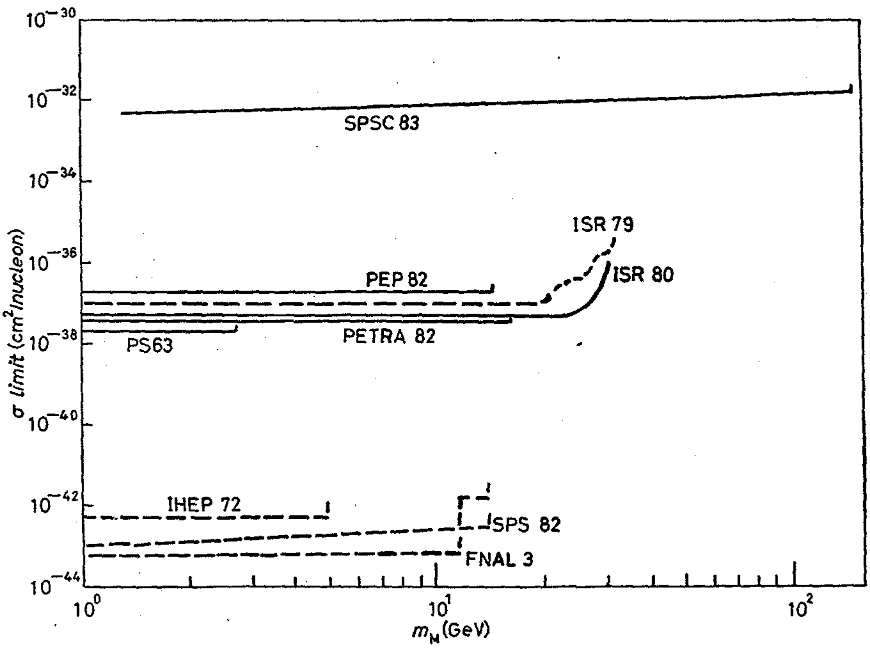

Fig. 7.1. – Compilation of upper limits for «classical»-magnetic-monopole production (at 95% c.l.) obtained at high-energy accelerators plotted *vs.* monopole mass. Solid and dashed lines refer to «direct» and «indirect» measurements (see text). The new limits from the SPS $p\bar{p}$ collider ($\sigma < 3 \cdot 10^{-32}$ cm^2) extend up to 150 GeV.

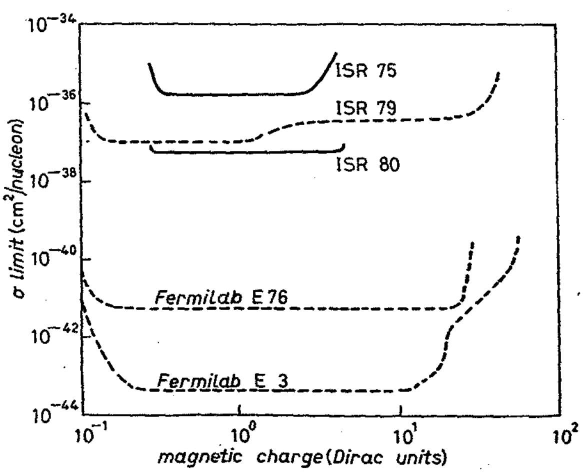

Fig. 7.2. – Compilation of upper limits for classical-monopole production (at 95% c.l.) in pp and p-nuclei collisions at accelerators plotted *vs.* magnetic charge. Solid and dashed lines refer to «direct» and «indirect» measurements (see text).

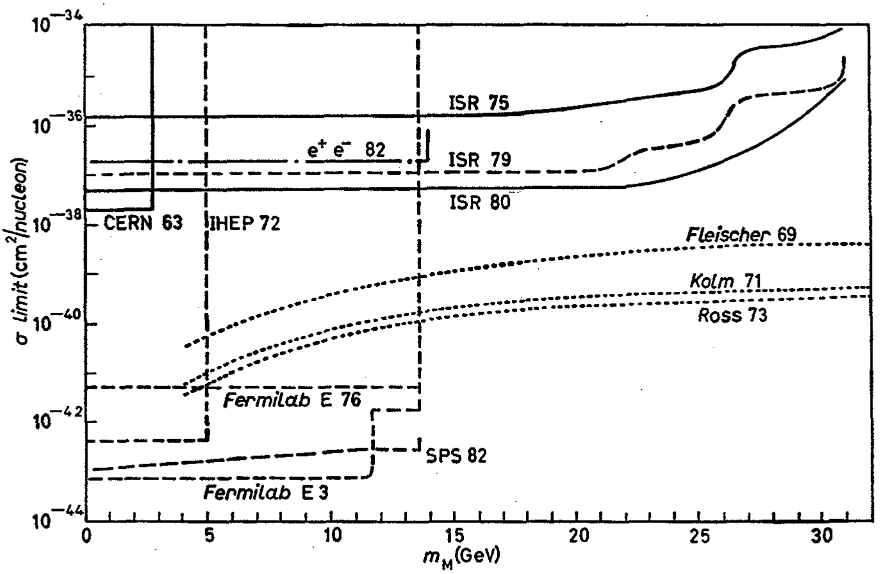

Fig. 7.3. – Compilation of upper limits for classical-magnetic-monopole production plotted *vs.* monopole mass. Solid and dashed lines refer to « direct » and « indirect » measurements at accelerators; dotted lines refer to cosmic-ray experiments.

TABLE V. – *Recent experimental searches for « classical monopoles » at the highest-energy accelerators.*

Accel-erator	Col-lision	$\sqrt{s}$ (GeV)	Tech-nique	Mass (GeV)	Range of magnetic charge (g_D)	Cross-section upper limit (cm^2)	Refer-rence
PEP	e^+e^-	29	CR39	< 14	$Z/\beta > 20$	10^{-37}	[82K2]
PETRA	e^+e^-	40	kapton	< 20	$0.8 \div 3$	$5 \cdot 10^{-38}$	[83M2]
SPS	$p\mathcal{N}$	28	W-grains	< 14	$0.1 \div 20$	10^{-43}	[83B9]
SPS col-lider	$\bar{p}p$	540	kapton foils	< 150	$0.8 \div 3$	10^{-32}	[83A4]

7·2 *Searches in the cosmic radiation.* – Searches for a flux F of *fast* magnetic monopoles were made using counters, track-etch detectors and nuclear emulsions. One assumed that poles could have been primordial or could have been produced in the upper atmosphere by energetic cosmic rays.

7·2.1. Searches with electronic detectors. Most of these searches were aimed at detecting lowly ionizing quarks at sea-level and at mountain altitude [78G1]. The information on magnetic poles was only indirect based on a reanalysis of the data. The experimental upper limits were modest, $F < 7 \cdot 10^{-11}\ \text{cm}^{-2}\ \text{s}^{-1}\ \text{sr}^{-1}$.

7'2.2. Searches with emulsion and track-ecth detectors. In 1975 a monopole candidate from a high-altitude, balloon-borne stack of plastic detectors, nuclear emulsions and a Čerenkov detector was reported [75P1, 78P1]. The detector had an area of 18 m², was quite elaborate (35 layers of lexan and 3 of nuclear emulsion) and was flown for 15 days. The main purpose of the experiment was the search for heavy nuclei, with $20 \leqslant Z \leqslant 83$, in the cosmic radiation. After a long debate the authors concluded that they had an unusual event, which could be i) a supermassive particle with $\beta \simeq 0.4$, $Z \simeq 95$ and $m > 10^3$ GeV; ii) a fast antinucleus with $Z/\beta \simeq -110$, $76 \leqslant |Z| < 96$; the antinucleus fragmented and lost one or two charges; iii) a very fast nucleus with $Z \simeq 112$, $\beta \geqslant 0.99$. Because of inconsistencies in the various detector readings, the authors excluded a monopole (*). From this exposure and from subsequent ones [81B1], one had an upper limit $F < 2 \cdot 10^{-13}$ cm^{-2} s^{-1} sr^{-1}.

7'2.3. Searches for ancient tracks in mica and obsidian. As stated in subsect. 3'12, mica and obsidian are track-etch detectors with high thresholds. Within this limitation, flux upper limits of $F < 10^{-19}$ cm^{-2} s^{-1} sr^{-1} in mica and $F < 3 \cdot 10^{-18}$ cm^{-2} s^{-1} sr^{-1} in obsidian were reported. These good limits were obtained because the materials had ages of approximately $2 \cdot 10^8$ y. The area scanned with optical microscopes was 380 cm² (see also subsect. 8'5.6).

7'2.4. Searches for poles drifting in the atmosphere. Magnetic poles from outer space or produced by cosmic rays at the top of the atmosphere may stop at sea-level if they are light and if their kinetic energy is not too high. If their mass is small, they could drift slowly in the Earth magnetic field. In some experiments it was assumed that the poles could be drifting in the atmosphere and could be sucked and accelerated by the magnetic lines of solenoids (for which the lines of force of the magnetic field were mostly supplied by the Earth magnetic field). Their detection would have been performed by counters or nuclear emulsions or track-etch detectors [58G1, 61F1, 65C1, 81B1]. The estimated upper limit for a flux of poles drifting in the atmosphere is $F \leqslant 10^{-15}$ cm^{-2} s^{-1} sr^{-1}.

7'3. *Searches in bulk matter.* – Several searches for magnetic monopoles trapped in bulk matter have been performed. In order to have a sensitive search, one has to establish where monopoles would stop, where they would be trapped and then device a sensitive method of detection. Classical monopoles were thought to be produced mostly by cosmic rays and to have relatively low kinetic energies. Thus they could stop at the surface of the Earth (or of the

---

(*) But they added that the event could also be compatible with a monopole with $\beta \simeq 0.4$, $n = 2$, $m > 10^{11}$ GeV; they said that « such a large mass is not excluded by theory; but is perhaps offensive ».

Moon), where they could be trapped in ferromagnetic materials (also in some paramagnetic materials). Samples of materials were passed through a superconducting loop, or placed in a high-field pulsed magnet, which would extract and accelerate the poles; these could have been detected in nuclear emulsions or counters.

An experiment used as detector a superconducting coil in which an electric field, and thus a current change, would be induced by a magnetically charged particle present in a sample which was moved through the coil [71E1, 74K1]. Using multiple traversals of the sample, the proper sensitivity was achieved. Samples of 20 kg of lunar material, several kilograms of magnetite from Earth mines and 2 kg of meterorites were used. The authors placed a limit of less than $2\cdot 10^{-4}$ monopoles per gram of lunar material. Assuming a constant monopole flux over the long time during which the Moon remained unaltered, they estimated a pole flux $F < 8\cdot 10^{-18}$ poles $cm^{-2}\,s^{-1}\,sr^{-1}$. This flux limit applies to poles of small mass and becomes less significant for poles with higher kinetic energies (it is irrelevant for kinetic energies $> 10^{8}$ GeV). Assuming instead, that monopoles could be produced by cosmic rays, the cross-section upper limits shown in fig. 7.3 were obtained.

Another group searched for monopoles in magnetite (from a surface mine), from ferromanganese nodules (from deep ocean sediments) and from sea water using a lay-out similar to the one described in subsect. 4'1.2 [69F1, 69F2, 76C2]. The poles should have been extracted, accelerated and sent towards a detector by a large magnetic field (pulsed or continuous). The detectors consisted of plastic sheets of lexan and nitrocellulose. While the field was sufficient to extract all poles, it would provide poles with sufficient velocities to produce ionization only if the pole masses were $< 10^{4}$ GeV. The experiment used 7.7 kg of material, having an age of approximately $1.6\cdot 10^{7}$ y. The authors estimated that this corresponds to a flux $F < 10^{-19}\,cm^{-2}\,s^{-1}\,sr^{-1}$ if the poles would have stopped at the surface of the Earth.

7'4. *Multi-γ events.* – Five peculiar photon showers were found in nuclear plates exposed to high-altitude cosmic rays [54S1, 55S1]. The five events are characterized by a very energetic narrow cone of tens of γ-rays, without any incident charged particle. The total energy in the photons is of the order of 10^{11} GeV. The radial spread of photons $\big((10^{-3}\div 10^{-4})\,\text{rad}\big)$ suggests a c.m. velocity corresponding to $\beta \gtrsim 10^{3}$. The energies of the photons in the overall c.m. system are very small, orders of magnitude too low to have π^0 decays as their source.

One of the possible explanations of these events could be the following: a high-energy γ-ray, with energy $\gtrsim 10^{12}$ eV, produces in the plate a pole-antipole pair, which then suffers bremsstrahlung and annihilation producing the final multi-γ events.

Experiments performed at the ISR and at Fermilab failed to observe these multigamma events [73C2, 75B1, 82D3]. The ISR experiment, at $E_{\text{c.m.}} = 53$ GeV, placed an upper-limit cross-section of 10^{-37} cm^2.

7'5. *Relevance of «classical» pole searches for larger-mass poles.* – As we have seen, classical monopoles have been searched in many ways, using different techniques. The experiments yielded null results; the significance in terms of production upper-limit cross-sections is shown in fig. 7.1 to fig. 7.3; in terms of flux limits in the cosmic radiation the significance is given in the third column of table VI. We shall now briefly discuss the relevance of these searches as searches for superheavy monopoles, in particular for poles with masses $m_M \sim 10^{16}$ GeV. These cannot be produced at any accelerator and are expected to have low velocities and high kinetic energies. Poles with masses $m_M \sim 10^4$ GeV would be in an intermediate situation. Table VI gives a summary of the searches, which will now be commented. Clearly searches at accelerators are relevant only for the production of poles with mass $m_M < 200$ GeV.

7'5.1. Measurements of poles as a flux in the cosmic radiation.

a) Experiments performed with counters were tuned to fast particles and were, therefore, insensitive to slow particles. The sensitivity was zero for $m_M \sim 10^{16}$ GeV; some sensitivity existed for poles with $m_M \sim 10^4$ GeV. Electronic experiments of this type, with the proper time windows and proper energy thresholds, play instead an important role in the present searches.

b) The experiment performed at high altitude using lexan plus emulsion detectors had a global threshold of $\beta n > 0.3$ (fixed by lexan). It would, therefore, be OK only for high-velocity monopoles, or if large values of n (eq. (1.1)) were allowed, or if the monopole would have attached a heavy nucleus (for instance ^{27}Al, subsect. **3**'3 and **8**'5*b*)).

c) The experiments which looked for fossil tracks in mica and obsidian had a high threshold, $\beta n > 2$; one can thus repeat the same comments of *b*).

d) Heavy poles would fall through the Earth and cannot be found in the atmosphere; thus the search for poles drifting in the atmosphere is not relevant.

7'5.2. Searches in bulk matter.

a) The use of a superconducting coil detector is a good method. On the other hand, it is improbable that heavy poles are stopped at the surface of the Moon, at the surface of the Earth or in meteorites. The search for poles trapped in ferromagnetic materials or in meteorites could be important for future searches, but only if large quantities of materials are analysed. As for the search performed with lunar rocks, one has to remember that the lunar material

TABLE VI. – *Summary of «classical» monopole searches and relevance to searches for* GUT *poles* ($m_M \simeq 10^{16}$ GeV) *and poles with* $m_M \simeq$ $\simeq 10^4$ GeV.

Search type	βn	Flux limit ($cm^{-2}\,s^{-1}\,sr^{-1}$)	Relevance for		Reasons
			10^{16} GeV	10^4 GeV	
at accelerators	—	—	none	none	energies too low
cosmic-ray fluxes					
counters	> 0.3	$< 7\cdot 10^{-2}$	none	some	short time of flight
lexan	> 0.3	$< 2\cdot 10^{-4}$	some	some	good for fast poles, large n, poles + nuclei
ancient tracks	> 2	$< 10^{-19}$	some	some	good for fast poles, large n, poles + nuclei
drifting poles	—	$< 10^{-16}$	none	some (n large)	improbable and not detectable
bulk matter					
lunar material	superconducting induction coil		doubtful	some	$m \simeq 10^{16}$: small capture; lost when coming to Earth
meteorites			possible	some	small capture probability
ferromagnetic			possible	some	small capture probability
ferromagnetic (solenoid)			none	some	not enough acceleration lexan → high thresholds
Multi γ			none	none	energies too low

was taken to the Earth, experiencing high decelerations, hundred times the acceleration of gravity at the Earth surface. Monopoles trapped in all materials, but ferromagnetic, would have been lost. Since all elements heavier than hydrogen and helium were presumably sinthesized inside stars and thrown into space in stellar explosions, it is unlikely that meteorites would originally be very rich in monopoles. They would have to pick up monopoles in their travel. Furthermore, monopoles in meteorites may get lost when they impact the Earth, since they experience decelerations of $\sim 10^3$ times the acceleration of gravity on the Earth surface; moreover, parts of the meteorites melt. Therefore, monopoles in nonferromagnetic materials (bound with $< \sim 1$ eV/Å) and from the melted parts would escape.

b) The search performed trying to extract with a strong magnetic field poles from magnetite and ferromanganese is not relevant because the velocities acquired by the poles would not have been sufficient to ionize; therefore, the poles could not have been detected with the detectors used.

In conclusion, most of the searches for classical monopoles performed until 1981 were not relevant to the question of the existence of very massive poles. We have also learned that heavy poles are «delicate» objects, which may be lost by small accelerations! It is instead possible to extract some limits for monopoles with $m_M \sim 10^4$ GeV.

8. – Experimental searches for GUT poles.

8'1. *Introduction.* – It has already been stated that a flux of cosmic monopoles may reach the Earth and may have done so far the whole life of the Earth. Assuming a mass $m_M \simeq 10^{16}$ GeV, the poles would acquire a kinetic energy of 10^8 GeV in their free fall to the Earth surface (1.2 GeV/m at the Earth surface). The gravitational binding to the Earth, at the Earth surface, is 0.1 eV/Å.

The velocity spectrum of the monopoles hitting the Earth could be of the type shown in fig. 4.5, from which one concludes that $3 \cdot 10^{-5} < \beta < 0.1$ is the experimentally interesting range for GUT monopole searches. Searches for cosmic poles may be classified as i) direct searches for a flux of poles reaching now the Earth, ii) searches for poles which over the ages have been trapped in Earth ferromagnetic materials and iii) searches for tracks left in certain materials over the ages by passing poles.

The searches for GUT poles do not differ in principle from the searches for classical poles, but, as was discussed in subsect. 7'5, there are major differences arising mainly from the low speed and large mass of the cosmic monopoles.

Immediately after the theoretical prediction of the possible existence of cosmic GUT poles with large masses, several small-scale experiments were set up, some of those being of the « quick and dirty » type. Later on, detectors specifically designed for low pole velocities were used. Then, also apparatuses which were originally designed for other purposes, like those for proton decay and for neutrinos, were employed.

In the following we shall discuss searches performed with superconducting induction coils, with electronics detectors, with track-etch detectors and in bulk matter.

8'2. *Searches with superconducting induction devices.* – The technique of looking for monopoles using small superconducting coils was first used by the Berkeley group [75E2] using multiple traversals of the sample. Since then the technique has been improved considerably and one is now able to detect the single passage of one magnetic monopole. The method of detection with a superconducting ring is based solely on the long-range electromagnetic interaction between the magnetic charge and the macroscopic quantum state of the superconducting ring. A passage of a monopole with the smallest Dirac charge and with any velocity would be observed as a jump of two flux quanta (fluxons). In fact, induction coils are the only known devices sensitive to poles of any velocity.

Figure 8.1 illustrates the schematic of a superconducting induction de-

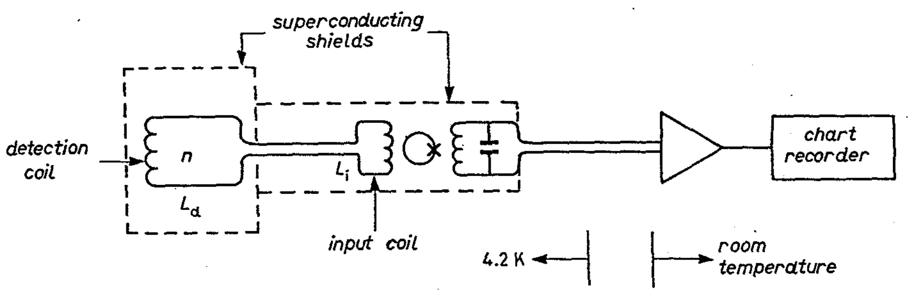

Fig. 8.1. – Schematic diagram of a superconducting induction detector for magnetic monopoles [83T2]. The detection coil is coupled to an input coil for the SQUID device, whose output is amplified and sent to a chart recorder.

tector. It consists of the detection coil coupled to a SQUID, a superconducting quantum interferometer device. The signal from a monopole is very small and an ultrasensitive magnetic monitor such as a SQUID is needed. The detector components, in particular the magnetometer, must be extremely well shielded from any variation of the ambient magnetic field. This places severe restrictions on the cross-sectional area of induction detectors. Variations in the ambient field may be suppressed by surrounding the detector with a superconducting shield placed inside an outer mu-metal shield. However, a flux jump occurring within the shield can produce a signal which may mimic that of a monopole.

In 1982 a Stanford group successfully operated a four-turn coil of 5 cm diameter (fig. 8.2) [82C1]. In 151 days of operation they recorded a single current jump corresponding to that expected from a monopole with $g = g_D$ (*).

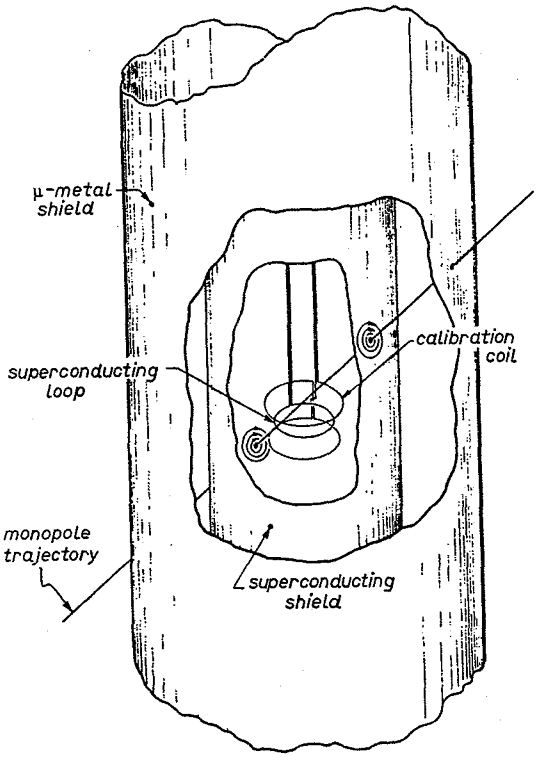

Fig. 8.2. – Schematic view of the first Standord superconducting loop [82C1]. Notice the magnetic shieldings (superconducting and mu-metal) and the two trapped magnetic fluxes in the superconducting shields.

No other jump was observed in subsequent runs. This candidate event generated a great deal of interest in induction detection of monopoles. The technique evolved quickly and now several experimental groups are running what may be called second-generation experiments, characterized by areas at least one order of magnitude larger, coincidence arrangements and sophisticated procedures for eliminating spurious events [83F4].

(*) The author stated that « although a spontaneous and large mechanical impulse seems highly unlikely in an unoccupied laboratory, the evidence presented by this single event does not preclude that possibility ». Thus he considered that the experiment set an upper limit $F < 0.53\ \mathrm{m^{-2}\,d^{-1}\,sr^{-1}}$ for an isotropic distribution of any moving particle with magnetic charge $> 0.06\, g_D$.

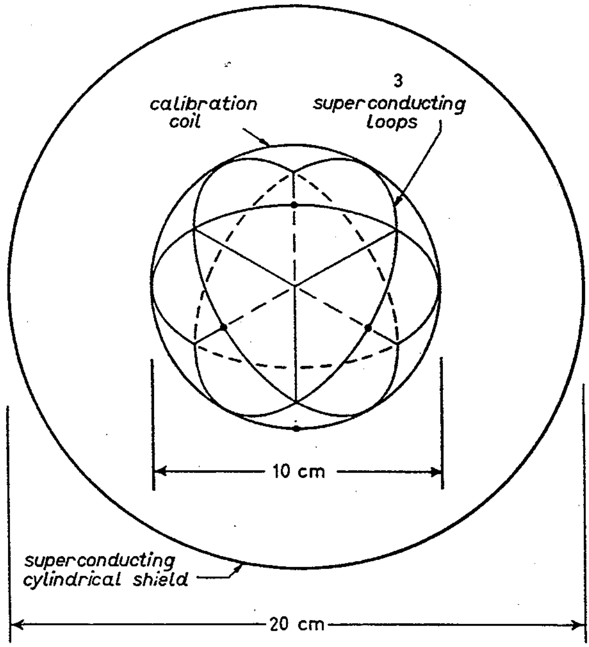

Fig. 8.3. – Schematic view of the Stanford three-loop superconducting induction detector [83C3].

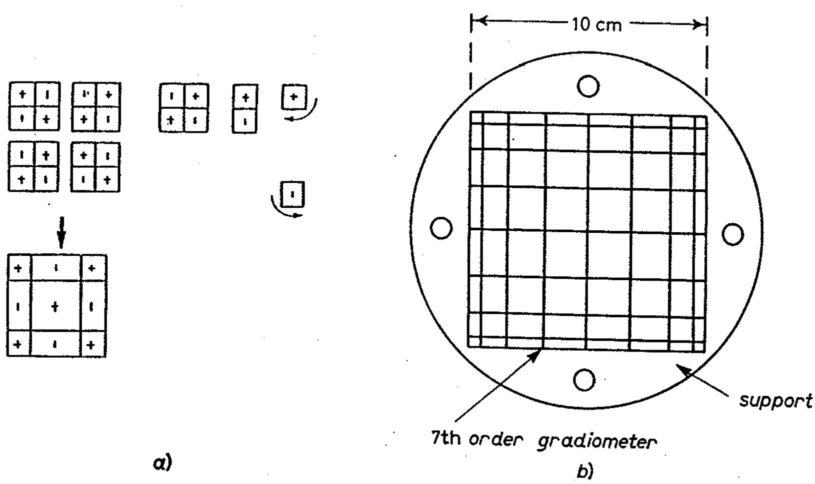

Fig. 8.4. – *a*) Illustration on how to generate a hierarchy of planar high-order gradiometers [83T2]. *b*) Schematic top view of the IBM 7th-order superconducting gradiometer [83F4].

The Stanford group is now running a detector which consists of three orthogonal loops, in a twofold coincidence arrangement (fig. 8.3). It has an effective area (averaged over 4π) of 71 cm² (405 cm² for « near miss » events).

At the IBM Research Centre a hierarchy of coplanar gradiometer coils has been developed. As a result the induction detector becomes relatively insensitive to spurious magnetic-flux changes. Figure 8.4*a*) illustrates how to generate a series of higher-order gradiometers [83T2]. The latest IBM detector consists of six independent planar gradiometer coils mounted on the faces of a rectangular parallelepiped of dimension $(15 \times 15 \times 60)$ cm³ (see fig. 8.5) [83C6, 83T3]. A monopole incident on the box would traverse two and only two of the faces. The detector has $S\Omega = 12\,500$ cm² sr.

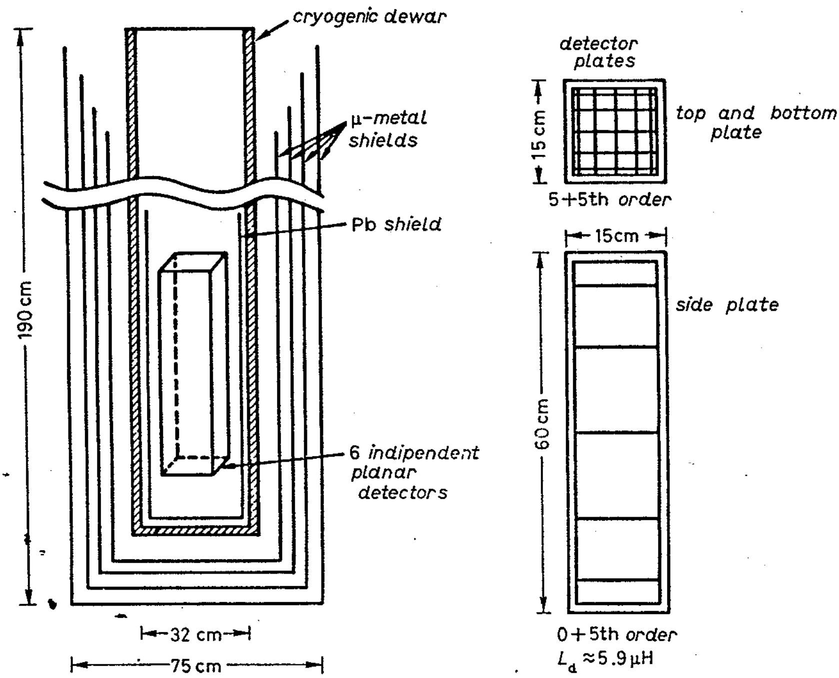

Fig. 8.5. – The present IBM detector. Six planar gradiometers placed on the faces of a parallelepiped are independently monitored by six SQUIDs (not shown). This provides a geometry with 100% coincident detection [83C6, 83T3].

The Stanford and IBM detectors are instrumented with accelerometers, r.f. detectors, magnetometers and ionization detectors to eliminate spurious events. Figure 8.6 shows the recording of the three-loop Stanford detector.

The Chicago-Fermilab-Michigan (CFM) collaboration has brought into operation a device with two 60 cm diameter loops, also of a gradiometer design with equal-size cells (they called it « macrame »), placed in coincidence (see fig. 8.7).

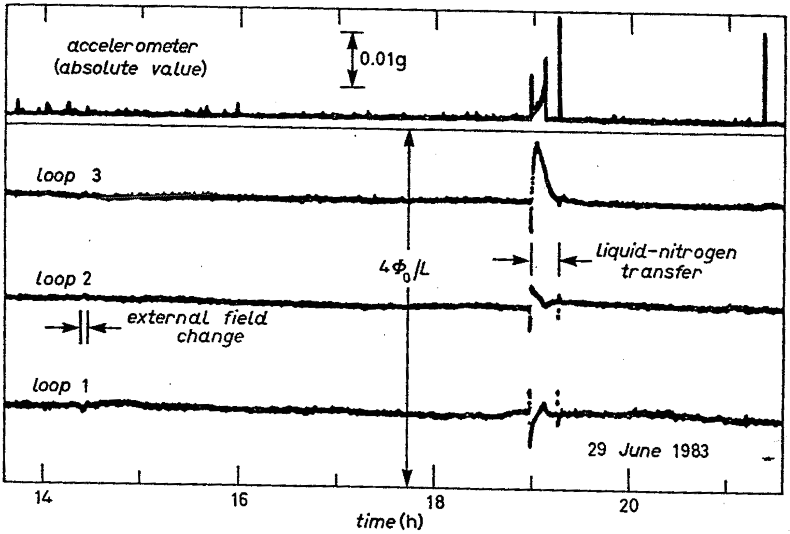

Fig. 8.6. – Chart recording of the three loops and of the accelerometer of the Stanford induction detector [83C3]. Notice the disturbances generated at the time of the liquid-nitrogen transfer in the outer cryostat.

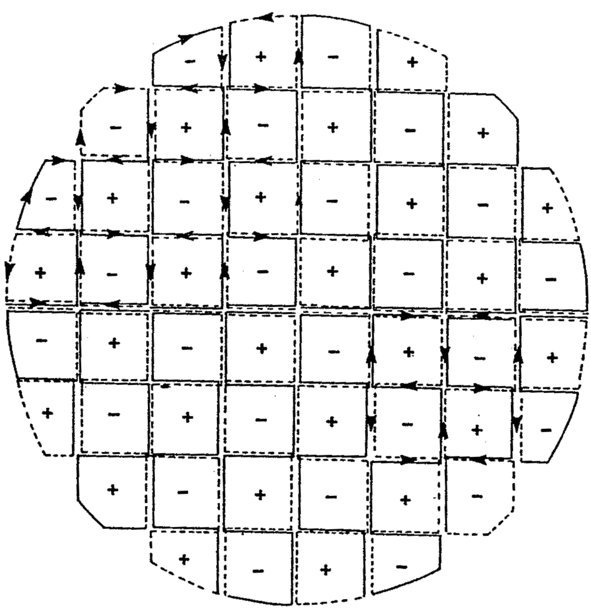

Fig. 8.7. – Illustration of the «macrame» superconducting structure of the Chicago detector [83F4].

No other event candidate was reported. Table VII summarizes the experiments with superconducting induction devices, their main features and the upper limits obtained. The global upper limit may be placed at $F < 4\cdot 10^{-12}\ \text{cm}^{-2}\ \text{s}^{-1}\ \text{sr}^{-1}$. This limit is also shown in fig. 6.1 and fig. 8.11.

TABLE VII. – *List of experiments searching for cosmic monopoles using superconducting induction devices. The table gives for each group the main feature of the apparatus, the effective area for which one has a 4π solid angle and the flux upper limit* (90% *confidence level; the first value corresponds to one event). The overall combined upper limit is presently about* $0.4\cdot 10^{-11}\ \text{cm}^{-2}\ \text{s}^{-1}\ \text{sr}^{-1}$.

Group	Main feature	Physical area (cm^2)	Area/4π ($\text{cm}^2/4\pi$)	Flux limit ($10^{-11}\ \text{cm}^{-2}\ \text{s}^{-1}\ \text{sr}^{-1}$)	Reference
Stanford 1	single coil	20	10	61	[82C1]
Stanford 2	3-axis coils	79	71(476) (*)	1.2	[83C3]
Chicago FNAL-Mich.	2 coils gradiometer	2800	700	1	[83F4]
IBM-1	gradiometer 2 coils	100	25	51(17) (**)	[82C6]
IBM-2	gradiometer 6 coils	225 900	1000	1.4	[83C6]
Kobe	single coil	50	25	46	[83F4]
IC	2 coils	625	300	8	[83F4]
NBS	background studies	—	—	—	[83Z1]

(*) Including «near miss» events.
(**) Using also noncoincident recordings.

8.3. *Counter searches.* – The simplest lay-out of an electronic detector designed to detect a flux of cosmic GUT poles consists of two counters, which should measure the energy loss and the times of flight. Large-area lay-outs consist of hodoscopes, arranged in several layers, often employing different types of electronics detectors, that is scintillation counters, proportional counters, limited streamer tubes, etc. Table VIII lists the electronics experiments, together with some relevant parameters, like the values $S\Omega$ = area times solid angle, the minimum $\mathrm{d}E/\mathrm{d}x$ detected and the β range covered.

No monopole was detected; the experiments can thus place only upper limits (usually at the 90 % confidence level) for the β range covered. A few comments on the lay-outs will now be made; for reasons of space, only few figures will be shown.

ULLMANN [81U1] performed at Brookhaven National Laboratory a search with a proportional-counter array having $S\Omega = 1.9\ \text{m}^2\ \text{sr}$. With this system he established an upper limit at the level of $(3 \div 7)\cdot 10^{-11}\ \text{cm}^{-2}\ \text{s}^{-1}\ \text{sr}^{-1}$ for monopoles with velocities between 100 and 350 km/s.

The Bologna search used the existing apparatus of a cosmic-ray station located on the roof of the physics building [82B1, 83B4]. This simple apparatus, enlarged to a reach a value $S\Omega = 36\ \text{m}^2\ \text{sr}$, yielded an upper limit $F < (2\div4)\cdot 10\ \text{cm}^{-13}\ \text{cm}^{-2}\ \text{s}^{-1}\ \text{sr}^{-1}$ for poles with $0.005 < \beta < 0.5$; the limit was $7\cdot10^{-13}$ for $0.001 < \beta < 0.005$.

At Tokyo three different searches were performed. The first utilized a detector with $S\Omega = 1.1\ \text{m}^2\ \text{sr}$ having six layers of scintillation counters [82M1]. The thresholds were first set at 1.2 $I_{\min}$ and later lowered to 0.025 $I_{\min}$. This detector was a prototype for a larger lay-out installed in the Kamioka mine (fig. 8.8). It had $S\Omega = 22\ \text{m}^2\ \text{sr}$ and counter thresholds at 1/16 th $I_{\min}$.

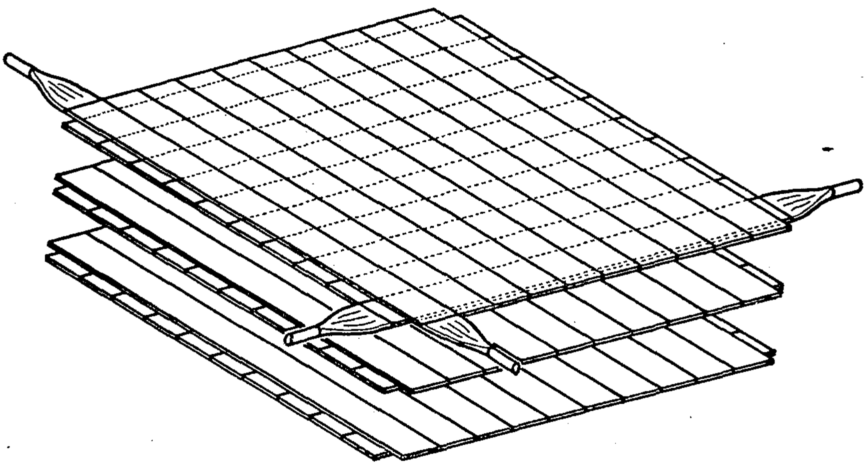

Fig. 8.8. – Lay-out of the Tokyo-Kamioka mine monopole detector [83M1], with 6 planes of counter hodoscopes.

The third lay-out with $S\Omega = 1.4\ \text{m}^2\ \text{sr}$ was specifically designed to detect very low ionization losses, down to 0.025 $I_{\min}$ [83A7, 83G3].

The University of Michigan search employed a horizontal stack of five scintillators, with $S\Omega = 3.16\ \text{m}^2\ \text{sr}$ and very low thresholds, at the level of 0.01 $I_{\min}$ [83A7].

The Utah-Stanford search, located in the Mayflower mine in Utah, used scintillation counters arranged in three double layers of four counters each (plus an extra layer). It had $S\Omega = 2.7\ \text{m}^2\ \text{sr}$ and its electronics was set to detect particles depositing more than 0.12 $I_{\min}$ [83G1].

The nucleon decay experiment located in the Soudan mine used arrays of proportional counters having $S\Omega = 71.6\ \text{m}^2\ \text{sr}$ [83B3]. The detector had thresholds at 0.5 $I_{\min}$ and is set up to cover the β range $3\cdot10^{-4}$ to $3\cdot10^{-2}$.

The experiment in the Baksan mountain, in the USSR, uses the existing cosmic-ray detector (fig. 8.9) [82A1]. For the monopole search the energy loss threshold was set at 0.25 $I_{\min}$. A limit $< 10^{-14}\ \text{cm}^{-2}\ \text{s}^{-1}\ \text{sr}^{-1}$ was reported for

TABLE VIII. – *List of experiments which searched or are searching for a flux of cosmic monopoles with scintillation counters, proportional tubes and track-etch detectors.*

Laboratory	Location	Detector	$S\Omega$ (m^2 sr)	dE/dx (minimum)	β range	Flux upper limit ($cm^{-2}\, s^{-1}\, sr^{-1}$)	References
1) BNL	building	proportional	1.9	2.0	$3\cdot 10^{-4} \div 1.2\cdot 10^{-3}$	$3.4\cdot 10^{-11}$	[81U1]
2) Bologna	building	scintillators	$10 \div 36$	$10 \div 25$	$10^{-3} \div 0.6$	$3.4\cdot 10^{-13}$	[83B4]
3) Tokyo	building	scintillators	1.1	1.2	$10^{-2} \div 10^{-1}$	$1.5\cdot 10^{-11}$	[82M1]
Tokyo	building	scintillators	1.4	0.025	$2\cdot 10^{-4} \div 5 \cdot 10^{-3}$	$1.5\cdot 10^{-11}$	[82M1]
Tokyo	Kamioka mine	scintillators	22.0	0.2	$6\cdot 10^{-4} \div 1$	$1.5\cdot 10^{-12}$	[83M1]
4) Michigan	building	scintillators	11.0	$0.01 \div 0.05$	$3\cdot 10^{-4} \div 10^{-2}$	$8.1\cdot 10^{-11}$	[83A7]
5) Utah-Stanford	Mayflower mine	scintillators	2.7	0.12	$2\cdot 10^{-4} \div 3 \cdot 10^{-2}$	$8.1\cdot 10^{-12}$	[83G1]
6) Minnesota-Argonne	Soudan mine	proportional	71.6	0.5	$10^{-3} \div 3 \cdot 10^{-2}$	$4.1\cdot 10^{-13}$	[83B3]
7) USSR	Baksan mine	scintillators	1800.0	0.25	$10^{-3} \div 5 \cdot 10^{-2}$	$1.5\cdot 10^{-14}$	[82A1]
8) India-Japan	Kolar mine	proportional	218.0	2.5	$2\cdot 10^{-3} \div 0.9$	$3.5\cdot 10^{-14}$	[82A7]
9) Mont Blanc	tunnel	streamer tubes	19.0	0.02	$10^{-3} \div 0.5$	$7.0\cdot 10^{-13}$	[83B8]
10) BNL-Brown-KeK	neutrino beam	drift+ +scintillator	14.5	0.3	$10^{-3} \div 0.2$	$5.2\cdot 10^{-12}$	[83C7]
11) Tokyo	building	proportional+ +Drell	24.7	—	$> 2\cdot 10^{-4}$	$1.6\cdot 10^{-12}$	[83K3]
12) Berkeley-Indiana	building	scintillator	17.5	1.2	$6\cdot 10^{-4} \div 2.1\cdot 10^{-3}$	$4.1\cdot 10^{-13}$	[83T2]
13) Berkeley	surface	CR39	150.0	$Z/\beta \geqslant 30$	$0.02 \div 1$	$1.5\cdot 10^{-13}$	[82B2]
14) Kitami	building	nitrocellulose	1000.0	$Z/\beta \geqslant 60$	$0.04 \div 1$	$5.2\cdot 10^{-15}$	[83D3]

monopoles with $10^{-3} < \beta < 5\cdot 10^{-2}$. At present this experiment has the largest $S\Omega$ ($= 1800\ \mathrm{m^2\,sr}$) and the highest sensitivity.

The India-Japan collaboration used the nucleon decay experimental lay-out, located in the Kolar gold mine in India [82A7]. The apparatus consists of arrays of proportional counters covering $S\Omega = 208\ \mathrm{m^2\,sr}$, set to count energy losses larger than $2.5\ I_{\min}$.

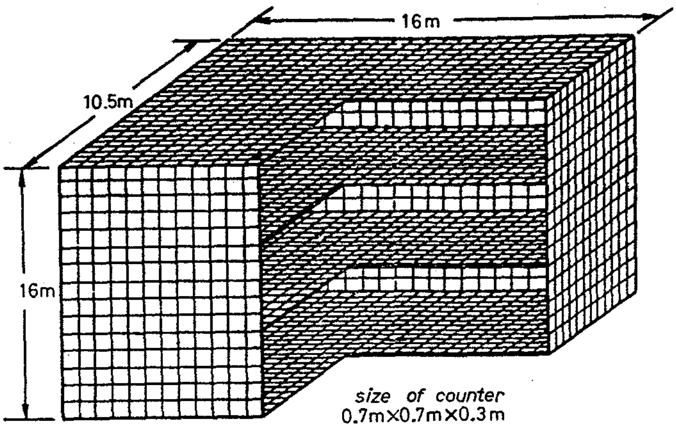

Fig. 8.9. – Lay-out of the Baksan mountain (USSR) liquid-scintillator detector [82A1].

One Tokyo group [83K3] used a stack of scintillation counters and of proportional chambers, employing 90 % gaseous helium and 10 % CH_4 (fig. 8.10). In the proportional chambers the monopoles could excite the helium atoms via the Drell mechanism discussed in subsect. 3'9

$$\mathrm{He} \xrightarrow[\text{pole}]{} \mathrm{He}^* . \tag{8.1}$$

Then, by the Penning effect, the excitation energy of the excited He* is transferred into ionization of the CH_4 molecule

$$\mathrm{He}^* + \mathrm{CH_4} \to \mathrm{He} + \mathrm{CH_4^+} + e^- . \tag{8.2}$$

Therefore, one may obtain an effective ionization also for low-velocity monopoles in the $10^{-4} < \beta < 10^{-3}$ range.

The Berkely-Indiana group [83T2] used a single thick slab (7.6 cm) of scintillator. Relativistic charged particles traverse the detector in a time much shorter than the response time of the detector system (~ 40 ns). A GUT pole travelling with $\beta = 10^{-3}$ takes at least 250 ns to traverse the scintillator. The signature of a monopole is thus given by an anomalously wide pulse with a constant pulse height in time. With this arrangement the experimenters should have reached the β limit given by ionization energy losses ($\sim 5\cdot 10^{-4}$).

The Mont Blanc detector for proton decay [83B8] is a cubic detector of 3.5 m side, made of 134 layers of limited streamer tubes, separated by 1 cm thick iron absorbers. The detector is capable of determining the path of a particle with a transverse precision of $\sim 1\ cm^2$. The identification may be made

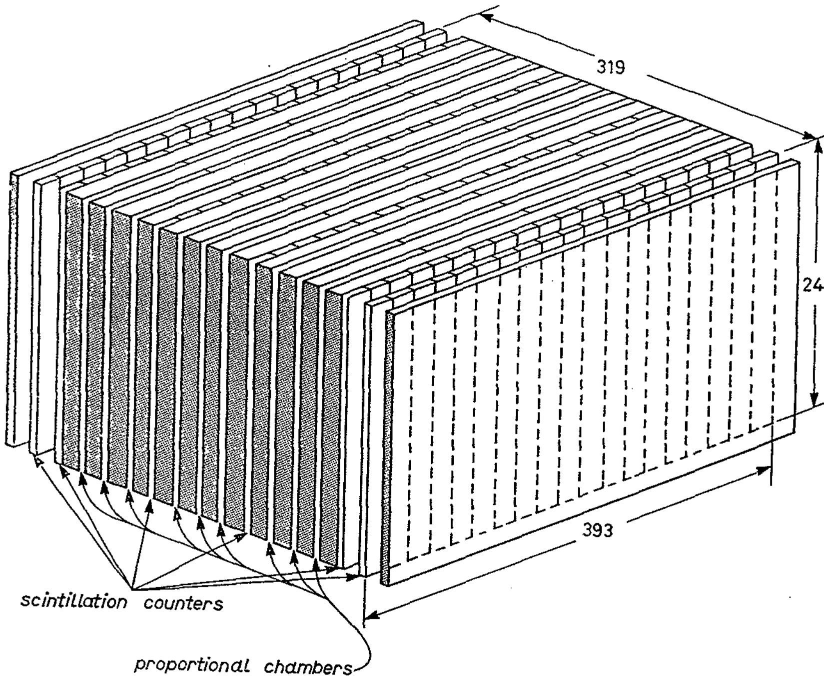

Fig. 8.10. – Lay-out of a Tokyo detector, which used the Drell and Penning effects (see text) [83A7]. Units in cm, ▒ iron layers.

by time of flight through the whole detector. Since many samples are involved, the apparatus is capable of detecting monopoles which ionize 1/100 of I_{min} because of the Landau tail in the energy loss distribution. The detector has $S\Omega = 19\ m^2\,sr$ and gave a flux limit $< 7\cdot 10^{-13}\ cm^{-2}\,s^{-1}\,sr^{-1}$.

The BNL Neutrino Experiment uses layers of $(4\times 4)\ m^2$ proportional drift tubes. As a monopole detector it has $S\Omega = 14.5\ m^2\,sr$, it is sensitive to $10^{-3} < \beta < 0.2$ and it has reached the upper limit $F < 5\cdot 10^{-12}\ cm^{-2}\,s^{-1}\,sr^{-1}$ [83C7].

The CHARM neutrino detector at CERN consists of 78 layers of $(3\times 3\times 0.03)\ m^3$ scintillation counters, separated by 0.2 m. It may search for poles with $10^{-3} < \beta < 0.5$; it has $S\Omega \simeq 50\ m^2\,sr$.

Figure 8.11 shows a compilation of upper limits (at the 90 % confidence level) for a flux of cosmic GUT poles plotted *vs.* the β of the monopole. It has to be remembered that for $\beta < 10^{-3}$ there are some doubts about the energy losses and consequently about the response of some electronics detectors.

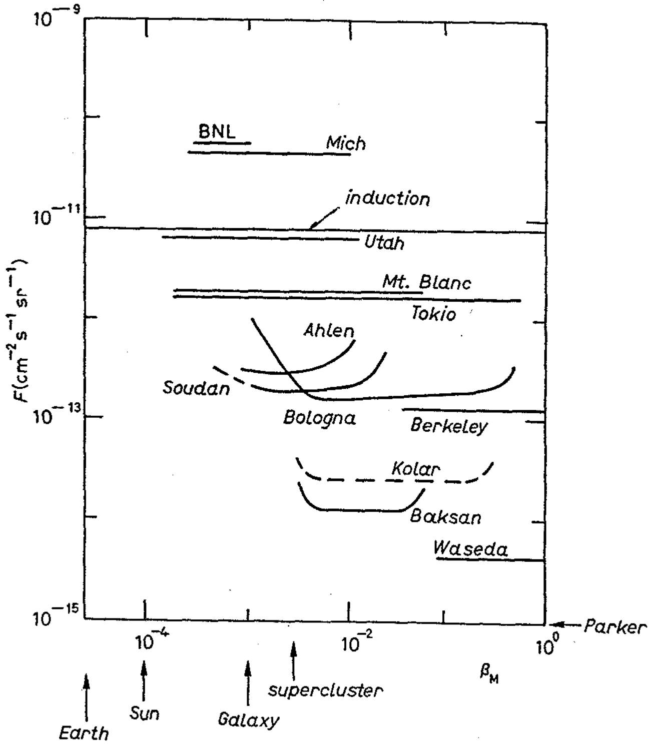

Fig. 8.11. – Compilation of upper limits for a flux of cosmic GUT monopoles plotted *vs.* the β of the monopoles (at 90% c.l.). The limits were obtained with induction devices, scintillation and gas tube detectors (tables VII and VIII). The Berkeley experiment was performed with CR39 plastics, the Kitami experiment with nitrocellulose sheets.

8'4. *Searches with track-etch detectors.* – A Berkeley group [82B2] exposed 15 m² of several layers of CR39 for about one year at ground level. They quoted an upper limit $F < 1.5 \cdot 10^{-13}\ \text{cm}^{-2}\ \text{s}^{-1}\ \text{sr}^{-1}$ for $\beta > 0.02$.

A Japanese group [83D2] exposed 100 m² of nitrocellulose sheets for 3.3 years at ground level at Kitami, Hokkaido. The experiment was originally designed to search for « classical monopoles ». It was modular, with each unit consisting of a stack of a pair of nitrocellulose sheets, a pair of polycarbonate sheets and a X-ray film. Only the nitrocellulose is useful for the detection of slow poles. The authors quoted an upper limit $F < 5.2 \cdot 10^{-15}\ \text{cm}^{-2}\ \text{s}^{-1}\ \text{sr}^{-1}$ for poles with $\beta > 0.04$.

The upper limits from these two experiments are also shown in fig. 8.11 and in table VIII.

8'5. *Searches in bulk matter.* – The Kobe group performed a search for relic monopoles trapped in iron sand using several tens of kilograms of material formed between 10^7 and 10^8 y ago [83E2]. The sand was heated above the

Curie point, at which temperature the material stops being ferromagnetic. The poles, which were trapped in the material, would leave it, would fall towards the Earth and would be detected in a superconducting induction coil through which they would pass. The Kobe group placed the upper limit of $2\cdot10^{-6}$ poles per gram of ore. It is difficult to extract from this an upper limit on the monopole flux: it was estimated to be of the order of 10^{-13} poles $cm^{-2}\,s^{-1}\,sr^{-1}$ for poles with $\beta<10^{-4}$. The sensitivity is much better for «classical» monopoles or for poles with an intermediate mass (like 10^4 GeV).

A Wisconsin group is proposing to perform an experiment of this type on a large scale, using the ancient iron ore processed in a steel mill in Wisconsin [83G3].

8'6. *Searches for ancient tracks in mica.* – Though as a track-etch detector has a high threshold, mica should detect the passage of a «monopolic atom», when the attached nucleus is, for instance, aluminium, if the speed of the system is of the order of $10^{-3}\,c$, where ionization losses of charged particles are largest.

Ahlen *et al.* [83A7] have taken a piece of mica from a mine 5 km deep in Brazil. The age of the mica was estimated to be $\sim4.6\cdot10^8$ y. After etching in hydrofluoric acid they scanned 14 cm^2 of mica with an optical microscope (see also subsect. 7'2.3). They estimated an upper limit $F<2\cdot10^{-17}\,cm^{-2}\,s^{-1}\,sr^{-1}$ for poles with $4\cdot10^{-4}<\beta<2\cdot10^{-3}$. The limits are obtained assuming that the poles attach an Al nucleus and that the mean free path for Al attachment in the Earth crust is ~5 km. The limit would be much poorer if the incoming monopoles would have already attached a proton.

9. – Monopole catalysis of proton decay.

9'1. *Introduction.* – It was suggested in 1980 [80D1] that a GUT monopole could catalyze baryon-number–violating processes such as

$$p+M\to M+e^{+}+\text{mesons}. \tag{9.1}$$

It was thought that the cross-section would be very small, of the order of the geometrical cross-section of the monopole core ($\sim10^{-58}\,cm^2$), where may be found the Y- and X-bosons which mediate the $\Delta B\neq0$ interactions. Later Rubakov [81R1, 82R2] and Callan [82C4] showed that the cross-section is independent of m_X and could be comparable with the cross-section of ordinary strong interactions. This possibility has stirred up considerable theoretical interest and some controversies. The implications are very interesting both in particle physics and in astrophysics.

One explanation of the large rate of monopole catalysis is the following.

The monopole core should be surrounded by a fermion-antifermion condensate (fig. 5.4). Some of the condensate with 4, 6 fermions have $\Delta B \neq 0$ terms extending up to the confinement region; hence they could induce baryon-number–violating processes at strong-interaction rates. For instance, in the SU_2 subgroup of SU_5 quarks and leptons appear as doublets

$$\begin{pmatrix}\bar{d}_3\\ e^-\end{pmatrix}_L \begin{pmatrix}e^+\\ d_3\end{pmatrix}_L \begin{pmatrix}u_1\\ \bar{u}_2\end{pmatrix}_L \begin{pmatrix}u_2\\ \bar{u}_1\end{pmatrix}_L, \tag{9.2}$$

where the indices 1, 2, 3 indicate colour states. One $\Delta B \neq 0$ interaction of the monopole with the condensate could be of the type

$$\mathrm{u}_1+\mathrm{u}_2+\mathrm{M} \rightarrow \mathrm{e}^+ + \bar{\mathrm{d}}_3 + \mathrm{M}\,, \tag{9.3}$$

which may be interpretated as the proton catalysis

$$\mathrm{u}_1+\mathrm{u}_2+\mathrm{d}_3+\mathrm{M} \rightarrow \mathrm{e}^+ + \mathrm{M} + \text{mesons}\,. \tag{9.4}$$

The catalysis reaction can be imagined pictorially as shown in fig. 9.1.

Positively charged dyons should not catalyze proton decay with large rate because of electrostatic repulsion between the proton and the dyon. Negatively charged dyons would instead have large effective cross-sections. Neutral monopoles could form monopolic atoms with protons (and with some nuclei), thus probably enhancing the catalysis cross-section.

In order to have a better understanding of the origin of the effect, CALLAN considered the problem of a charged fermion scattering on a point Dirac monopole; he recalled that physics is not defined at $r = 0$. The total angular

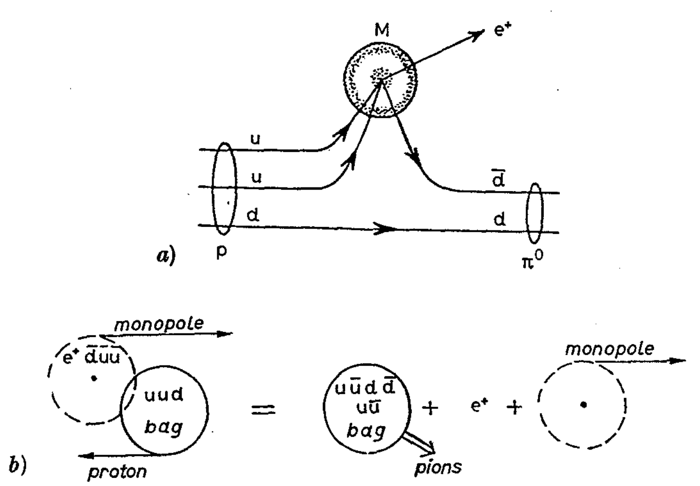

Fig. 9.1. – a), Illustrations of the monopole catalysis of proton decay; b) shows the effect of the presence of a $\Delta B \neq 0$, 4-fermion condensate ($\bar{\mathrm{d}}_3\mathrm{e}^+\bar{\mathrm{u}}_2\bar{\mathrm{u}}_1$) [83P2].

momentum of the system is given by (subsect. 2·3)

$$J = L + S + eg\hat{r}/c\,, \tag{9.5}$$

where $\boldsymbol{L}$ is the orbital angular momentum, $\boldsymbol{S}$ is the spin of the fermion, $eg\hat{r}/c$ is the field angular momentum, which gives rise to 1/2 units of $\boldsymbol{J}$, because of the Dirac condition. For S-wave fermions the spin orientation may cancel the latter piece, giving rise to a $\boldsymbol{J} = 0$ state. As the fermion passes the core and $\boldsymbol{r} \to -\boldsymbol{r}$, the angular momentum will not be conserved unless $\boldsymbol{S} \to -\boldsymbol{S}$ (helicity flip) or $e \to -e$ (charge exchange). But a gauge monopole is not singular at $r = 0$. Studies of the gauge monopole-fermion system at close distances indicate that when a S-wave fermion reaches the core of a gauge monopole, it will come out with a change of identity, *e.g.* $\mathrm{d} \to \mathrm{e}$, $\mathrm{u}_1 \to \bar{\mathrm{u}}_2$, etc. The monopole is a state of indefinite fermion number and it distorts the fermionic vacuum around it. As a consequence baryon-number–violating processes can occur outside the core of the monopole.

CALLAN pointed out that the problem with the S-wave Dirac equation is that it does not conserve probability, because flux leaks into and out of the monopole core. The core can be substituted with a boundary condition. Considering the problem in one dimension, one may picture what happens as sketched in fig. 9.2: an incoming S-wave soliton, describing an e^+, is reflected from the monopole bag, sending back a $\bar{\mathrm{d}}_3$ soliton. Now the symmetry-breaking boundary condition replaces the details of the monopole core, which leads to processes like (9.3), which would exhibit a typical S-wave behaviour of strong-interaction processes

$$\sigma_c = \sigma_{\Delta B \neq 0} \simeq \frac{\pi}{E^2} \simeq \frac{\sigma_0 \sigma_R}{\beta}\,, \tag{9.6}$$

that is the size of the cross-section depends on E, not on core size. In other words, quarks and leptons around the core can fall into the monopole and pop out with a different identity, $\bar{\mathrm{d}} \to \mathrm{e}^-$, $\mathrm{u}_1 \to \bar{\mathrm{u}}_2$, etc. The above picture is in terms of quarks. In order to apply it to baryon decay, one needs a picture of hadrons as confined quarks. This leads to the same cross-section (eq. (9.6)), where $1/\beta$ is a purely kinematical flux factor, $\sigma_0 \simeq 4 \cdot 10^{-28}\,\mathrm{cm}^2$ and σ_R is a fudge factor which absorbs all the uncertainties in the cross-section; it could be of order unity, of order 10^{-5} [82E1] or much smaller [84R1].

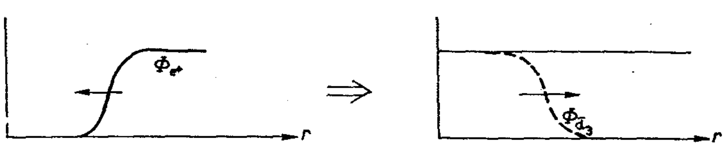

Fig. 9.2. – A different picture of monopole catalysis of proton decay: an e^+ soliton scatters by the boundary conditions into a $\bar{\mathrm{d}}_3$ antisoliton [82C6].

In order to have catalysis with strong interaction rates, one needs at least an enancement of the S-wave electron wave function at the monopole core and baryon-number–violating fields inside the core. The first condition should be met by all unified groups, while the second condition may vary from one model to another. Moreover, there are several unsettled issues, like the role of the weak-interaction scale, the effects of higher partial waves, the effects of higher fermion generations, the confinement scale and the question of the boundary condition at the monopole core. For these reasons it is not clear if strong catalysis is a general feature of all GUT theories. It may be that catalysis does occur but at considerably lower rates (see the discussions in [82C3, 83K5, 83W1, 84R1, 84S2]).

According to recent papers [83A2, 84R1] the monopole catalysis cross-section could have a $(1/\beta^2)$-dependence, $\sigma_c \sim 1\ (\text{GeV})^2/\beta^2$, at least for sufficiently low monopole-proton relative velocities. Clearly, more theoretical work is needed.

If the $\Delta B \neq 0$ cross-section for monopole catalysis of the proton decay were large, then a monopole would trigger a chain of baryon « decays » along its passage through a large detector, such as those designed to study baryon decay. The mean free path $\lambda = (N_A \varrho \sigma)^{-1}$ between two successive monopole-induced proton decays would be, for slow monopoles,

$$\lambda_c = \frac{1}{N_0 \varrho \sigma_c} \simeq \frac{4200}{\varrho\ (\text{g cm}^{-3})} \frac{\beta}{\sigma_R}, \tag{9.7}$$

where it was assumed $\sigma_0 = 4 \cdot 10^{-28}\ \text{cm}^2$ and a $(1/\beta)$-dependence. ϱ is the density of the material in g cm^{-3}. The time between two successive monopole-induced proton decays would be

$$\tau = \frac{\lambda}{\beta c} = \frac{1}{c N_A \varrho \sigma_0 \sigma_R} \simeq \frac{1.4 \cdot 10^{-7}}{\sigma_R\, \varrho\ (\text{g cm}^{-3})}. \tag{9.8}$$

Table IX gives values of λ and σ assuming $\varrho = 1$ g cm^{-3}, $\beta = 10^{-3}$ and 10^{-4} and $\sigma_R = 1,\ 10^{-2},\ 10^{-4},\ 10^{-6}$.

TABLE IX. – *Catalysis of proton decay. Values of λ and τ for various σ_R when $\beta = 10^{-3}$, 10^{-4}, $\sigma_0 = 4 \cdot 10^{-28}$ cm^2 and the density of the medium is $\varrho = 1$ g cm^{-3}* (see text).

	σ_R	$\sigma = \sigma_0 \sigma_R/\beta$ (cm^2)	$\lambda = 4200\beta/\varrho\sigma_R$ (cm)	$\tau = 1.4 \cdot 10^{-7}/\sigma_R \varrho$ (s)
$\beta = 10^{-3}$	1	$4 \cdot 10^{-25}$	4.2	$1.4 \cdot 10^{-7}$
	10^{-2}	$4 \cdot 10^{-27}$	$4.2 \cdot 10^{2}$	$1.4 \cdot 10^{-5}$
	10^{-4}	$4 \cdot 10^{-29}$	$4.2 \cdot 10^{4}$	$1.4 \cdot 10^{-3}$
	10^{-6}	$4 \cdot 10^{-31}$	$4.2 \cdot 10^{6}$	1.4
$\beta = 10^{-4}$	1	$4 \cdot 10^{-24}$	0.42	$1.4 \cdot 10^{-7}$
	10^{-2}	$4 \cdot 10^{-26}$	42.0	$1.4 \cdot 10^{-5}$
	10^{-4}	$4 \cdot 10^{-28}$	$4.2 \cdot 10^{3}$	$1.4 \cdot 10^{-3}$
	10^{-6}	$4 \cdot 10^{-30}$	$4.2 \cdot 10^{5}$	1.4

9'2. *Experimental searches for monopole catalysis of nucleon decay.* – As soon as the idea of monopole catalysis of proton decay became known, some rough upper limits were established from bubble chamber information and indirect astrophysical considerations. Then, some quick experiments were performed and better astrophysical limits established. Later, all large-scale proton decay experiments added new triggers to be sensitive to multiple «proton decays». The signature for a monopole-catalyzed nucleon decay should be different from that of a spontaneous nucleon decay. In the last case the laboratory momentum has to be balanced, which leads to back-to-back configurations. In the case of monopole-induced decays, the events may have the same general appearance of low-energy (< 2 GeV) atmospheric neutrino interactions in the detector. For this reason the search for «unbalanced proton decays» as expected from catalysis has an intrinsic background from neutrino interactions. Proton decay experiments were planned for very rare events and did not have the possibility to record events which happened immediately after a first candidate; in other words, they were biased against a string of proton decays. To overcome this difficulty, buffer memories and electronics logics were added.

No string of events consistent with monopole catalysis of nucleon decay was found. Table X gives a summary of the upper limits established by the various experiments, which will now be reviewed.

TABLE X. – *Upper limits on the monopole flux from the no-observation of a string of* $\geqslant 2$ *nucleon decays, assuming a catalysis cross-section of* 10 mb.

Experiment	Approximate linear dimensions of detector (m)	Approximate flux limit F ($cm^{-2}\,s^{-1}\,sr^{-1}$)	Reference
Kolar gold mine	4	$2 \cdot 10^{-12}$	[83B8]
Mt. Blanc	3.5	10^{-14}	[83E1]
IMB	18	$3 \cdot 10^{-15}$	[83E1]
Kamioka	14	$8 \cdot 10^{-15}$	[83E3]
Soudan	2.9	$1.5 \cdot 10^{-13}$	[83E3]

The Aachen-Hawaii-Tokyo group performed a quick experiment using a water Čerenkov counter filled with 12 t of water. From a twelve-day run they obtained an upper-limit flux of $2 \cdot 10^{-12}\,cm^{-2}\,s^{-1}\,sr^{-1}$ valid for $\sigma_R = 10^{-2}$ and $5 \cdot 10^{-4} < \beta < 5 \cdot 10^{-2}$ [83B8].

The Mont Blanc proton decay detector, which was already mentioned in subsect. 8'3, has an average density of $3\,g\,cm^{-3}$. The detector is located at a depth of 5000 m w.e. (metres of water equivalent). The size of the detector limits the sensitivity to $\lambda =$ few metres. The limit from the nonobservation of single unbalanced events is $F < 3 \cdot 10^{-13}\,cm^{-2}\,sr^{-1}\,s^{-1}$; it is determined by neutrino interactions and thus cannot be improved. The limit from the nonobservation of a string of $\geqslant 2$ proton decays is at the level of $F < 10^{-14}\,\mathrm{cm^{-2}\,sr^{-1}\,s^{-1}}$ (assuming $\sigma_c = 10$ mb).

The Irvine-Michigan-Brookhaven (IMB) water Čerenkov detector is a parallelepiped of $(17 \times 22.5 \times 18)\,\mathrm{m^3}$, viewed by 2048 photomultipliers. It is located at a depth of ~ 2000 m w.e. in the Morton salt mine near Cleveland, Ohio [83E1, 84F1]. The upper limits obtained are shown in fig. 9.3 as a function

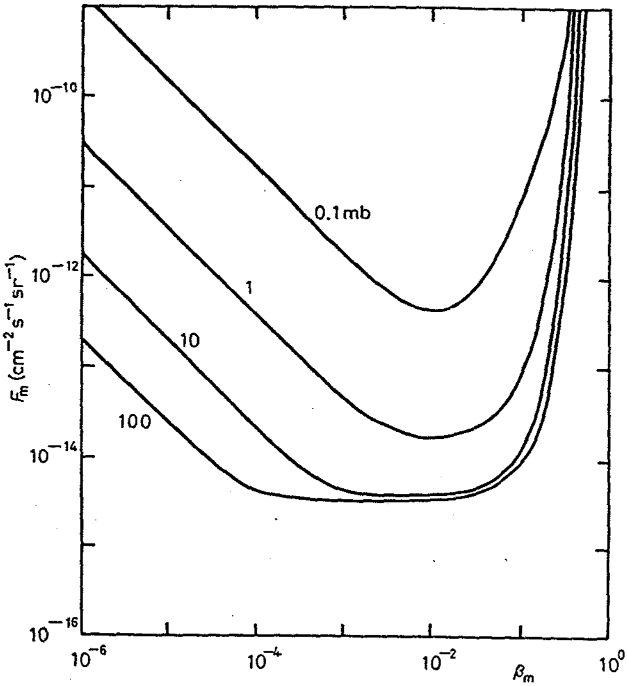

Fig. 9.3. – Upper limits (90% c.l.) on the monopole flux *vs.* monopole velocity for the multiple catalysis of proton decay in the IMB water Čerenkov detector for several values of the catalysis cross-section [83E1].

of the monopole velocity for several values of the catalysis cross-section σ_c. The cut-off at low β is due to the geometrical limitations of the apparatus, while the sharper cut-off at high β is due to limitations in the electronics timings. The best upper limit is $F < 3 \cdot 10^{-15}\,\mathrm{cm^{-2}\,s^{-1}\,sr^{-1}}$ for $\sigma_c = 10$ mb, or $F\sigma_c < 3 \cdot 10^{-41}\,\mathrm{sr^{-1}\,s^{-1}}$ for β around $10^{-3} \div 10^{-2}$.

The Tokyo water Čerenkov counter is a cylinder of 15 m diameter and 16 m height (3000 t of water, about 1000 t fiducial mass) viewed by 1000, 20″ photomultiplers (specifically designed for the experiment) which cover 20% of the outer surface of the detector [83E3]. The apparatus is placed in the Kamioka mine at a depth of ~ 2700 m w.e. (fig. 9.4). They obtained an upper limit $F < 8 \cdot 10^{-15}\,\mathrm{cm^{-2}\,s^{-1}\,sr^{-1}}$ (for $\sigma_c = 10$ mb and $(1/\beta^2)$-dependence) (fig. 9.5).

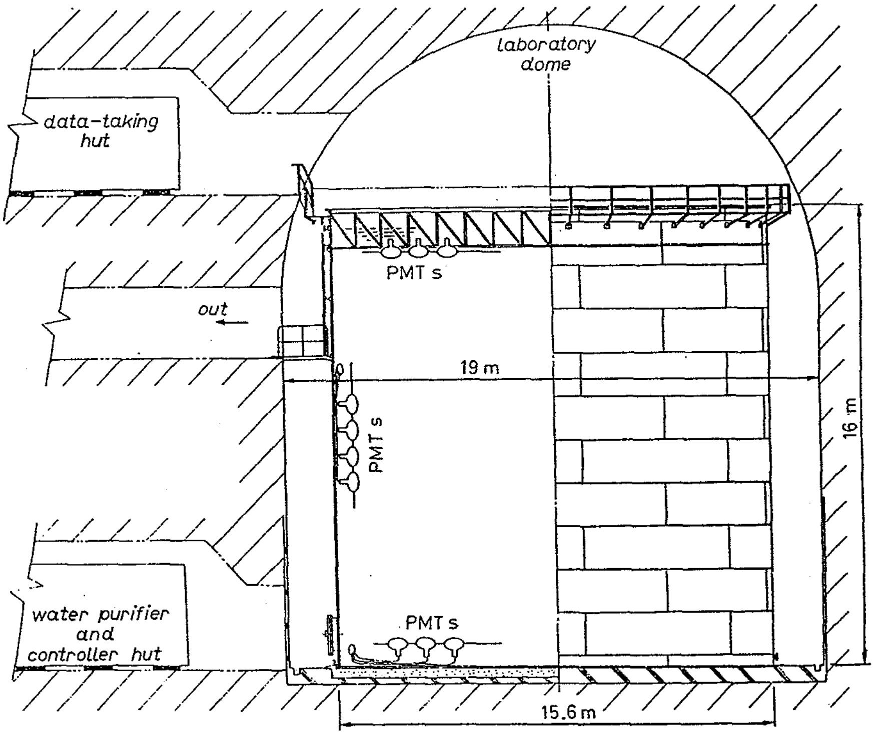

Fig. 9.4. – A schematic view of the $3000\ m^3$ water tank and phototube support system of the Kamioka proton decay experiment [84K3].

The Tata-Osaka-Tokyo detector in the Kolar gold field, at a depth of 7600 m.w.e. is composed of 34 layers of proportional counters with 1.2 cm iron plates between layers. The counters are $(10 \times 10)\ cm^2$ by 6 m length. The detector, a $(6 \times 4 \times 3.7)\ m^3$ parallelepiped with a total weight of 140 t and an average density of $1.6\ g\ cm^{-3}$ [84K3], was the first large-scale proton decay detector. It yielded $F < 2 \cdot 10^{-12}\ cm^{-2}\ s^{-1}\ sr^{-1}$ for $10^{-3} < \beta < 10^{-1}$ and $\sigma_c \simeq 10$ mb.

The Soudan-1 prototype, at a depth of 1800 m w.e., consists of horizontal layers of proportional tubes, each 4 cm in diameter, held in a matrix of taconite (iron-loaded concrete). The average density of the detector is $1.6\ g\ cm^{-3}$; the detector is $(2.9 \times 2.9 \times 1.9)\ m^3$ and wheighs 31 t [83A7]. It yielded $F < 1.5 \cdot 10^{-13}\ cm^{-2}\ s^{-1}\ sr^{-1}$ for $\beta > 10^{-3}$ and $\sigma_c = 10$ mb.

9·3. *Astrophysical limits on monopole catalysis of nucleon decay.* – The number of monopoles inside a star or a planet should keep increasing with time, because of a constant capture rate and of a probably small pole-antipole annihilation rate (see sect. 6). The catalysis of nucleon decay by magnetic monopoles could be another source of energy for these astrophysical bodies. It could lead to observable effects in those bodies which do not have an important

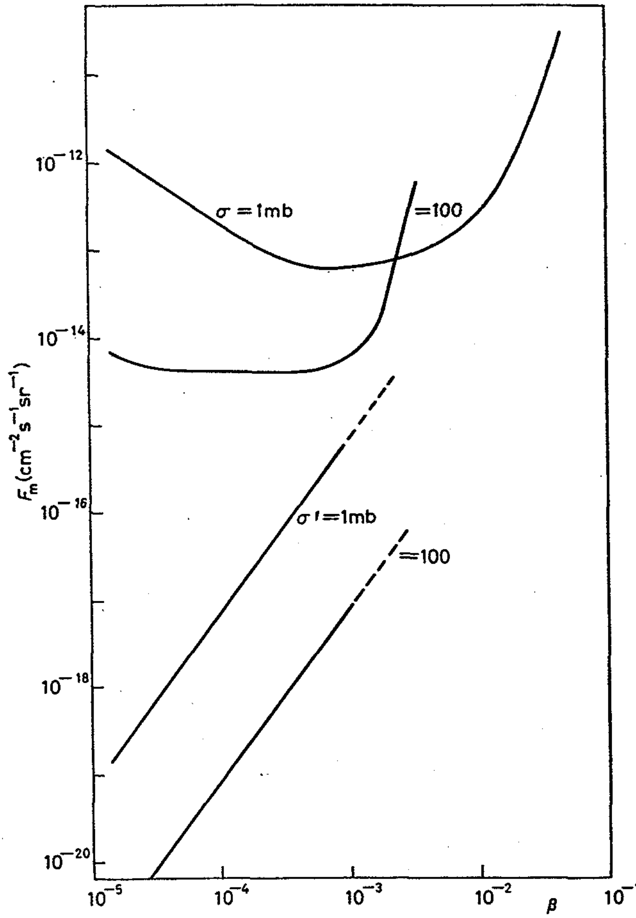

Fig. 9.5. – Upper limits (90% c.l.) on the monopole flux *vs.* monopole velocity for the multiple catalysis of proton decay in the Kamioka water Čerenkov detector for several values of the catalysis cross-section [84K3]. Also shown are upper limits from solar neutrinos (see text).

internal source of energy, like the planets, or which have used up most of the nuclear fuel, like the neutron stars and the white dwarfs. It is easy to perform a first-order estimate of the effect, which leads to strong constraints. But, there are many hypotheses which could vitiate the conclusion. For instance, a very small catalysis cross-section would make most of the following discussion irrelevant as far as limits for the monopole flux are concerned. The catalysis cross-section could be large in a hydrogen medium and small in a medium of heavy nuclei [83A9]. There is then the problem of how long have the monopoles been accumulating on each celestial body, what has happened to them, how many annihilated, etc. Table IX and fig. 9.6 give summaries of the astrophysical limits on monopole catalysis.

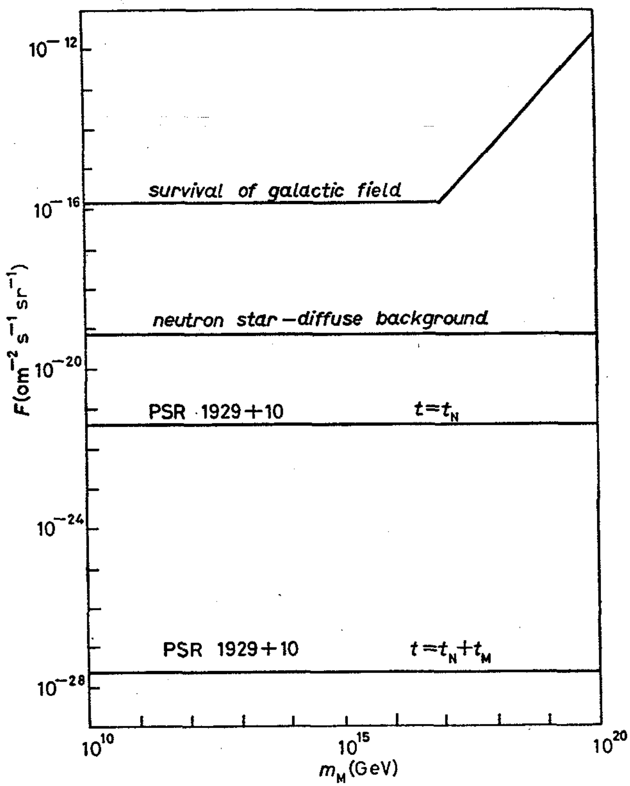

Fig. 9.6. – Monopole flux upper limits obtained from analyses of the monopole catalysis of nucleon decay in various astrophysical bodies for poles with $\beta = 10^{-3}$. The Parker bound (survival of galactic field) is shown for comparison.

9·3.1. Monopole catalysis of nucleon decay in the Earth. Turner [83T4] estimated an upper bound on the total number of monopoles present inside the Earth assuming that the total energy released by monopole catalysis of nucleon decay in the Earth should not exceed the surface heat flow. The Earth should stop monopoles with $\beta < 10^{-4}$, which are velocities typical of a local monopole flux, not of the galactic flux. The stopped monopoles will go towards the centre of the Earth, where they will have drift velocities of the order of $\beta_d \sim 10^{-5}$. At these low velocities the catalysis cross-section may have reached a constant value, $\sigma_{\Delta B \neq 0} \simeq 10^{-28} \sigma_R$. Thus the rate of catalysis is

$$\Gamma_{cat} = n_N \beta_d c \sigma_{\Delta B \neq 0} = n_N c \cdot 10^{-27} \beta_d \sigma_R \simeq 10^8 \beta_d \sigma_R \,, \tag{9.9}$$

where $n_N = 3.3 \cdot 10^{24}\ \mathrm{cm}^{-3}$ is the average density of nucleons in the Earth. In one nucleon decay is released an energy $w = 0.94\ \mathrm{GeV} = 1.5 \cdot 10^{-3}$ erg.

The power produced by catalysis in the Earth is

$$\left(\frac{\mathrm{d}W}{\mathrm{d}t}\right)_{\mathrm{cat}} = N_{\mathrm{M}} w \Gamma_{\mathrm{cat}}, \tag{9.10}$$

which should be smaller than the known heat flow ($L = 3\cdot 10^{20}$ erg/s). The total number of monopoles stopped by the Earth in its history is given by eq. (6.14). One has

$$\beta_{\mathrm{d}}\sigma_{\mathrm{R}}F \leqslant \frac{L}{4\pi^2 R_{\mathrm{E}}^2 t_{\mathrm{E}} w n_{\mathrm{N}} c\sigma_0} \simeq 0.8\cdot 10^{-20}\ \mathrm{cm}^{-2}\,\mathrm{s}^{-1}\,\mathrm{sr}^{-1}. \tag{9.11}$$

If $\sigma_{\mathrm{R}} = O(1)$, this would be a very strong bound. According to ARAFUNE *et al.* [83A9] the catalysis cross-section for slowly moving monopoles is suppressed for spinless nuclei and for nuclei with spin with a negative anomalous magnetic moment. A suppression factor of $1.9\cdot 10^{-6}$ for $\beta = 10^{-4}$ has been estimated for iron [83A2].

9'3.2. Limits from Jupiter and Saturn. The same reasoning may be repeated for the Jovian planets [83A9, 83T4]. The magnitude of the intrinsic heat for Jupiter and Saturn was well measured by the Pioneer and Voyager flights. Jupiter releases $1.76\cdot 10^{-6}$ erg/g s, while Saturn $1.52\cdot 10^{-6}$ erg/g s. From these values, the limit $F\sigma_{\mathrm{R}}\beta_{\mathrm{d}} < 4\cdot 10^{-18}\ \mathrm{cm}^{-2}\,\mathrm{s}^{-1}\,\mathrm{sr}^{-1}$ was obtained for Jupiter, valid for a flux of monopoles with $\beta \leqslant 3\cdot 10^{-4}$. The limit for Saturn is similar, while those for Uranus and Neptune are an order of magnitude worse. Since Jupiter and Saturn are predominantly made of hydrogen, the limit could be more reliable than that from the Earth (unless they have a small iron core) [83A9].

9'3.3. Limits from neutron stars. Neutron stars should be very effective in stopping monopoles, because of the good conductivity of the star medium, which enhances eddy-current losses. The energy released in catalyzed proton/neutron decays would be thermalized and radiated in the form of photons and neutrinos. Neutron stars are born very hot; in the absence of internal heat sources one expects that old neutron stars ($\sim 10^{10}$ y) are quite cold ($\leqslant 10^5$ K). Catalysis with a strong cross-section could heat the old neutron stars, yielding surface temperatures of ~ 50 eV ($\simeq 6\cdot 10^5$ K) and thus a strong X-ray emission. Upper limits on the monopole flux times the catalysis cross-section can be obtained by looking at the sky general X-ray background or at the total X luminosity of some particular neutron stars [82D1, 82K1, 83B6, 83O2, 84K2]. We may repeat the arguments used for the Earth keeping well in mind the peculiar properties of a neutron star, in particular its small radius ($R_{\mathrm{N}} \sim 10$ km) and its extremely high density. The interior of the star should behave as a very good conductor, yielding very high energy losses for monopoles, estimated to be $\mathrm{d}E/\mathrm{d}x \simeq 10^{11}\beta$ (GeV/cm). The escape velocity from a neutron star is $\beta_{esc} \simeq 0.5\ c$; all monopoles will reach these velocities when they encounter the surface of the star after falling in the star gravitational field. The high rate of energy loss ensures that all poles with masses between 10^4 and 10^{17} GeV are stopped in the star; poles with $m_M < 10^4$ GeV will be accelerated away, poles with $10^{17} < m_M < 10^{23}$ will not stop, but will lose enough energy so as to be gravitationally bound, and will eventually end in the star. Because of the high magnetic fields the effective star surface for intercepting monopoles is larger than the geometric cross-section. In a Newtonian approximation it is

$$\Sigma \doteq 4\pi R_N^2\left[1+\left(\frac{\beta_{esc}}{\beta}\right)^2\right] \simeq 4\pi R_N^2\frac{\beta_{esc}^2}{\beta^2} \simeq \frac{\Sigma_0}{\beta^2}. \tag{9.12}$$

One has:

total number of captured monopoles: $N_M = \pi\Sigma F t$;
catalysis rate: $\Gamma_{cat} = n_N c\beta_d\sigma_0\sigma_R$;
energy release by catalysis: $(\mathrm{d}W/\mathrm{d}t)_{cat} = N_M\Gamma_{cat}$.

For the young pulsar 1929 + 20, which is ~ 60 parsec from us, one obtains the following rough estimate:

$$\beta_d\sigma_R F \leqslant \frac{L\beta^2}{\pi\Sigma_0 t n_N c\sigma_0 w} \simeq 10^{-21}\ \mathrm{cm^{-2}\ s^{-1}\ sr^{-1}}. \tag{9.13}$$

In (9.13) one assumed $T_{surface} = 2\cdot 10^5$ K, $L_{tot} \simeq L_\gamma = 2.6\cdot 10^{30}$ erg/s (*), $\Sigma_0 = 8\cdot 10^{11}\ \mathrm{cm}^2$, $n_N = 2\cdot 10^{38}$ nucleons/cm³, $\sigma_0 = 0.1$ mb, $t = t_N \simeq 3\cdot 10^6$ y and $\beta = 10^{-3}$. A more precise estimate is given in table XI. If one considers also the time spent by the star in the main sequence (assuming that poles are not lost in the supernova phase), then $t = t_N + t_M \simeq t_M \simeq 10^{10}$ y and the limit (9.13) becomes $3\div 4$ orders of magnitude better.

Table XI gives a summary of the various upper-limit estimates of the product $F\sigma_R\beta$ together with a comment on their reliability. (It is clearly important to have a better knowledge of the neutron star interior.) The monopole-nucleon relative velocity is the thermal velocity inside the astrophysical body. For very small velocities the catalysis cross-section should at most reach a saturation value. The table quotes also limits obtained from the Earth, Jupiter and white dwarfs.

If a neutron star has a core of pion condensate, it may have magnetic-flux tubes with the same flux of a magnetic monopole. It would then be possible

(*) The total luminosity of a neutron star may be estimated from the measured photon luminosity, L_γ, according to some model of the equation of state and of the internal structure of a neutron star.

TABLE XI. – *Astrophysical limits on monopole catalysis* [84K2]. The first six lines refer to limits from neutron stars. The table gives the star photon luminosity (L_γ), the ratio r of total luminosity over photon luminosity, the thermal velocity β_d of poles inside the star, the limit for $F\sigma_R\beta_d$ and the main uncertainties in the calculations. Some of the values have been corrected for photon absorption in the interstellar medium (ISM). A value $\sigma_0 = 0.1$ mb was chosen. The last two lines give limits for the monopole catalysis in the Earth and in Jupiter. The flux limits would here apply to the local flux of low-velocity monopoles ($\beta < 10^{-4}$ and $< 3\cdot 10^{-4}$ respectively, while stars capture monopoles with $\beta < 10^{-3}$).

Method	L_γ (erg/s)	$r = L_T/L_\gamma$	β_d	$F\sigma_R\beta_d$ ($cm^{-2}\,s^{-1}\,sr^{-1}$)	Uncertainties	Reference
diffuse X-ray background	$< 2\cdot 10^{32}$	$1 \div 10^3$	0.3	$r\cdot 10^{-24}$	equation of state, ISM	[82D1]
diffuse X-ray background	$< 3\cdot 10^{30}$	$1 \div 10^3$	0.3	$3r\cdot 10^{-23}$	equation of state, ISM	[84K2]
diffuse X-ray background ($E_\gamma > 200$ eV)	$< 2\cdot 10^{32}$	$5 \div 10^3$	0.3	$r\cdot 10^{-22}$	equation of state, ISM	[82K1]
serendipitous searches for X-ray point sources	$< 10^{31}$	10^2	0.3	$5r\cdot 10^{-24}$	equation of state.	[82K1]
1129 + 10 (young neutron star, $\tau \sim 10^6$ y)	$< 3\cdot 10^{30}$	1	0.3	$7r\cdot 10^{-22}$	distance, age, r, $M\bar{M}$ annihilation	[84K2]
1129 + 10 including main sequence lifetime	$< 3\cdot 10^{30}$	1	0.3	$7r\cdot 10^{-27}$	above+main sequence pole end in n-star?	[84K2]
white dwarfs	$< 10^{30}$	1	10^{-3}	$2\cdot 10^{-21}$	r, internal structure, annihilation	[83K5]
Earth	$< 3\cdot 10^{20}$	—	10^{-5}	$3\cdot 10^{-20}$	capture, nuclear suppression	[83T4]
Jupiter	$< 5\cdot 10^{24}$	—	$10^{-3} \div 10^{-4}$	$4\cdot 10^{-18}$	capture, iron core? (nuclear suppression)	[83T4]

for a monopole which entered one such flux tube to be accelerated to velocities larger than the escape velocity of the star: thus the neutron star would absorb monopoles with $\beta \sim 10^{-3}$ and eject a very small percentage of them with $\beta \sim 0.5$ and kinetic energies $K \sim 10^{17}$ GeV! [83H4, 83K1].

9'3.4. Limit from neutrinos from the Sun. The catalysis argument applied to the protons of our Sun leads to the possibility that the Sun could emit electron neutrinos, with an average energy of 35 MeV, coming from muon decays [83A9]. This process could lead to about $3 \cdot 10^4$ electron neutrinos incident on the Earth per cm^2 and per second (if $\leqslant 1\%$ of the solar luminosity is due to monopole catalysis; this is of the same order of magnitude as the limit from Jupiter). The electron neutrinos may elastically scatter on electrons. The Kamioka proton decay detector is sensitive to electrons with energies larger than 10 MeV. From three possible candidates the authors estimate an upper limit $F < 8 \cdot 10^{-10} \beta^2$ if the monopole catalysis cross-section is 1 mb [84K3]. (The espected background from atmospheric neutrinos with $E_\nu \sim 35$ MeV is about 1.) From limits of this sort one could place a limit on the number of poles in the Sun, at the approximate level of less than 1 pole per 10^{12} g.

10. – Other types of searches.

Among the other types of searches one may mention the searches for protons with a monopole-antimonopole structure [75O1, 79B1], the searches for magnetic currents [45E1, 51E1] and the searches for tachyon monopoles, that is for monopoles which should be travelling faster than light [72B1, 78B1]. In this section we shall briefly mention some of these searches.

Most experiments cannot establish if the magnetic-dipole moment of the proton is made from a monopole-antimonopole distribution rather than from a distribution of current loops or of intrinsic moments, since the experiments are sensitive only to the proton's magnetic field outside the distribution [75O1, 79B2]. An exception is the hyperfine transition in the neutral hydrogen atom which leads to the emission of the 21 cm wave. The interaction energy between the electron and proton magnetic moments is of the form

$$w = -A\boldsymbol{\mu}_e \cdot \boldsymbol{\mu}_p , \tag{10.1}$$

where $A = (-4\pi/3)|\psi(0)|^2$ for the normal proton; it would be $(8\pi/3)|\psi(0)|^2$ for a proton dipole moment equal to the observed one, but arising from a monopole-antimonopole distribution. In this case the hyperfine transition would lead to a 42 cm radiation.

The fact that ordinary matter leads to the 21 cm radiation and not to the 42 cm one is a result which denies magnetic charge any role in the structure of ordinary matter. If one assumes that the magnetic moment of the proton is given by a normal part term and by a second term $\mu' = \delta\mu_p$ due to a pole-antipole structure, then the precision measurement of the 21 cm wave yields for the parameter δ the limit $\delta < 2\cdot 10^{-6}$. If one writes $\mu' = g_D d = \delta\mu_p$, one obtains $d < \delta\mu_p/g_D < 10^{-8}$ fm [75O1].

There remains the logical possibility that some small fraction of protons could be anomalous and have their moments made from magnetic-charge distributions rather than from current distributions. In this case there is no real guarantee that the magnetic-dipole moment would be numerically equal to the normal one, but one has to hypothesize the equality. BRODERICK *et al.* [79B1] analysed the radiation emitted by three supernova remnants and the radio galaxy 3C353. These are strong sources of continuum emission, with a strong absorption line at the 21 cm radiation. The absorption is interpreted as due to neutral galactic hydrogen located in the line of sight from the sources to the detecting radiotelescope. The authors did not find any absorption at 42 cm. Thus they exclude the presence of anomalous protons in the neutral galactic hydrogen at a level of $2\cdot 10^{-4}$ of the normal protons.

RAUTIAN *et al.* [77R1] have proposed a method of detecting magnetic monopoles by searching for anomalies in the maser emission of large interstellar clouds of OH molecules. The monopoles may change the scale of splitting of Zeeman sublevels or change the polarization of one optical line (from circular to linear). The effects depend on the square of the magnetic charge.

11. – Future detectors.

In this section we shall mention new methods of monopole detection and then discuss the large-area experimental lay-outs which are coming into operation or which are planned.

11'1. *New detectors.*

Superconducting scanning detector. The Stanford group has proposed a new type of superconductive detector, which uses a thin superconducting sheet, in the form of a cylinder, for recording magnetically charged particle tracks [83F1]. A magnetic charge traversing the cylinder would leave, in the walls of the cylinder, doubly quantized trapped flux vortices, which would remain in the same location as long as the sheet remains superconducting. The surface area of the cylinder could be periodically scanned; quantized vortices could be recorded by a small scanning coil coupled to a SQUID, mounted on a mechanichal system which rotates about the axis of the cylinder. The authors estimate that the superconducting sheet would have about one quantized vortex per square centimetre, corresponding to the ambient trapped flux from the 10^{-7} G field inside the shielding. Regular scanning would provide the records for individuating new vortices.

Superconducting colloid detector. A superconducting colloid detector consists of a collection of normal metal grains coated with a thin layer of superconductor. They are held at low temperature in a dielectric filler material under a magnetic field. The field and temperature are so adjusted that a small temperature jump will flip the grains into the normal state. The energy deposited by the passage of a single particle can flip the grains, since the specific heat is low at low temperature. As a grain goes normal, the magnetic field in and around the grain changes, leading to a relatively large electromagnetic signal, which can be picked up by a read-out coil.

The proposed detectors [83D5, 83G4] would use a superconducting colloid ~ 1 cm thick, filled with grains of ~ 20 μm size, at $T \sim 2$ K. A monopole would cross ~ 50 grains. Each grain is made of aluminium coated with a thin layer of type I superconductor. The read-out could be somewhat similar to those of multiwire proportional chambers (thus having time information to < 0.1 μs and space information to $\simeq 1$ cm). The relatively large energy losses of a monopole in a metal allow us to set a threshold at few hundred keV, thus reducing background from minimum ionizing particles. The noise from fission fragments and cosmic-ray showers should be minimized.

Inductive nonsuperconducting coils. Several reports have been written on inductive nonsuperconductive coils [81B3, 82R4, 83P1]. A magnetic charge moving with constant velocity in a direction perpendicular to the plane of a circular loop and passing through its centre produces an electric field tangent to the circumference of the loop (see (3.7), where we neglected the $\partial B/\partial t$ term of eq. (2.3)). Thus in the loop there is an induced electromotive force

$$V = \oint \boldsymbol{E}\cdot d\boldsymbol{l} = \frac{2\pi r^2 \beta\gamma g}{(r^2+\gamma^2 v^2 t^2)^{3/2}} \,. \tag{11.1}$$

For slow moving poles $\gamma \sim 1$, and for a coil with N turns one has a voltage pulse of approximate Gaussian shape

$$V \simeq \frac{2\pi g}{r}\beta N\left[1+\frac{v^2t^2}{r^2}\right]^{-3/2} \tag{11.2}$$

with a maximum value $V_{\max} = 2\pi g N\beta/r$ (for $N = 10^3$, $\beta = 10^{-4}$, $r = 5$ cm $\rightarrow V_{\max} = 120$ μV) and a full width at half height $\Delta t \simeq 1.5\, r/v$. The integrated value of the induced voltage gives the magnetic charge g

$$\int V\,\mathrm{d}t = \frac{4\pi}{c}\,gN\,. \tag{11.3}$$

The situation does not change significantly for off-axis monopoles.

The thermal noise is concentrated in the resistive component of the coil. One has an approximate signal-to-noise ratio [82R4]

$$\frac{\mathrm{S}}{\mathrm{N}} \simeq g\left[16KT\varrho_0\beta c\,\frac{l^2}{ab}\right]^{1/2} \tag{11.4}$$

which does not depend on the number of turns. The best situation seems to be that of a massive coil with $l \simeq a \simeq b$. The S/N ratio could be improved by a factor of 5 going to liquid-nitrogen temperatures.

Tests of inductive nonsuperconducting coils were performed at CERN [83P1] and at Berkeley [82F2]. At Berkeley a 15 cm diameter, 3 cm thick coil with 10^4 turns of 0.15 mm copper wire is placed inside a Cu shield. The container and the pick-up are kept at liquid-helium temperature. The signal is amplified with a FET amplifier. At CERN a 15 cm diameter, 10 cm thick coil with 10^4 turns of 0.2 mm copper wire is kept at room temperature.

Acoustic detection of monopoles. When a monopole passes through a conductor, the energy loss due to eddy current is deposited within a radius of $\simeq 1000$ Å of the particle track. The heated metal expands and thus produces an acoustic wave in a rather broad band of very high frequencies. The wave travels through the material and reaches an acoustic transducer where it is detected.

Since the monopole β is always larger than $3.8\cdot10^{-5}$, the poles travel faster than the sound velocity in the medium. If the medium has tipical dimensions larger than 1 m, then the maximum useful frequency is limited to ~ 10 MHz by the attenuation length (which decreases fast with increasing frequency). AKERLOF [82A3, 83A3] estimated that at most 0.45 eV of the total energy loss may reach the detector. The signal has to be compared with various noises: the thermal noise in the medium does not seem to pose problems, the corresponding S/N ratio being of the order of ten. The noise problems arise from the thermal noise via the transducer, in the preamplifier and in the electronics. The Caltech group [82B3] has S/N $\sim 10^{-2}$. The ratio could be improved by shaping the metal so as to achieve focusing of the sound wave. One could also lower the temperature and/or change the type of transducer.

11'2. *Future large-area lay-outs.* – The present trend towards larger experiments may be summarized as follows.

1) *Superconducting induction experiments.* Several groups are developing and testing superconducting induction devices with $S \simeq 1\ \mathrm{m}^2$; they could be duplicated to achieve surface areas $S \simeq (10 \div 100)\ \mathrm{m}^2$ [84E3]. The final goal will probably be a co-operative effort to mount a detector with $S\Omega \sim 1000\ \mathrm{m}^2\ \mathrm{sr}$.

The Stanford group is building a new detector consisting of eight planar twisted loops mounted on the walls of a cylinder. Each loop has an area of $1.5\ \mathrm{m}^2$ and is composed of an array of oppositely coupled square elements, each 8 cm on a side (total $S\Omega \simeq 18\ \mathrm{m}^2\ \mathrm{sr}$) [84G2].

The IBM group is presently designing a new larger box of six independent gradiometers (fig. 11.1), with $S\Omega \simeq 50\ \mathrm{m}^2\ \mathrm{sr}$.

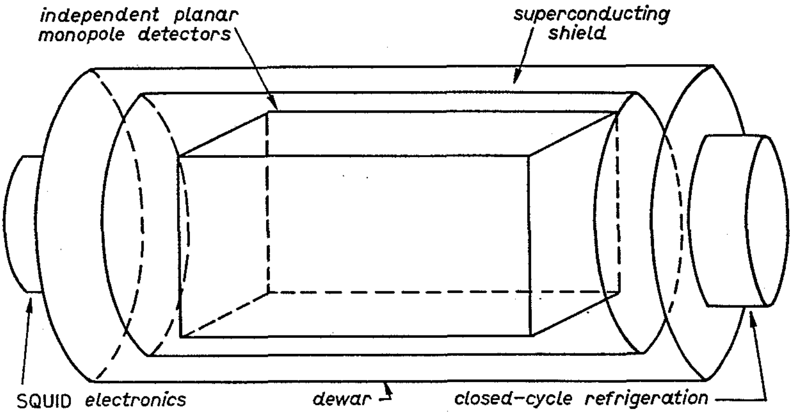

Fig. 11.1. – Sketch of the proposed IBM superconducting induction lay-out.

The Chicago-Fermilab-Michigan group is designing a basic unit of $1\ \mathrm{m}^2$ surface, with two « macrame » coils in coincidence (fig. 11.2). In a dewar there could be 5 of these units for a total $S\Omega \simeq 50\ \mathrm{m}^2\ \mathrm{sr}$ [84S1].

2) *Track-etch detectors.* In the Kamioka mine a Japanese group is installing $1000\ \mathrm{m}^2$ of CR39 track-etch detectors [83K2]. A similar system may be installed in the Gran Sasso tunnel in Italy [84L1].

3) *Electronics experiments.* The present largest lay-out is the Baksan detector with $S\Omega = 1800\ \mathrm{m}^2\ \mathrm{sr}$. Other large detectors in various stages of development are [83A7, 83G3]:

The University of Pennsylvania and BNL groups are designing a hollow-box detector of $(8 \times 8 \times 16)\ \mathrm{m}^3$ with 200 scintillation counters covering all six sides of the box. Each counter is a $(0.3 \times 0.3 \times 8)\ \mathrm{m}^3$ box filled with mineral oil-based liquid scintillator. Two 5″ photomultipliers view the ends of the box. This detector will cover the existing tetrachloroethylene solar-neutrino tank

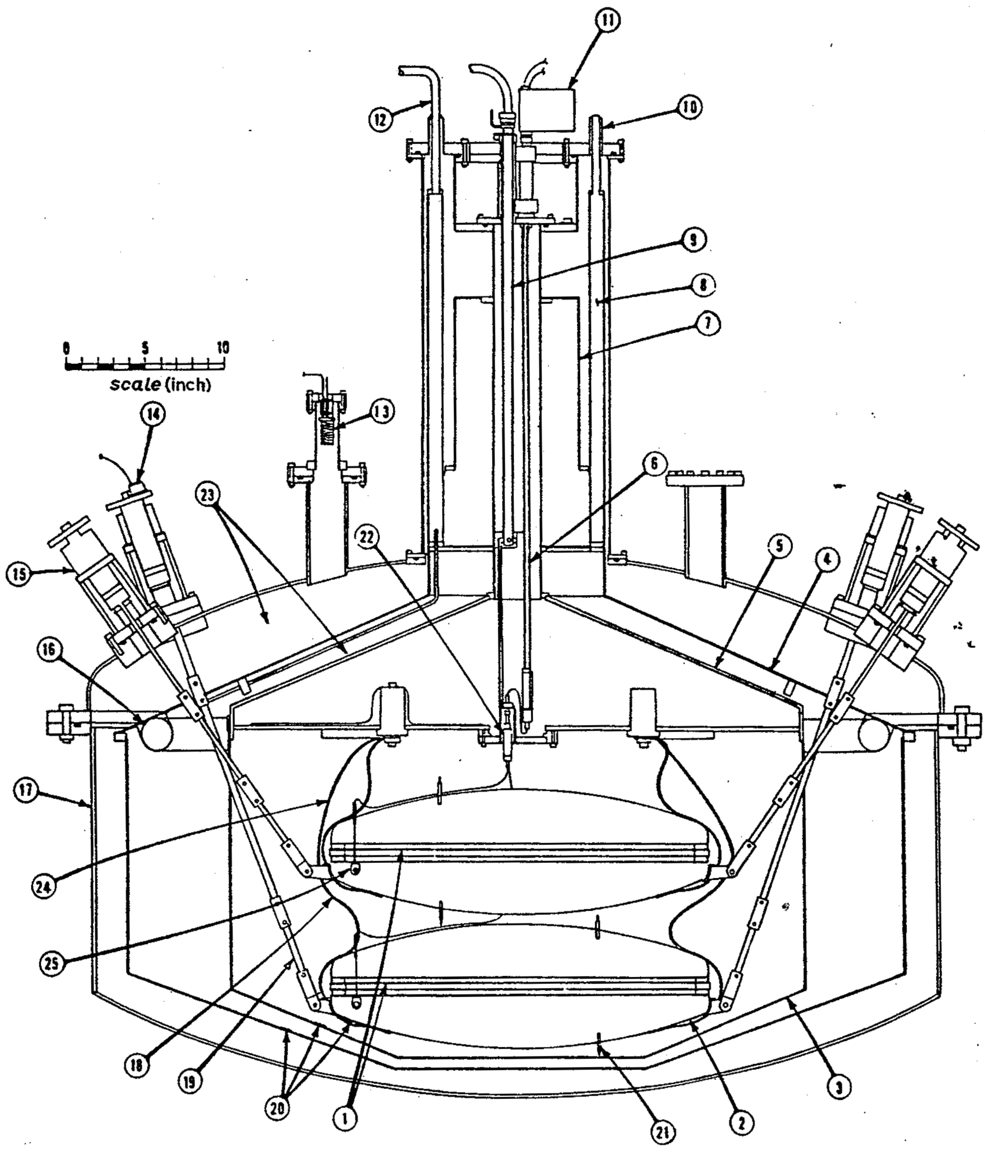

Fig. 11.2. – The Chicago-Fermilab-Michigan prototype detector. The scale is set by the diameter of the loops, which is two feet [83F4].

in the Homestake mine. It should have $S\Omega \simeq 1500\ \text{m}^2\,\text{sr}$ and be sensitive to $4\cdot 10^{-3} < \beta < 0.5$.

A group at Texas A & M University is designing a large three-layer scintillation counter detector with an effective area of $150\ \text{m}^2$. It is made of 108 ($4' \times 8' \times 3/8''$) acrylic-based scintillators located on the surface of a 24 feet cube. It may first detect poles with $0.04 < \beta < 1$ and later down to β of few 10^{-4}.

The fly's eye detector at Utah scans the entire night sky for high-energy ($>10^{17}$ eV) cosmic-ray–induced showers. These are detected via sixty-seven 1.5 m diameter mirrors each viewed by 14 photomultipliers. For each shower the system allows the recording of the time of arrival of the light signals in conjunction with the geometry of the tracks, thus giving an estimate of the cosmic-ray shower energy. The detector may look for monopole-antimonopole annihilation events.

The proton decay experiment in the Frejus tunnel, between France and Italy, is a fine-grain calorimeter of $(6\times6\times13)$ m^3 dimension and weighs ~1000 t. It is made of 1000 flash-tube planes interspersed with two 1.5 mm iron plates; 120 Geiger tube planes serve as trigger. As a monopole detector it may detect poles with few $10^{-4}<\beta<10^{-1}$; it has $S\Omega\sim1000$ m^2 sr.

The second Mont Blanc detector is made of 72 tanks (each 1.5 m^3 in volume) of liquid scintillator (a total mass of $\sim$ 90 t). Its primary purpose is the search for $\sim$10 MeV neutrinos resulting from stellar collapse. It may be used as a monopole detector with $S\Omega\sim700$ m^2 sr covering a β range $4\cdot10^{-3}<\beta<10^{-2}$.

There are preliminary plans and discussions for larger detectors (Stanford, Baikal Lake, Soudan, etc). In particular, there is the intent to install in the Gran Sasso underground laboratory, in Italy, an electronic detector with $S\Omega\geqslant10\,000$ m^2 sr [84L1]. The detector would have two planes of thick scintillation counters, 6 planes of limited streamer tubes and four planes of proportional tubes to make use of the Drell+Penning effects. A CR39 track-etch detector should be incorporated.

Catalysis of proton decay. All proton decay experiments have installed new electronics and are improving it in order to be able to detect a string of catalyzed proton decays.

12. – Conclusions and outlook.

In the last few years we have witnessed a large increase of the number of papers on magnetic monopoles: it started with a large increase in theoretical works, then in phenomenological papers, including astrophysical implications, and now with the results of several experimental searches. We have learned that the list of what monopoles could do has become longer. Besides producing an intense magnetic field, they may catalyze proton decay, induce nuclear fission of heavy elements, induce β-decay, attach nuclei, destroy magnetic fields, etc. The mass of the monopole is expected to be very large; it could be so large that poles could even be little black holes. The number of monopoles produced in the early Universe could be so small that their detection could be impossible, but it could also be so large that they could significantly contribute to the dark matter in the Universe.

The field of magnetic monopoles has evolved into a fascinating interdisciplinary field of physics, with implications in fundamental theories, in particle physics, in astrophysics and in cosmology. In certain aspects it represents a connection between physics and cosmology.

Monopoles are required by unified gauge theories. It seems that they would fill a specific gap, that their basic properties are known and also that some of

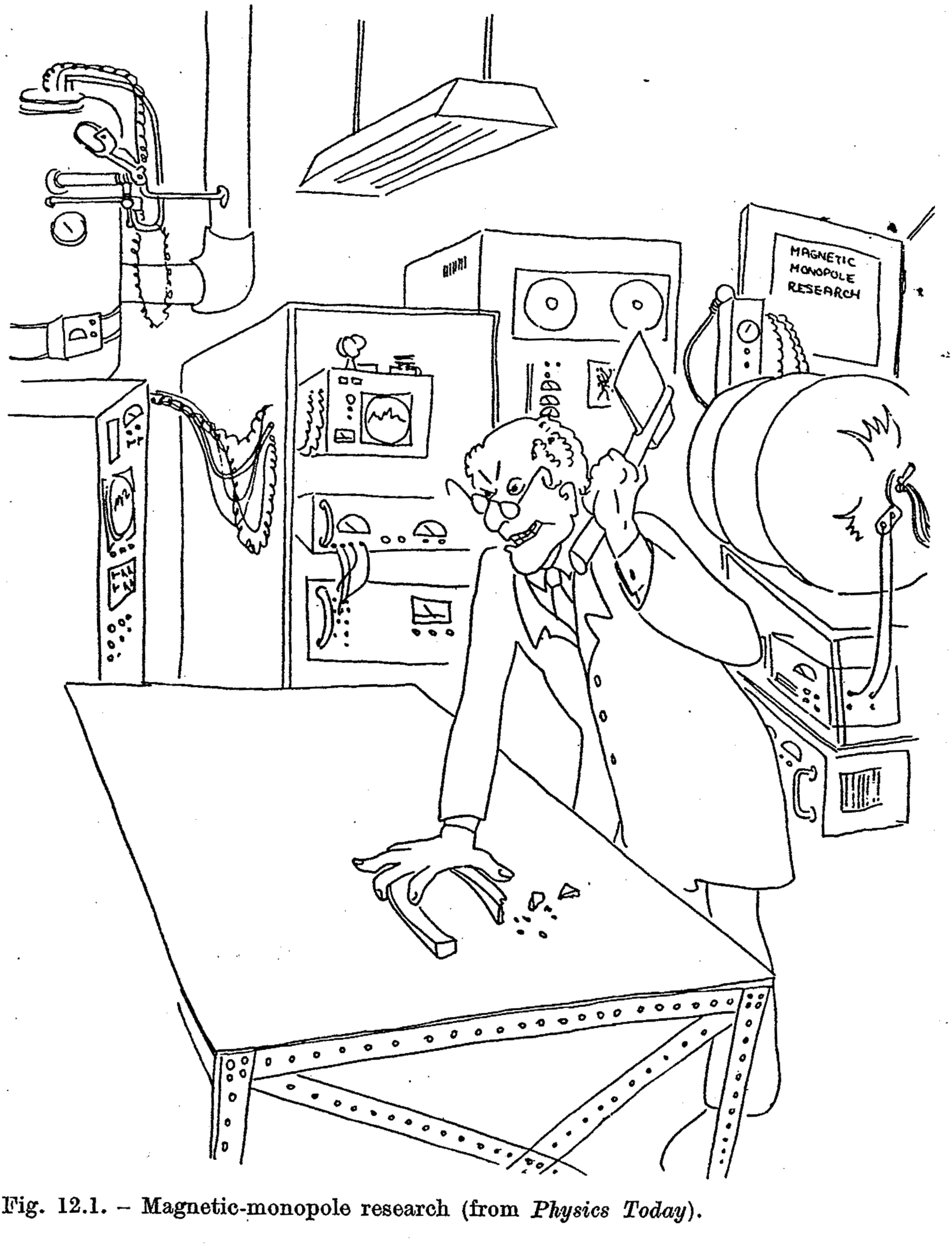

Fig. 12.1. – Magnetic-monopole research (from *Physics Today*).

the consequences from their existence are predictable. The discovery of superheavy magnetic monopoles would have far-reaching implications: it would confirm the unification hypothesis, fix its energy scale and give cosmological evidence that the Universe was once extremely hot. If the magnetic charge is one unit Dirac charge, it would presumably imply quark confinement, thus forbidding free quarks with fractional charges [82L2].

The theoretical and phenomenological understanding of monopoles has improved considerably in the last few years. But new possibilities have opened up. I refer in particular to the various differing predictions of the monopole mass and of the monopole production rates in the early Universe. Therefore, theoretical guidance to experiments is not really adequate.

From the experimental point of view, one clearly observes the trend towards larger and costlier experiments. Moreover, it has been pointed out by several people that in the searches for rare events it is normal to get a candidate which is difficult to reject [83F4]. This forces the experimenters to use at the same time, at least in large lay-outs, more than one technique in order to obtain redundancy and gain in « convincingness » [83C4]. But, what if one finds nothing convincing? In order to overcome this possibility several of the larger experiments are planning to add « worthy by-products », like detection of multi-muon events, neutrinos from supernovae explosions, neutrinos from the Sun, and in general measurements of astrophysical significance. But what the field of monopole would really need would be some real monopoles! (fig. 12.1).

* * *

I would like to acknowledge a large number of colleagues for explanations, for co-operation and for sending material before publication. I would like to mention and to thank in particular Drs. S. P. Ahlen, B. Barish, J. M. Barkov, B. Cabrera, P. Capiluppi, C. L. Chi, R. A. Carrigan jr., D. Cline, N. S. Craigie, R. J. Crewther, I. D'Antone, A. De Rujula, G. Fiorentini, E. Fiorini, H. Frisch, L. Gonzales, E. Iarocci, M. Koshiba, G. Mandrioli, V. P. Martemyanov, P. Musset, P. Picchi, P. B. Price, A. M. Rossi, A. Sen, J. Stone, N. Straumann, C. D. Tesche, C. C. Tsuei and G. Venturi.

MONOPOLE BIBLIOGRAPHY

This bibliography on magnetic monopoles from 1931 till 1984 is far from complete. It is meant to be comprehensive of all experimental papers and of the most recent results. A more comprehensive bibliography is reported in the specialized papers [73S1], [77C1], [80R1], [81C1] and [82C3].

[31D1] P. A. M. Dirac: *Proc. R. Soc. London,* **133**, 60 (1931).
[31T1] J. Tamm: *Z. Phys.*, **71**, 141 (1931).

[33T1] M. A. TUVE: *Phys. Rev.*, **43**, 770 (1933).
[35G1] B. O. GRÖNBLOM: *Z. Phys.*, **98**, 283 (1935).
[38J1] P. JORDAN: *Ann. Phys. (N. Y.)*, **32**, 66 (1938).
[44E1] F. EHRENHAFT: *Phys. Rev.*, **65**, 62 (1944).
[44F1] M. FIERZ: *Helv. Phys. Acta*, **17**, 27 (1944).
[45E1] F. EHRENHAFT: *Phys. Rev.*, **67**, 201 (1945).
[46B1] P. P. BANDERET: *Helv. Phys. Acta*, **19**, 503 (1946).
[48C1] H. CHANDRA: *Phys. Rev.*, **74**, 883 (1948).
[48D1] P. A. M. DIRAC: *Phys. Rev.*, **74**, 817 (1948).
[49E1] F. EHRENHAFT: *Phys. Rev.*, **75**, 1334 (1949).
[49S1] M. N. SABRA: *Phys. Rev.*, **75**, 1968 (1949).
[51B1] E. BAUER: *Proc. Cambridge Philos. Soc.*, **47**, 777 (1951).
[51C1] H. J. D. COLE: *Proc. Cambridge Philos. Soc.*, **47**, 196 (1951).
[51E1] F. EHRENHAFT: *Acta Phys. Austriaca*, **5**, 12 (1951).
[51F1] K. FORD and J. A. WHEELER: *Phys. Rev.*, **81**, A 656 (1951).
[51M1] W. V. R. MALKUS: *Phys. Rev.*, **83**, 899 (1951).
[52S1] S. SHANNUGADHASAN: *Can. J. Phys.*, **30**, 218 (1952).
[54S1] M. SCHEIN, D. M. HASKIN and R. G. GLASSER: *Phys. Rev.*, **95**, 855 (1954).
[55S1] M. SCHEIN, D. M. HASKIN and R. G. GLASSER: *Phys. Rev.*, **99**, 643 (1955).
[58F1] H. C. FITZ, W. B. GOOD, J. L. KASSNER and A. E. RUARK: *Phys. Rev.*, **111**, 1406 (1958).
[58G1] E. GOTO: *J. Phys. Soc. Jpn.*, **13**, 1413 (1958).
[58R1] N. F. RAMSEY: *Phys. Rev.*, **109**, 225 (1958).
[59A1] Y. AHARONOV and D. BOHM: *Phys. Rev.*, **115**, 485 (1959).
[59F1] K. W. FORD and J. A. WHEELER: *Ann. Phys. (N. Y.)*, **7**, 287 (1959).
[59H1] H. BRADNER and W. M. ISBELL: *Phys. Rev.*, **114**, 603 (1959).
[59K1] R. KATZ and O. R. PARNELL: *Phys. Rev.*, **116**, 236 (1959).
[60L1] I. R. LAPIDUS and J. L. PIETENPOL: *Am. J. Phys.*, **28**, 17 (1960).
[60P1] N. A. PORTER: *Nuovo Cimento*, **16**, 958 (1960).
[61F1] M. FIDECARO, G. FINOCCHIARO and G. GIACOMELLI: *Nuovo Cimento*, **22**, 657 (1961).
[62C1] N. CABIBBO and E. FERRARI: *Lett. Nuovo Cimento*, **23**, 1146 (1962).
[62E1] C. J. ELIEZER: *Proc. Cambridge Philos. Soc.*, **58**, 401 (1962).
[63A1] E. AMALDI, G. BARONI, A. MANFREDINI, H. BRADNER, L. HOFFMANN and G. VANDERHAEGHE: *Nuovo Cimento*, **28**, 773 (1963).
[63A2] E. AMALDI, G. BARONI, H. BRADNER, H. G. DE CARVALHO, L. HOFFMANN, A. MANFREDINI and G. VANDERHAEGHE: *Search for Dirac magnetic poles*, CERN 63-13 (1963), unpublished.
[63G1] E. GOTO: *Prog. Theor. Phys.*, **30**, 700 (1963).
[63G2] E. GOTO, H. M. KOHM and K. W. FORD: *Phys. Rev.*, **132**, 387 (1963).
[63P1] V. A. PETUKHOV and M. N. YAKIMENKO: *Nucl. Phys.*, **49**, 87 (1963).
[63P2] E. M. PURCELL, G. B. COLLINS, T. FUJII, J. HORNBOSTEL and F. TURKOT: *Phys. Rev.*, **129**, 2326 (1963).
[64R1] R. A. FERRELL: *Physics (N. Y.)*, **1**, 1 (1964).
[64S1] S. SEYFFERTH: *Naturwissenschaften*, **51**, 547 (1964).
[65C1] R. A. CARRIGAN: *Nuovo Cimento*, **38**, 638 (1965).
[65H1] C. R. HAGEN: *Phys. Rev.*, **140**, B 804 (1965).
[65K1] R. KATZ and J. J. BUTTS: *Phys. Rev.*, **137**, B 148 (1965).
[65T1] L. J. TASSIE: *Nuovo Cimento*, **38**, 1935 (1965).
[65T2] D. R. TOMPKINS: *Phys. Rev.*, **138**, 248 (1965).
[65W1] S. WEINBERG: *Phys. Rev.*, **138**, 988 (1965).

[66A1] R. K. Adair, W. C. Carithers and R. Stefanski: *Phys. Rev.*, **149**, 1070 (1966).
[66H1] M. B. Hague: *J. Nat. Sci. Math.*, **6**, 41 (1066).
[66S1] J. Schwinger: *Phys. Rev.*, **144**, 1087 (1966).
[66S2] J. Schwinger: *Phys. Rev.*, **151**, 1048 (1966).
[66S3] J. Schwinger: *Phys. Rev.*, **151**, 1055 (1966).
[67G1] P. J. Green: *Sea level cosmic-ray search for fast small-pole strength magnetic charges*, Thesis, Luisiana University (1967), unpublished.
[67K1] H. H. Kolm: *Phys. Today*, **20**, 69 (1967).
[68A1] E. Amaldi: *On the Dirac magnetic poles*, in *Old and New Problems in Elementary Particles* (Academic Press, New York, N.Y., 1968), p. 1.
[68H1] L. L. Vant-Hull: *Phys. Rev.*, **173**, 1412 (1968).
[68K1] H. H. Kolm: *Sci. J.*, **4**, 60 (1968).
[68P1] R. F. Palmer and J. C. Taylor: *Nature (London)*, **219**, 1033 (1968).
[68P2] N. A. Porter: *Nature (London)*, **217**, 329 (1968).
[68S1] J. Schwinger: *Phys. Rev.*, **173**, 1536 (1968).
[69A1] F. Ashton: *Izv. Adak. Nauk SSSR*, **33**, 1817 (1969).
[69E1] A. D. Erlykin and V. I. Yakovlev: *Sov. Phys. JETP*, **29**, 992 (1969).
[69F1] R.L. Fleischer, I.S. Jacobs, W.M. Schwarz, P.B. Price and H.G. Goodell: *Phys. Rev.*, **177**, 2029 (1969).
[69F2] R. L. Fleischer, H. R. Hart, I. S. Jacobs, P. B. Price, W. M. Schwarz and F. Aumento: *Phys. Rev.*, **184**, 1393 (1969).
[69F3] R. L. Fleischer, P. B. Price and R. T. Woods: *Phys. Rev.*, **184**, 1398 (1969).
[69R1] M. A. Ruderman and D. Zwanziger: *Phys. Rev. Lett.*, **22**, 146 (1969).
[69S1] J. Schwinger: *Science*, **165**, 757 (1969).
[70A1] L. W. Alvarez, P. H. Eberhard, R. R. Ross and R. D. Watt: *Science*, **167**, 701 (1970).
[70B1] M. I. Blagov, V. A. Murashova, T. I. Syreitshikova, Yu. Ya. Tel'nov, Yu. D. Usachev and M. N. Yakimenko: *Search for magnetic charge particles produced by a photon beam*, in *Proccedings of the 1970 Kiev Conference* (1970), p. 314.
[70F1] R. L. Fleischer, H. R. Hart jr., I. S. Jacobs, P. B. Price, W. M. Schwarz and R. T. Woods: *J. Appl. Phys.*, **41**, 958 (1970).
[70G1] G. Giacomelli: *New frontiers of high energy physics*, in *Evolution in Particle Physics*, edited by M. Conversi (New York, N.Y., 1970), p. 147.
[70G2] I. I. Gurevich, S. Kh. Khakimov, V. P. Marthemianov, A. P. Mishakova, V. V. Ogurtzov, V. G. Tarasenko, L. M. Barkov and N. M. Tarakanov: *Phys. Lett. B*, **31**, 394 (1970).
[70H1] M. Y. Han and L. C. Biederharn: *Phys. Rev. Lett.*, **24**, 118 (1970).
[70O1] W. Z. Osborne: *Phys. Rev. Lett.*, **24**, 1441 (1970).
[70P1] E. N. Parker: *Astrophys. J.*, **160**, 383 (1970).
[70P2] E. N. Parker: *Astrophys. J.*, **162**, 665 (1970).
[70S1] K. H. Schatten: *Phys. Rev. D*, **1**, 2245 (1970).
[70S2] D. Sivers: *Phys. Rev. D*, **2**, 2048 (1970).
[70Y1] C. N. Yang: *Phys. Rev. D*, **1**, 2360 (1970).
[71A1] L. W. Alvarez, M. Jr. Autuna, R. A. Byrns, P. H. Eberhard, R. E. Gilmer, E. H. Hoyer, R. R. Ross, H. H. Stellrecht, J. D. Taylor and R. D. Watt: *Rev. Sci. Instrum.*, **4**, 326 (1971).
[71B1] I. Bialynicki-Birula: *Phys. Rev. D*, **3**, 2413 (1971).
[71C1] R. A. Carrigan jr. and F. A. Nezrick: *Phys. Rev. D*, **3**, 56 (1971).
[71D1] J. Dooher: *Phys. Rev. D*, **3**, 2652 (1971).

[71E1] P. H. Eberhard, R. R. Ross and L. W. Alvarez: *Phys. Rev. D*, **4**, 3260 (1971).

[71F1] R. L. Fleischer, H. R. Hart, G. E. Nichols and P. B. Price: *Phys. Rev. D*, **4**, 24 (1971).

[71H1] M. Y. Han and L. C. Biedenharn: *Nuovo Cimento A*, **2**, 544 (1971).

[71K1] H. H. Kolm, F. Villa and A. Odian: *Phys. Rev. D*, **4**, 1285 (1971).

[71P1] E. N. Parker: *Astrophys. J.*, **163**, 255 (1971).

[71P2] E. N. Parker: *Astrophys. J.*, **186**, 279 (1971).

[71T1] D. R. Tompkins: *Phys. Rev. D*, **4**, 1268 (1971).

[72B1] D. F. Bartlett and M. D. Lahana: *Phys. Rev. D*, **6**, 1817 (1972).

[72B2] L. M. Barkov, I. I. Gurevich and M. S. Zolotarev: *Sov. Phys. JETP*, **34**, 917 (1972).

[72B3] A. O. Barut: *Phys. Lett. B*, **38**, 97 (1972).

[72G1] I. I. Gurevich, S. Kh. Khakimov, V. P. Martemianov, A. P. Mishokova, L. A. Makar'ina, V. V. Ogurtzov, V. G. Tarasenkov, L. A. Chernyshova, L. M. Barkov, M. S. Zolotarev, V. S. Ohapkin and N. M. Tarkanov: *Phys. Lett. B*, **38**, 54 (1972); *Sov. Phys. JETP*, **34**, 917 (1972).

[72M1] V. P. Martemianov and S. Kh. Khakimov: *Sov. Phys. JETP*, **35**, 20 (1972).

[72N1] J. L. Newmeyer and J. S. Trefil: *Phys. Lett. B*, **38**, 524 (1972).

[72N2] J. L. Newmeyer and J. S. Trefil: *Nuovo Cimento A*, **8**, 703 (1972).

[72V1] J. P. Vinti: *J. Geophys. Res.*, **77**, 2404 (1972).

[72V2] P. Vinciarelli: *Phys. Rev. D*, **6**, 3419 (1972).

[72W1] J. M. Wilcox: *Comments Astrophys. Space Phys.*, **4**, 141 (1972).

[73C1] R. A. Carrigan jr., F. A. Nezrick and B. P. Strauss: *Phys. Rev. D*, **8**, 3717 (1973).

[73C2] G. B. Collins, J. R. Ficenec, D. M. Stevens, W. P. Trower and J. Fischer: *Phys. Rev. D*, **8**, 892 (1973).

[73R1] R. R. Ross, P. H. Eberhard, L. W. Alvarez and R. D. Watt: *Phys. Rev. D*, **8**, 698 (1973).

[73S1] D. M. Stevens: *Magnetic monopoles, an updated bibliography*, VPI-EPP-735-(1973).

[74C1] R. A. Carrigan jr., F. A. Nezrick and B. P. Strauss: *Phys. Rev. D*, **10**, 3867 (1974).

[74H1] G. 't Hooft: *Nucl. Phys. B*, **79**, 276 (1974).

[74H2] R. Howard: *Solar Phys.*, **38**, 283 (1974).

[74K1] L. Karlsson: *Nucl. Instrum. Methods*, **116**, 275 (1974).

[74P1] P. Peregrinus: *A Source Book in Medieval Science*, edited by E. Grant (Harvard University Press, Cambridge, Mass., 1974), p. 368.

[74P2] A. M. Polyakov: *JETP Lett.*, **20**, 194 (1974).

[74S1] M. Stix and E. Wiehr: *Solar Phys.*, **37**, 493 (1974).

[74Z1] V. P. Zrelov, L. Kollarova, D. Kollar, V. P. Lupil'tsev, P. Pavlovic, J. Ruzicka, V. I. Sidorova, M. F. Shaboshov and R. Janik: *Search for Dirac monopoles over the Vavilov-Cherenkov radiation using the* 70 GeV IHEP *synchrotron*, JINR-P1-7996 (1974).

[75B1] D. L. Burke, H. R. Gustafson, L. W. Jones and M. L. Longo: *Phys. Lett. B*, **60**, 113 (1975).

[75B2] Yu. S. Biza: *Isv. Akad. Nauk BSSR*, **2**, 110 (1975).

[75C1] R. A. Carrigan jr. and F. A. Nezrick: *Nucl. Phys. B*, **91**, 279 (1975).

[75E1] P. H. Eberhard, R. R. Ross, J. D. Taylor, L. W. Alvarez and H. Oberlack: *Phys. Rev. D*, **11**, 3099 (1975).

[75E2] P. H. Eberhard, R. R. Ross and J. D. Taylor: *Rev. Sci. Instrum.*, **46**, 362 (1978).

[75G1] G. GIACOMELLI, A. M. ROSSI, G. VANNINI, A. BUSSIERE, G. BARONI, S. DI LIBERTO, S. PETRERA and G. ROMANO: *Nuovo Cimento A*, **28**, 21 (1975).
[75G2] G. GIACOMELLI and A. THORNDIKE: *Monopole searches at Isabelle*, in *Proceedings of the 1975 Isabelle Summer Study* (1975).
[75H1] R. HAGSTROM: *Phys. Rev. Lett.*, **25**, 1677 (1975).
[75M1] R. MIGNANI and E. RECAMI: *Lett. Nuovo Cimento*, **13**, 589 (1975).
[75O1] G. I. OPAT: *Limits placed on the existence of magnetic charge in the proton by the ground state hyperfine splitting of hydrogen*, University of Melbourne Rep., UM-P-75/29 (1975).
[75P1] P. B. PRICE, E. K. SHIRK, W. Z. OSBORNE and L. S. PINSKY: *Phys. Rev. Lett.*, **35**, 487 (1975).
[75T1] D. R. TOMPKINS jr. and P. F. RODNEY: *Phys. Rev. D*, **12**, 2610 (1975).
[75W1] T. T. WU and C. N. YANG: *Phys. Rev. D*, **12**, 3845 (1975).
[75Y1] P. C. M. YOCK: *Nucl. Phys. B*, **86**, 216 (1975).
[76A1] S. P. AHLEN: *Phys. Rev. D*, **14**, 2935 (1976).
[76B1] S. A. BLUDMAN and M. A. RUDERMAN: *Phys. Rev. Lett.*, **36**, 840 (1976).
[76C1] W. C. CARITHERS, R. STEFANSKI and R. K. ADAIR: *Phys. Rev.*, **149**, 1070 (1966).
[76C2] R. A. CARRIGAN jr., F. A. NEZRICK and B. P. STRAUSS: *Phys. Rev. D*, **13**, 1823 (1976).
[76C3] J. M. CORNWALL and H. H. HILTON: *Phys. Rev. Lett.*, **36**, 900 (1976).
[76E1] P. H. EBERHARD and R. R. ROSS: *Are monopoles trapped by ferromagnetic materials?*, LBL-4614 (1976).
[76G1] A. S. GOLDHABER: *Phys. Rev. Lett.*, **36**, 1122 (1976).
[76K1] G. KALMAN and D. TER HAAR: *Nature (London)*, **259**, 467 (1976).
[76O1] O. OTGONSUREN, V. P. PERELYGIN, S. G. STETSENKO, N. N. GAVRILOVA, C. FIEENI and P. PELLAS: *Astrophys. J.*, **210**, 258 (1976).
[76O2] G. E. OPAT: *Phys. Rev. Lett. B*, **60**, 205 (1976).
[76S1] D. M. STEVENS: *Phys. Rev. D*, **14**, 2207 (1976).
[76W1] T. T. WU and C. N. YANG: *Nucl. Phys. B*, **107**, 365 (1976).
[77C1] R. A. CARRIGAN jr.: *Magnetic Monopole Bibliography* (1973-1976).
[77K1] Y. KAZAMA, C. N. YANG and A. S. GOLDHABER: *Phys. Rev. D*, **15**, 2287 (1977).
[77K2] Y. KAZAMA and C. N. YANG: *Phys. Rev. D*, **15**, 2300 (1977).
[77K3] C. KITTEL and A. MANOLIN: *Phys. Rev. B*, **15**, 333 (1977).
[77P1] V. F. PEREPELITSA: *A search for tachyon monopoles*, ITEP-82, Moscow (1977).
[77R1] S. G. RAUTIAN, V. P. SAFONOV and G. I. SMIRNOV: *Phys. Lett. B*, **70**, 278 (1977).
[78A1] S. P. AHLEN: *Phys. Rev. D*, **17**, 229 (1978).
[78B1] D. F. BARTLETT, D. SOO and M. G. WHITE: *Phys. Rev.*, **180**, 2253 (1978).
[78C1] R. A. CARRIGAN jr., B. P. STRAUSS and G. GIACOMELLI: *Phys. Rev. D*, **17**, 1754 (1978).
[78D1] P. A. M. DIRAC: *Int. J. Theor. Phys.*, **17**, 235 (1978).
[78G1] G. GIACOMELLI: *Searches for missing particles*, invited paper at *The 1978 Singapore Meeting on Frontiers of Physics, Proceedings of the Conference* (1978).
[78G2] P. GODDARD and D. OLIVE: *Rep. Prog. Phys.*, **41**, 91 (1978).
[78H1] H. HOFFMANN and G. KANTARDJIAN: *Lett. Nuovo Cimento*, **23**, 357 (1978).
[78P1] P. B. PRICE, E. K. SHIRK, W. Z. OSBORNE and L. S. PINSKY: *Phys. Rev. D*, **18**, 1382 (1978).
[78Z1] YA. B. ZEL'DOVICH and M. YU. KHLOPOV: *Phys. Lett. B*, **79**, 239 (1978).
[78Z2] V. P. ZRELOV: *Nucl. Instrum. Methods*, **153**, 145 (1978).
[79B1] J. J. BRODERICK, J. R. FICENEC, D. C. TEPLITZ and V. L. TEPLITZ: *Phys. Rev. D*, **19**, 1046 (1979).

[79B2] M. BONNARDEAU and A. K. DRUKIER: *Astrophys. Space Sci.*, **60**, 375 (1979).
[79O1] D. OLIVE: *Phys. Rep.*, **49**, 165 (1979).
[79P1] J. P. PRESKILL: *Phys. Rev. Lett.*, **43**, 1365 (1979).
[79S1] I. A. SATIKOV and V. I. STRAZHEV: *Sov. J. Nucl. Phys.*, **30**, 716 (1979).
[80A1] S. P. AHLEN: *Rev. Mod. Phys.*, **52**, 121 (1980).
[80C1] R. A. CARRIGAN jr.: *Nature (London)*, **288**, 348 (1980).
[80C2] R. A. CARRIGAN jr.: *Down to earth speculations on grand unification magnetic monopoles*, FERMILAB-Pub 80/58-EXP.
[80D1] C. P. DOKOS and T. N. TOMARA: *Phys. Rev. D*, **21**, 2940 (1980).
[80E1] M. B. EINHORN, D. L. STEIN and D. TOUSSAINT: *Phys. Rev. D*, **21**, 3295 (1980).
[80K1] T. W. B. KIBBLE: *Phys. Rep.*, **67**, 183 (1980).
[80L1] G. LAZARIDES and Q. SHAFI: *Phys. Lett. B*, **94**, 149 (1980).
[80L2] P. LANGACKER: *Phys. Rev. Lett.*, **45**, 1 (1980).
[80R1] J. RUZICKA and V. P. ZRELOV: *Fifty Years of Dirac Monopole: Complete Bibliography*, JINR-1-2-80-850 (1980).
[80S1] D. M. SCOTT: *Nucl. Phys. B*, **171**, 109 (1980).
[81B1] D. F. BARTLETT, D. SOO, R. L. FLEISCHER, H. HART and A. MAGRO-CAMPERO: *Phys. Rev. D*, **24**, 612 (1981).
[81B2] M. BONNARDEAU: *Phys. Rev. D*, **23**, 323 (1981).
[81B3] R. BONARELLI, P. CAPILUPPI, I. D'ANTONE, G. GIACOMELLI, G. MANDRIOLI, C. MERLI and A. M. ROSSI: *Ricerca di monopoli magnetici cosmici*, University of Bologna, Rep. IFUB (1981), unpublished.
[81C1] R. E. CRAVEN, W. P. TROWER and R. A. CARRIGAN jr.: *Magnetic Monopole Bibliography*, FERMILAB 81/37 (1981).
[81D1] A. K. DRUKIER: *Astrophys. Space Sci.*, **74**, 245 (1981).
[81E1] P. H. EBERHARD: *Phys. Rev. D*, **4**, 3260 (1981).
[81G1] G. GIACOMELLI: *Review of the experimental status (past and future) of monopole searches*, in *Proceedings of the Conference on Monopoles in Quantum Field Theory, Trieste* (1981). Revised for the 1982 Zuoz Spring School of Physics.
[81G2] G. GIACOMELLI and G. KANTARDJIAN: *Magnetic monopole searches at Isabelle*, in *Proceedings of the 1981 Isabelle Summer Workshop* (1981).
[81G3] S. GEER and W. G. SCOTT: *Calculation of the energy loss for slow monopoles in atomic hydrogen*, CERN $p\bar{p}$ Note (1981).
[81G4] A. H. GUTH: *Phys. Rev. D*, **23**, 347 (1981).
[81K1] T. W. B. KIBBLE: *Monopoles in the early universe*, in *Proceedings of the 1981 Meeting on Monopoles in Quantum Field Theory, Trieste* (1981).
[81L1] G. LAZARIDES, Q. SHAFI and T. F. WALSH: *Phys. Lett. B*, **100**, 21 (1981).
[81R1] V. A. RUBAKOV: *JETP Lett.*, **33**, 644 (1981).
[81U1] J. D. ULLMANN: *Phys. Rev. Lett.*, **47**, 289 (1981).
[82A1] E. N. ALEXEYEV, M. M. BOLIEV, A. E. CHUDAKOV, B. A. MAKOEV, S. P. MIKHEYEV and YU. V. STEN'KIN: *Lett. Nuovo Cimento*, **35**, 413 (1982).
[82A2] S. P. AHLEN and K. KINOSHITA: *Phys. Rev. D*, **26**, 2347 (1982).
[82A3] C. W. AKERLOF: *Phys. Rev.*, **260**, 1116 (1982).
[82A4] D. S. AYRES, D. B. CLINE, K. HELLER, W. MARCIANO and R. SHROCK: *Future search for GUT monopoles*, Wisconsin U-Print 82-0863 (1982).
[82A5] L. W. ALVAREZ: *Some thoughts on monopoles*, LBL-Phys. Notes 932 (1982), unpublished.
[82B1] R. BONARELLI, P. CAPILUPPI, I. D'ANTONE, G. GIACOMELLI, G. MANDRIOLI, C. MERLI and A. M. ROSSI: *Phys. Lett. B*, **112**, 100 (1982).
[82B2] P. B. BUFORD-PRICE: *Searches for exotic particles*, in *Proceedings of the Workshop on Magnetic Monopoles* (Wingspread, 1982).

[82B3] B. C. BARISH: *Acoustic detection of monopoles*, in *Proceedings of the Workshop on Magnetic Monopoles* (Wingspread, 1982).
[82C1] B. CABRERA: *Phys. Rev. Lett.*, **48**, 1378 (1982).
[82C2] S. COLEMAN: *The magnetic monopole fifty years later*, HUTP-82/A032.
[82C3] R. E. CRAVEN and W. P. TROWER: *Magnetic Monopole Bibliography 1981-1982*, FERMILAB-82/96.
[82C4] C. G. CALLAN: *Phys. Rev. D*, **26**, 2058 (1982).
[82C5] C. G. CALLAN jr.: *Phys. Rev. D*, **25**, 2141 (1982).
[82C6] R. J. CREWTHER: *Introduction to the theory of magnetic monopoles*, in *Proceedings of the* 1982 *Zuoz Spring School*, SIN Switzerland.
[82D1] S. DIMOPOULOS and J. PRESKILL: *Phys. Lett. B*, **119**, 320 (1982).
[82D2] A. K. DRUKIER and S. NUSSINOV: *Phys. Rev. Lett.*, **49**, 102 (1982).
[82D3] G. F. DELL, L. C. L. YUAN, L. E. ROBERTS and J. DOOHER: *Nucl. Phys. B*, **209**, 45 (1982).
[82D4] S. DIMOPOULOS, S. L. GLASHOW and E. M. PURCELL: *Nature* (*London*), **298**, 824 (1982).
[82E1] J. ELLIS, D. V. NANOPOULOS and K. A. OLIVE: *Phys. Lett. B*, **116**, 127 (1982).
[82F1] G. W. FORD: *Phys. Rev. D*, **26**, 2519 (1982).
[82F2] K. FREESE and M. S. TURNER: *Phys. Lett. B*, **123**, 293 (1982).
[82G1] G. GIACOMELLI: *Experimental status of monopoles*, in *Proceedings of the Workshop on Magnetic Monopoles* (Wingspread, 1982). X
[82G2] B. GROSSMAN, G. LAZARIDES and A. I. SANDA: *Phys. Rev. D*, **28**, 2109 (1982).
[82G3] F. GOLDHABER: *Monopoles and gauge theories*, in *Proceedings of the Workshop on Magnetic Monopoles* (Wingspread, 1982).
[82H1] K. HAYASHI: *Lett. Nuovo Cimento*, **33**, 324 (1982).
[82H2] K. HAYASHI: *Lett. Nuovo Cimento*, **34**, 10 (1982).
[82I1] M. IZAWA and K. SATO: *Prog. Theor. Phys.*, **68**, 1574 (1982).
[82K1] E. W. KOLB, S. A. COLGATE and J. A. HARVEY: *Phys. Rev. Lett.*, **49**, 1373 (1982).
[82K2] K. KINOSHITA, P. B. PRICE and D. FRYBERGER: *Phys. Rev. Lett.*, **48**, 77 (1982).
[82L1] M. J. LONGO: *Phys. Rev. D*, **25**, 2399 (1982).
[82L2] G. LAZARIDES, Q. SHAFI and W. P. TROWER: *Phys. Rev. Lett.*, **49**, 1756 (1982).
[82M1] T. MOSHIMO, K. KAWAGOE and M. KOSHIBA: *J. Phys. Soc. Jpn.*, **51**, 3065 (1982).
[82N1] D. V. NANOPOULOS: *Cosmological implications of grand unified theories*, in *Proc. S.I.F.*, Course LXXXI (Amsterdam, 1982), p. 156.
[82R1] L. E. ROBERTS and J. P. DOOHER: *Nuovo Cimento A*, **72**, 191 (1982).
[82R2] V. A. RUBAKOV: *Nucl. Phys. B*, **203**, 311 (1982).
[82R3] D. M. RITSON: *Magnetic monopole energy losses*, SLAC-PUB-2950 (1982).
[82R4] C. RUBBIA: *Hunting the supermassive monopole without superconductivity*, CERN-EP Internal Report 82-01 (1982).
[82S1] N. STRAUMANN: *Cosmological production of magnetic monopoles*, SIN PR 82-09 (1982).
[82S2] K. SATO and M. IZAWA: *Black hole and worm hole creation by phase transition and monopole problem*, KUNS 664 (1982).
[82S3] E. E. SALPETER, S. L. SHAPIRO and I. WASSERMAN: *Phys. Rev. Lett.*, **49**, 1114 (1982).
[82T1] M. S. TURNER: *Phys. Rev. D*, **26**, 1296 (1982).
[83A1] S. P. AHLEN and G. TARLÉ: *Phys. Rev. D*, **27**, 688 (1983).
[83A2] J. ARAFUNE: *Phys. Rev. Lett.*, **50**, 1901 (1983).
[83A3] C. W. AKERLOF: *Phys. Rev. D*, **27**, 1675 (1983).

[83A4] B. Aubert, P. Musset, M. Price and J. P. Vialle: *Phys. Lett. B*, **120**, 465 (1983).

[83A5] S. N. Anderson, J. J. Lord, S. C. Strausz and R. J. Wilkes: *Possible evidence for magnetic monopole interactions: anomalous long range alpha particle tracks deep underground*, VTL PUB-9 (1983).

[83A6] A. M. Allega and N. Cabibbo: *Acoustic detection of superheavy monopoles in gravitational antennas*, INFN report (1983).

[83A7] S. P. Ahlen: *Status of monopole detection by ionization/excitation techniques*, invited paper at *Monopoles 83 Workshop* (Ann Arbor, Mich., 1983).

[83A8] J. Arafune and M. Fugugita: *Phys. Lett. B*, **133**, 380 (1983).

[83A9] J. Arafune, M. Fugugita and S. Yanagita: *Monopole abundance in the solar system and the intrinsic heat in the Jovian planets*, Kyoto report RIFP-531 (1983).

[83B1] L. Bracci and G. Fiorentini: *Phys. Lett. B*, **124**, 493 (1983).

[83B2] J. Bartelt, H. Courant, K. Heller, T. Joyce, M. Marshak, E. Peterson, K. Ruddick, M. Shupe, D. S. Ayres, J. W. Dawson, T. H. Fields, E. N. May and L. E. Price: *Phys. Rev. Lett.*, **50**, 655 (1983).

X [83B3] R. Bonarelli, P. Capiluppi, I. D'Antone, G. Giacomelli, G. Mandrioli, C. Merli and A. M. Rossi: *Phys. Lett. B*, **126**, 137 (1983).

[83B4] L. Bracci and G. Fiorentini: *Phys. Lett. B*, **124**, 29 (1983).

[83B5] F. A. Bais, J. Ellis, D. V. Nanopoulos and K. A. Olive: *Nucl. Phys. B*, **219**, 189 (1983).

[83B6] G. Battistoni, E. Bellotti, G. Bologna, P. Campana, C. Castagnoli, V. Chiarella, A. Ciocio, D. C. Cundy, B. D'Ettorre-Piazzoli, E. Fiorini, P. Galeotti, E. Iarocci, C. Liguori, G. Mannocchi, G. P. Murtas, P, Negri. G. Nicoletti, P. Picchi, M. Price, A. Pullia, S. Ragazzi, M. Rollier, O. Saavedra, L. Satta, L. Trasatti and L. Zanotti: *Phys. Lett. B*, **133**, 454 (1983).

[83B7] J. M. Barkov, A. P. Bugorsky, G. Giacomelli, I. I. Gurevich, S. Kh. Khakimov, P. Lazeyras, V. P. Martemianov, A. P. Mishakova, V. V. Ogurtzov, V. G. Tarasenkov, V. N. Vyrodov, M. A. Kotov, L. A. Makarina and A. A. Filippov: *Search for Dirac monopoles in* pN *collisions at* 400 GeV/c, CERN/EP 83-194 (1983).

[83B8] P. C. Bosetti, P. W. Gorham, F. A. Harris, J. G. Learned, M. McMurdo, D. J. O'Connor, V. J. Stenger and S. Thompson: *Phys. Lett. B*, **133**, 265 (1983).

[83B9] S. W. Barwick, K. Kinoshita and P. B. Price: *Phys. Rev. D*, **28**, 2838 (1983).

[83C1] R. A. Carrigan jr. and W. P. Trower: *Magnetic monopoles: a status report*, FERMILAB-Pub-83/31.

[83C2] C. G. Callan jr.: *Nucl. Phys. B*, **212**, 391 (1983).

[83C3] B. Cabrera and W. P. Trower: *Found. Phys.*, **13**, 195 (1983).

[83C4] G. Charpak: *Detectors for rare events*, invited paper at *Monopoles 83 Workshop* (Ann Arbor, Mich., 1983).

[83C5] B. Cabrera: *Upper limit on flux of cosmic-ray monopoles obtained with a three-loop superconductive detector*, Stanford University preprint (1983).

[83C6] C. C. Chi: *Monopole search at* IBM: *present status and future plans*, invited paper at the *Monopoles 83 Workshop* (Ann Arbor, Mich., 1983).

[83C7] P. L. Connolly: *A monopole search using an accelerator detector*, BNL-3444 (1983).

[83D1] S. D. Drell, N. M. Kroll, M. T. Mueller, S. J. Parke and M. A. Ruderman: *Phys. Rev. Lett.*, **50**, 644 (1983).

[83D2] T. DOKE, T. HAYASHI, R. HAMASAKI, T. AKIOKA, T. NAITO, K. ITO, T. YANAGIMACHI, S. KOBAYASHI, T. TAKENAKA, M. OHE, K. NAGATA and T. TAKAHASHI: *Phys. Lett. B*, **129**, 370 (1983).

[83D3] A. K. DRUKIER: *Acta Astron.*, **32**, 1 (1983).

[83D4] S. DAWSON and A. N. SCHELLEKENS: *Phys. Rev. D*, **28**, 3125 (1983).

[83D5] A. K. DRUKIER: *Search for superheavy magnetic monopoles with superconducting colloid detector, A preliminary study*, MPI-PAE/Pth 58/83 (1983).

[83E1] S. ERREDE, J. L. STONE, J. C. VANDERVELDE, R. M. BIONTA, G. BLEWITT, C. B. BRATTON, B. G. CORTEZ, G. W. FOSTER, W. GAJEWSKI, M. GOLDHABER, J. GREENBERG, T. J. HAINES, T. W. JONES, D. KIELCZEWSKA, W. R. KROPP, J. C. LEARNED, E. LEHMANN, J. M. LOSECCO, P. V. RAMANA MURTHY, H. S. PARK, F. REINES, J. SCHULTZ, E. SHUMARD, D. SINCLAIR, D. W. SMITH, H. W. SOBEL, L. R. SULAK, R. SVOBODA and C. WUEST: *Phys. Rev. Lett.*, **51**, 245 (1983).

[83E2] T. EBISU and T. WATANABE: *J. Phys. Soc. Jpn.*, **52**, 2617 (1983).

[83E3] P. ECKERT, D. ALTSCHÜLER, T. SCHÜCKER and G. WANNER: *Nucl. Phys. B*, **226**, 387 (1983).

[83F1] A. FUKUHARA, K. SHINAGAWA, A. TONOMURA and H. FUJIWARA: *Phys. Rev. B*, **27**, 1839 (1983).

[83F2] K. FREESE and M. S. TURNER: *Phys. Lett. B*, **123**, 293 (1983).

[83F3] D. FARGION: *Phys. Lett. B*, **127**, 35 (1983).

[83F4] H. FRISCH: *Monopole detection by induction techniques*, invited paper at *Monopoles 83 Workshop* (Ann Arbor, Mich., 1983).

[83G1] D. E. GROOM, E. C. LOH, H. N. NELSON and D. M. RITSON: *Phys. Rev. Lett.*, **50**, 573 (1983).

[83G2] G. GIACOMELLI: *Magnetic monopoles*, invited paper to ICOMAN 1983, Frascati 17-22 January 1983.

[83G3] G. GIACOMELLI: *Conference high-lights and summation. Experimental*, invited paper at *Monopoles 83 Workshop* (Ann Arbor, Mich., 1983).

[83G4] L. GONZALES-MESTRES and D. PERRET-GALLIX: *Proposal for an all-beta monopole detector*, LAPP-EXP-83-04 (1983).

[83G5] C. GOEBEL: *Binding of monopoles to nuclei*, in *Proceedings of the Monopoles 83 Workshop* (Ann Arbor, Mich., 1983).

[83H1] D. K. HONG, J. KIM, J. E. KIM and K. S. SOH: *Phys. Rev. D*, **27**, 1651 (1983).

[83H2] D. J. HEGYI and K. A. OLIVE: *Phys. Lett. B*, **126**, 28 (1983).

[83H3] C. T. HILL: *Nucl. Phys. B*, **224**, 469 (1983).

[83H4] J. HARVEY: *Neutron star physics and monopole flux limits*, invited paper at the *Monopoles 83 Workshop* (Ann Arbor, Mich., 1983).

[83K1] V. A. KUZMIN and V. A. RUBAKOV: *Phys. Rev. Lett. B*, **125**, 372 (1983).

[83K2] K. KAVAGOE, K. NAGANO, S. NAKAMURA, M. NOZAKI, S. ORITO, T. DOKE, T. HAYASHI, I. MATSUMI, M. MATSUSHITA, H. TAWARA and K. OGURA: *A search for magnetic monopoles with* 1000 m^2 *of plastic track detector*, Status report, University of Tokyo report (1983).

[83K3] F. KAJINO: *A scintillator-proportional counter search for monopoles*, in *Monopoles 83 Workshop* (Ann Arbor, Mich., 1983).

[83K4] C. KOUNNAS, D. V. NANOPOULOS and M. QUIROS: *Phys. Lett. B*, **129**, 223 (1983).

[83K5] E. W. KOLB: *Monopole catalyzed nucleon decay: the astrophysical connection*, FERMILAB Conf. 83/103-AST (1983).

[83I1] M. IZAWA and K. SATO: *Prog. Theor. Phys.*, **70**, 1024 (1983).

[83L1] G. LAZARIDES and Q. SHAFI: *Phys. Lett. B*, **124**, 26 (1983).

[83L2] H. J. LIPKIN: *Monopole catalysis of nuclear beta-decay and spontaneous fission*, invited paper at the *Monopoles 83 Workshop* (Ann Arbor, Mich., 1983).

[83M1] T. MASHIMO, S. ORITO, K. KAWAGOE, S. NAKAMURA and M. NOZAKI: *Phys. Lett. B*, **128**, 327 (1983).

[83M2] P. MUSSET, M. PRICE and E. LOHRMANN: *Phys. Lett. B*, **128**, 333 (1983).

[83M3] V. F. MIKHAILOV: *Phys. Lett. B*, **130**, 331 (1983).

[83O1] K. OLAUSEN, H. A. OLSEN, P. OSLAND and I. ØVERBØ: *Nucl. Phys. B*, **228**, 567 (1983).

[83O2] K. A. OLIVE and D. N. SCHRAMM: *Phys. Lett. B*, **130**, 267 (1983).

[83P1] M. J. PRICE: *The detection of cosmic monopoles using a room temperature coil*, CERN/EF 83-2 (1983).

[83P2] R. D. PECCEI: *Theoretical review of monopole bounds*, Munich preprint MPI-PAE/PTh 83-22 (1983).

[83P3] E. N. PARKER: *Monopole abundance implied by the magnetic fields of the galaxy*, in *Proceedings of the Monopoles 83 Workshop* (Ann Arbor, Mich., 1983).

[83P4] M. J. PERRY: *Monopoles in Kaluza-Klein theories*, invited paper at the *Monopoles 83 Workshop* (Ann Arbor, Mich., 1983).

[83R1] Y. RAPHAELI and M. S. TURNER: *Phys. Lett. B*, **121**, 115 (1983).

[83R2] TH. W. RUJGROK, J. A. TJON and T. T. WU: *Monopole chemistry*, DESY 83-036 (1983).

[83S1] K. H. SCHATTEN: *Phys. Rev. D*, **27**, 1525 (1983).

[83S2] A. N. SCHELLEKENS and C. K. ZACHOS: *Phys. Rev. Lett.*, **50**, 1242 (1983).

[83S3] J. STEIN-SCHABES and J. B. BARROW: *Phys. Lett. B*, **122**, 31 (1983).

[83T1] TAI TSUM WU: *Interaction of a fermion with a monopole*, DESY 83-021.

[83T2] C. D. TESCHE, C. C. CHI, C. C. TSUEI and P. CHAUDHARI: *Appl. Phys. Lett.*, **43**, 384 (1983).

[83T3] J. S. TREFIL, H. P. KELLY and R. T. ROOD: *Nature (London)*, **302**, 111 (1983).

[83T4] M. S. TURNER: *Nature (London)*, **302**, 804 (1983).

[83W1] T. F. WALSH and T. T. WU: *Monopole catalysis of proton decay*, DESY 83-002 (1983).

[83W2] E. J. WEINBERG: *Monopoles and grand unification*, invited paper at *Monopoles 83 Workshop* (Ann Arbor, Mich., 1983).

[83Y1] T. M. YAN: *Breaking of conservation laws induced by magnetic monopoles in the Rubakov-Callan model*, to be published in *Phys. Rev. D*.

[83Z1] J. F. ZIEGLER, C. C. TSUEI, C. C. CHI, C. D. TESCHE, P. CHAUDARI and K. W. JONES: *Phys. Rev. D*, **28**, 1793 (1983).

[84B1] L. BRACCI, G. FIORENTINI and R. TRIPICCIONE: *On the energy loss of very slowly moving magnetic monopoles*, Pisa preprint IFUP-TH 83/26 (1983).

[84B2] A. P. BALACHANDRAN and J. SCHECHTER: *Phys. Rev. D*, **29**, 1184 (1984).

[84B3] L. BRACCI, G. FIORENTINI, G. MEZZORANI and P. QUARATI: *Formation of monopole-proton bound states in the hot universe*, University of Pisa preprint IFUP TH 84-3 (1984).

[84B4] L. BRACCI and G. FIORENTINI: *On the capture of protons by magnetic monopoles*, University of Pisa IFUP TH 84-5 (1984).

[84B5] C. BERNARD, A. DE RUJULA and B. LAUTRUP: *Nucl. Phys. B*, **242**, 93 (1984).

[84C1] W. COLLINS and M. S. TURNER: *Phys. Rev. D*, **29**, 2158 (1984).

[84E1] S. ERREDE, E. SHUMARD and J. STONE: *Update of the* IMB *monopole catalysis flux limits*, University of Michigan preprint PDK 1984-20 (1984).

[84E2] P. ECKERT, D. ALTSCHULER and T. SCHUKER: *Nucl. Phys. B*, **231**, 40 (1984).

[84E3] T. EBISU and T. WATANABE: *Present status of monopole search with superconducting induction coils*, KOBE-84-03 (1984).

[84E4] K. Enqvist and D. V. Nanopoulos: *Phys. Lett. B*, **142**, 349 (1984).
[84F1] R. Farouki, S. L. Shapiro and I. Wasserman: *Numerical simulation of the plasma and gravitational dynamics of the galactic magnetic monopole halo*, Cornell preprint CRSR 811 (1984).
[84F2] D. Fryberger, T. E. Coan, K. Kinoshita and P. B. Price: *Phys. Rev. D*, **29**, 1524 (1984).
[84F3] J. N. Fry and G. M. Fuller: *Supermassive monopole stars*, University of Chicago Astrophysics preprint (1984).
[84G1] C. L. Gardner: *Phys. Rev. Lett.*, **52**, 879 (1984).
[84G2] R. Gardner, B. Cabrera, M. Taber and M. Huber: *Large scale superconductive monopole detector*, paper contributed to the LT-17 Conf. Germany (1984).
[84K1] N. M. Kroll: *Excitation of simple atoms by slow magnetic monopoles*, SLAC-PUB-3281 (1984).
[84K2] E. W. Kolb and M. S. Turner: *Limits from the soft X-ray background on the temperature of old neutron stars and on the flux of superheavy magnetic monopoles*, FERMILAB-PUB-84-30 (1984).
[84K3] M. Koshiba: *Kamioka results on proton decay*, invited paper at the *Fifth Workshop on Grand Unification* (Providence, R.I., 1984).
[84L1] Letter of intent for a large area detector dedicated to monopole search, cosmic-ray physics and astrophysics at the Gran Sasso laboratory (1984).
[84O1] K. Olausen: *Phys. Rev. Lett.*, **52**, 325 (1984).
[84P1] P. B. Price, S. Guo, S. P. Ahlen and R. L. Fleischer: *Phys. Rev. Lett.*, **52**, 1265 (1984).
[84P2] P. B. Price: *Limit on flux of supermassive monopoles and charged relic particles using plastic track detectors*, CERN-EP/84-28 (1984).
[84R1] V. A. Rubakov and M. S. Serebryakov: *Nucl. Phys. B*, **237**, 329 (1984).
[84S1] S. Somalwar, H. Frisch, I. Incandela and M. Kuchnir: *Series-parallel gradiometers for monopole detectors*, University of Chicago preprint EFI 84-10 (1984).
[84S2] A. Sen: *Phys. Rev. Lett.*, **52**, 1755 (1984).
[84T1] G. Tarlé, S. P. Ahlen and T. M. Liss: *Phys. Rev. Lett.*, **52**, 90 (1984).
[84T2] C. D. Tesche, C. C. Chi, C. C. Tsuei, P. Chaudari and S. Bermon: *Large area inductive monopole detectors. The planar gradiometer approach*, paper of IBM group for technical assessment panel (1984).
[84W1] I. Wasserman, S. L. Shapiro and R. Farouki: *Do cosmic magnetic monopoles cause rapid decay of the galactic magnetic field?*, Cornell University preprint CRSR 810 (1984).

CONFERENCES ON MAGNETIC MONOPOLES

Proceedings of the Monopoles in Quantum Field Theory, December 1981, Trieste, Italy, edited by N. S. Craigs, P. Goddard and W. Nahm (World Scientific, Singapore, 1981).

Proceedings of the Workshop on Magnetic Monopoles, 14-17 October 1982, Wingspread, Wisconsin, edited by R. Carrigan and P. Trower, NATO ASI series Vol. **102** (1982).

Workshop on Monopoles and Proton Decay, 18-20 October 1982, Kamioka, Japan (1982).

Monopoles 83, 6-9 October 1983, The University of Michigan (Ann Arbor, Mich., 1983).

Les monopoles magnetiques en physique et en astrophysique, 25-27 mai 1983 (Orsay, 1983).

Workshop on Monopoles, GUTS *and the Early Universe, 31 October - 4 November 1983, Copenhagen, Denmark* (1983).

LAST PUBLISHED PAPERS

M. Dragoni and M. Gasperini – On the localization of seismic events.

M. Bacci – Spectroscopic and structural properties of metallo-proteins.

E. Ferrari – On the scattering from an experimental beam of wave packets.

G. Marmo, N. Mukunda and J. Samuel – Dynamics and symmetry for constrained systems: a geometrical analysis.

L. Angelini, L. Nitti, M. Pellicoro, G. Preparata and G. Valenti – Fire string theory of e^+e^- annihilation.

J. C. Owen and G. Ripka – The ground state of a strongly interacting fermion system.

P. I. Fomin, V. P. Gusynin, V. A. Miransky and Yu. A. Sitenko – Dynamical symmetry breaking and particle mass generation in gauge field theories.

F.-L. Navarria – Polarization and high-energy lepton-nucleon scattering.

C. Pellacani – Shear instabilities in stratified fluids; linear theory.

A. Quattropani and R. Girlanda – Two-photon absorption in atoms and solids.

R. Hagedorn – Multiplicities, p_T distributions and the expected hadron quark-gluon phase transition.

S. Focardi and R. A. Ricci - Historical introduction the β-decay and the fundamental properties of weak interactions.

P. G. Bizzeti – Weak interactions in nuclei.

M. Ademollo – Cabibbo theory and current algebra.

A. Pullia – Structure of charged and neutral weak interactions at high energy.

G. Altarelli – Future perspectives in particle physics.

G. Goggi – Gauge vector bosons and unified electroweak interaction.

M. Giffon and E. Predazzi – High-energy physics after the SPS collider.

A. Devoto and D. W. Duke – Table of integrals and formulae for Feynman diagram calculations.

A. Bertin and A. Vitale – Pure Leptonic Weak Processes.

A. Bertin and A. Vitale – Strangeness-conserving semi-leptonic weak processes.

F. Palmonari – Nonleptonic weak interactions.

G. F. Bignami – Galactic high-energy astrophysics after the gamma-ray astronomy mission of the ESA COS-B satellite.

G. Iadonisi – Electron-phonon interaction: effects on the excitation spectrum of solids.

FORTHCOMING PAPERS (in alphabetical order)

E. Bussoletti – Interstellar grains.

C. A. Dominguez – The Goldberger-Treiman relation: a probe of the chiral symmetries of quantum chromodynamics.

A. Dupasquier and A. Zecca – Atomic and solid-state physics experiments with slow-positron beams.

P. Furlan – Conformal quantum electrodynamics and nondecomposable representation.

M. M. Giannini – Photoreactions above the giant dipole resonance.

I. Mannelli – Neutral K-K mixing and *CP* violation.

D. V. Nanopoulos – Superunification.

B. Olivo-Melchiorri and F. Melchiorri – Progress in cosmology.

V. N. Pervushin – The vacuum in gauge theories.

P. Ruggiero and M. Zanetti – Stochastic quantization at finite temperature.

C. Tomasi and F. Trombetti – Absorption and emission by minor atmospheric gases in the radiation balance of the Earth.

S. Twareque Ali – Stochastic localization, quantum mechanics on phase space and quantum space-time.

Direttore responsabile: RENATO ANGELO RICCI

Stampato in Bologna dalla Tipografia Compositori
coi tipi della Tipografia Monograf

Questo fascicolo è stato licenziato dai torchi il 22-V-1985

Questo periodico
è iscritto
all'Unione Stampa
Periodica Italiana